UNIVERSITEIT VAN PRETORIA
UNIVERSITY OF PRETORIA
YUNIBESITHI YA PRETORIA

Development of a breast cancer spheroid model for use in drug discovery and cancer biology research

Thesis submitted in partial fulfilment of the requirements for the degree,

PhD in the Department of Physiology,

at the Faculty of Health Sciences,

University of Pretoria

2020

Student	**Supervisor**
Tamarin Jurgens	Dr. Iman van den Bout
Student number: 28169982	Senior Lecturer
Department: Physiology	Department: Physiology
School of Medicine	School of Medicine
Faculty of Health Sciences	Faculty of Health Sciences
University of Pretoria	University of Pretoria
Co-supervisor	**Head of Department**
Prof. Annie Joubert	Prof. Annie Joubert
Department: Physiology	Department: Physiology
School of Medicine	School of Medicine
Faculty of Health Sciences	Faculty of Health Sciences
University of Pretoria	University of Pretoria

Declaration of originality

UNIVERSITY OF PRETORIA

The Department of Physiology places great emphasis upon integrity and ethical conduct in the preparation of all written work submitted for academic evaluation.

While academic staff teach you about referencing techniques and how to avoid plagiarism, you too have a responsibility in this regard. If you are at any stage uncertain as to what is required, you should speak to your lecturer before any written work is submitted.

You are guilty of plagiarism if you copy something from another author's work (e.g. A book, and article, or a website) without acknowledging the source and pass it off as your own. In effect, you are stealing something that belongs to someone else. This is not only the case when you copy work word-for-word (verbatim), but also when you submit someone else's work in a slightly altered form (paraphrase) or use a line of argument without acknowledging it. You are not allowed to use work previously produced by another student. You are also not allowed to let anybody copy your work with the intention of passing if off as his/her work.

Students who commit plagiarism will not be given any credit for plagiarised work. The matter may also be referred to the Disciplinary Committee (Students) for a ruling. Plagiarism is regarded as a serious contravention of the University's rules and lead to expulsion from the University.

The declaration which follows must accompany all written work submitted while you are a student of the Department of Physiology. No written work will be accepted unless the declaration has been completed and attached.

Full names of student:	Tamarin Jurgens
Student number:	26182699
Topic of work:	Development of a breast cancer spheroid model for use in drug discovery and cancer biology research

Declaration

1. I understand what plagiarism is and am aware of the University's policy in this regard.
2. I declare that this dissertation is my own original work. Where other people's work has been used (either from a printed source, Internet or any other source), this has been properly acknowledged and referenced in accordance with departmental requirements.
3. I have not used work previously produced by another student or any other person to hand in as my own.
4. I have not allowed, and will not allow, anyone to copy my work with the intention of passing it off as his or her own work.

SIGNATURE

SUMMARY

The screening of lead compounds during cancer drug discovery still results in many hits that never reach the clinic. This is in part due to the distance between 2D cell culture, which is mostly used for screening assays and the complexity of an *in vivo* tumour setting. It is thus essential that screening setups are developed that better bridge the gap between *in vitro* and *in vivo* studies. Culturing cells in 3D has been shown to provide an architecture and gene expression profile that better resembles that found in tumours. A number of methods have been developed but many are laborious, require specialised equipment, or are prohibitively costly. In Southern Africa, we do not always have access to expensive machinery and reagents. Therefore, in this thesis, we aimed to set up a simple, easy to use, cost-effective 3D spheroid methodology for triple negative breast cancer that could be used in any laboratory with minimal reagents.

The non-metastatic triple negative breast cancer cell line, BT-20, was identified as the cell line most amenable to spheroid formation and measurement, compared to the metastatic cell lines MDA-MB-231 and MCF-7. Both these cell lines formed inconsistent, difficult to measure spheroids. A low attachment methodology was settled on to induce cell aggregation and spheroid formation. This proved to be an easy, low-cost, and reproducible method. Using the developed methodology, the efficacy of several novel compounds with anti-proliferative activity in 2D cancer cell line cultures were tested for their ability to affect cell survival in the spheroid model.

Our studies show that one non-sulfamoylated 2-methoxyestradiol derivative, EE-15-one, caused a loss of cells in the 2D cell survival assay while it had no effect on BT-20 spheroids. In contrast, two other 2-methoxyestradiol derivatives had similar effects in 2D and 3D. Another novel anticancer compound, STX1972, also had anti-proliferative capabilities in 2D which were lost in cells grown in 3D. As a result, our screening approach on a small number of samples was able to identify 2 of 5 compounds that had no effect on cancer cell growth in 3D. Further analysis of EE-15-one suggests that this compound does not inhibit cell cycle progression like

the other derivatives tested but instead inhibits cell adhesion. Our data shows that integrin-based adhesion is replaced by cadherin-dependent cell-cell adhesion in spheroids. Changing the mode of adhesion correlates strongly with the efficacy of this compound suggesting that it is an inhibitor of integrin dependent cell adhesion. Further analysis show that the efficacy of this compound was not dependent on hypoxia, further strengthening the suggestion that it directly acts on cell adhesion.

It is commonly accepted that a tumour consists of a heterogeneous mix of subpopulations of cancer cells, each with altered genetic backgrounds. Furthermore, such subpopulations can affect each other changing behaviours of neighbouring cells. To replicate this scenario *in vitro*, we initiated the development of a co-culture spheroid system of different triple negative breast cancer cell lines to investigate how they behave within a spheroid. Our data shows that when a co-culture spheroid system of BT-20 and MDA-MB-231 cells is generated, the cells with migratory ability were able to migrate away from the spheroid onto rigid surfaces. In contrast, the non-metastatic BT-20 cells remained within the confines of the spheroid. This suggests that indeed different cell populations will continue to behave differently within a 3D cell culture setting.

In conclusion, we have developed a robust, cost-effective 3D culture system that has shown great potential for used in high throughput screening of novel anti-proliferative compounds. We have shown that these spheroids use different adhesive strategies than their counterparts kept in 2D. This suggests that these cells also change their cellular behaviour which is essential for better mimicking the *in vivo* tumour setting.

Key words: Spheroid, 3D cell culture, tumour microenvironment, extracellular matrix, 2-methoxyestradiol, novel 2-methoxyestradiol derivatives, microscopy, cancer, breast cancer, drug discovery

PEER REVIEWED RESEARCH OUTPUTS

Oral Presentations

- Faculty of Health Sciences symposium – "Faculty Day 2015" *(University of Pretoria, 18 Aug 2015).* Jurgens, T., Joubert, A.M., van den Bout, I. **Using a new 3D cell culture model to analyse the effects of novel estradiol analogues on triple negative breast cancer under physiological conditions** (2015).
- The 43rd Annual Physiology Society of Southern Africa (PSSA) Conference *(Parys, 6-9 Sept 2015).* Jurgens, T., Joubert, A.M., van den Bout, I. **Using a new 3D cell culture model to analyse the effects of novel estradiol analogues on triple negative breast cancer under physiological conditions** (2015).
- Faculty of Health Sciences symposium – "Faculty Day 2016" *(University of Pretoria, 24 Aug 2016).* Jurgens, T., Joubert, A.M., van den Bout, I. **Determination of the effects of novel estradiol analogues on triple negative cancer grown under hypoxic conditions** (2016).
- The 54th Annual Microscopy Society of South Africa (MSSA) Conference *(Port-Elizabeth, 5-8 Dec 2016).* Jurgens, T., Joubert, A.M., van den Bout, I. **Using spheroids to analyse the effects of novel estradiol analogues on triple negative breast cancer** (2015).
- Faculty of Health Sciences symposium – "Faculty Day 2017" *(University of Pretoria, 7 Sep 2017).* Jurgens, T., Joubert, A.M., van den Bout, I. **Using 3D Spheroids as a compound testing platform for cancer drug development** (2017).
- The 45th Physiology Society of Southern Africa (PSSA) Conference *(University of Pretoria, 29 Aug 2017).* Jurgens, T., Botes, M., Joubert, A.M., van den Bout, I. **Using 3D Spheroids as a compound testing platform for cancer drug development** (2017).
- The 55th Annual Microscopy Society of South Africa (MSSA) Conference. *(Bela-Bela, Limpopo, 4-7 Dec 2017).* Jurgens, T., Botes, M., Joubert, A.M., van den Bout, I. **Using 3D Spheroids as a compound testing platform for cancer drug development** (2017).

Poster Presentations

- The 53rd Annual Microscopy Society of South Africa (MSSA) Conference. *(Pretoria, 29 Nov – 4 Dec 2015).* Jurgens, T., Joubert, A.M., van den Bout, I. **Using 3D Spheroids to analyse the effects of novel estradiol analogues on breast cancer** (2015).
- EACR-AACR-SIC Special Conference 2017: The Challenges of Optimising Immuno and Targeted Therapies: From Cancer Biology to the Clinic. *(Florence, Italy, 22-27 June 2017).* Jurgens, T., Joubert, A.M., van den Bout, I. **Using 3D Spheroids to analyse the effects of novel estradiol analogues on breast cancer** (2017).

Publications

- Jurgens, T., Botes, M., Riahi, Z., Visagie, M., Janse van Vuuren, R., Joubert, A.M., van den Bout, I. **A novel non-sulphamoylated 2-methoxyestradiol derivative causes detachment of breast cancer cells by rapid disassembly of focal adhesions**. *Cancer Cell international.* **18**, 188 (2018)
- Janse van Vuuren, R., Botes, M., Jurgens, T., Joubert, A.M., van den Bout, I. **Novel non-sulphamoylated 2-methoxyestradiol derivative inhibits breast cancer migration by disrupting microtubule turnover and organization.** *Cancer Cell international.* **19:1** (2019)

ACKNOWLEDGEMENTS

The work presented in this thesis would not have been possible without the financial support from the National Research Foundation of South Africa and the German Academic Exchange Service (Deutscher Akademischer Austauschdienst - DAAD), the Cancer Association of South Africa, the Medical Research Council of South Africa, the Ernst and Ethel Eriksen Trust, and the School of Medicine Research Committee of the University of Pretoria. I will forever be grateful for the opportunities given to me during my post graduate years.

Firstly, I would like to express my sincere gratitude to my supervisor, Dr Iman van den Bout, for the continuous support and guidance during every stage of my PhD research. For his patience, encouragement, motivation, and knowledge. Thank you for the final push, without you there would be no thesis. I will forever be indebted to you, and I appreciate how much work you put into your first PhD student. I can only hope that I have made you proud and managed to give you several grey hairs in the process. A special thanks goes to my lab siblings Rustelle Janse Van Vuuren (middle child) and Mandie Botes (little one) who completed our little research family. Thank you for the insightful conversations and late nights in the lab. Thank you for the endless jokes and fun, you kept me sane.

I am also incredibly grateful to my co-supervisor and head of department, Prof Annie Joubert, for providing me with a space in her lab for my research. I have appreciated all her many insightful comments, constant support, and words of encouragement over the years. Thank you to all the post docs and students who formed part of the physiology department and the cancer biology lab, you made me feel at home and provided many hours of guidance.

My sincere thanks also go to Prof Robert Miller, Dr Claire Newton, Dr Ross Anderson and all my lab mates at the Centre of Neuroendocrinology. Thank you for giving me access to the laboratory and research facilities and making me feel part of the group. You are an incredible group of researchers and it was a privilege to learn from you.

On a more personal note, I would like to thank all the friends that have pulled me through my university days and pushed me right to the finish line, in particular I would like to thank Sam Beckley for being a PhD trooper with me and always being there to listen. No matter which way our paths go they always seem to cross and for that I am grateful.

To my two best friends, the two Sam's who make me whole. Page and Waterworth, it is an honour to have you both in my life and I could never have made it this far without your unfailing love and support. Thank you for dragging me out the dark and into the light. You are both incredible humans and I cannot wait for all the adventures we will have together in the future.

To my incredibly patient and supportive husband, Scott. You stuck with me from undergrad to PhD, you supported every decision I made, and you never once complained. You continually raise me up to reach for the stars and help me achieve all my goals. Without you believing in me I would never have made it this far; you earned this degree right next to me. Thank you for the gentle pushes of encouragement, all the late nights and early mornings, and above all thank you for being my best friend, I owe you everything.

Finally, my deep and sincere gratitude goes to my parents, my brother, and my entire extended family for their unparalleled love, help, and support. In particular, I will be forever grateful to my parents for giving me the opportunities and experiences that have made me who I am. You have never once doubted me, you have picked me up when I was down and supported me in every single one of my adventures. You made me who I am today, and I love you with my whole heart. This journey would not have been possible without you, I dedicate this thesis to you.

TABLE OF CONTENTS

ETHICAL CLEARANCE

Ethical clearance for this project was obtained by The Faculty of Health Sciences Research Ethics Committee, University of Pretoria. Ethics reference number: 51/2016 (Appendix III, IV, and V).

LIST OF FIGURES

LIST OF TABLES

LIST OF ABBREVIATIONS

2D	Two-dimensional
2ME	2-Methoxyestradiol
2n	Diploid
3D	Three-dimensional
4n	Tetraploid
ANOVA	Analysis of variance
Blc-2	B-cell lymphoma 2
BSA	Bovine serum albumin
BT-20	Breast Tumour-20
Ca^{2+}	Calcium
$CaCl_2$	Calcium chloride
CAIX	Carbonic anhydrase IX
CAM	Cell adhesion molecule
CO_2	Carbon dioxide
ddH_2O	Double distilled water
DAPI	4',6-Diamidino-2-phenylindole
DMEM	Dulbecco's Eagle's minimal essential medium
DMSO	Dimethyl sulfoxide
DNA	Deoxyribonucleic acid
ECM	Extracellular matrix
ECL	Enhanced chemiluminescence
EE-15-one	2-Ethyl-estra-1,3,5(10),15-tetraen-3-ol-17-one
EE-one	2-Ethylestrone
EDTA	Ethylenediaminetetraacetic acid
EGTA	Ethylene glycol-bis (β-aminoethyl ether)-N,N,N',N'-tetra acetic acid
EGF	Epidermal Growth Factor
EMT	Epithelial to Mesenchymal Transition
ER	Oestrogen receptor

ERK	Extracellular signal-regulating kinase
ESE-15-one	2-Ethyl-3-O-sulfamoyl-estra-1,3,5(10),15-tetraen-3-ol-17-one
ESE-one	2-Ethyl-13-methyl-17-oxo-7,8,9,11,12,13,14,15,16,17-decahydro-6-cyclopenta[a]phenanthrane-3 sulfamate
FAK	Focal adhesion kinase
FCS	Fetal calf serum
FDA	Fluorescein diacetate
FITC	Fluorescein isothiocyanate
GFP	Green fluorescent protein
HEK293FT	Human embryonic kidney 293T
HER2	Human epidermal growth factor receptor 2
HIF-1α	Hypoxia inducible transcription factor alpha
HRP	Horse radish peroxidase
LDS	Lithium dodecyl sulfate
Mg^{2+}	Magnesium
MAPK	Mitogen-activated protein kinase
MCF-7	Michigan Cancer Foundation 7
MDA-MB-231	M.D. Anderson-metastatic breast-231
mL	Millilitre
mM	Millimolar
nM	Nanomolar
ns	Not statistically significant
O_2	Oxygen
PBS	Phosphate-buffered saline
PEI	Polyethyleneimine
PI	Propidium Iodide
PR	Progesterone receptors
SAC	Spindle assembly checkpoint
SD	Standard deviation (±)

SDS	Sodium dodecyl sulfate
SDS-PAGE	Sodium dodecyl sulfate polyacrylamide gel electrophoresis
S.E.M	Standard error of the mean
TNBC	Triple negative human breast cancers
v/v	Volume per volume
VEGF	Vascular endothelial growth factor
w/v	Weight per volume
µg	Microgram
µM	Micromolar

CHAPTER 1

INTRODUCTION

1 INTRODUCTION

1.1 CANCER

1.1.1 Background and introduction to cancer

Uncontrolled growth induced by genetic mutations in proto-oncogenes and tumour suppressors is the first step towards the formation of a tumour.[1–3] Most mutated genes affect signal transduction pathways that normally monitor and regulate cell cycle progression and cell survival, while other mutations affect processes such as motility. [1]

The characteristics that most cancers have in common and the processes that are altered have been summarised previously by Hanahan and Weinberg in 2000 and further updated in a follow up publication in 2011.[2,4] The traits affected in cancer listed by Hanahan and Weinberg are: (1) programmed cell death and evasion of apoptosis, (2) growth signals specifically supplied by the tumour, (3) lack of anti-growth signals from surrounding cells in the microenvironment, (4) the induction of angiogenesis to provide a steady supply of oxygen and nutrients to the cancer cells that make up the tumour, (5) unlimited proliferative ability and cell immortality, (6) metastatic capabilities including migration and invasion, (7) deregulation and modifications to the cellular metabolism, such as aerobic glycolysis, to support cell growth, (8) avoidance of destruction attempts from the immune system, (9) a mutated genome causing genetic instability within cells, and (10) tumour-promoting inflammation.[2,4]

All these traits have the potential to cause changes in homeostasis individually, but more importantly, these traits are more powerful in combination. It has been shown that many of the characteristics of cancer cells are regulated or influenced by biochemical and biomechanical signals from the tumour microenvironment, especially the extracellular matrix (ECM), which is continuously evolving throughout the process of malignancy.[2,5] The process of metastasis is complex and involves several contributing factors, but without the signalling, structure, and scaffolding of the components of the ECM within the tumour microenvironment cancer cells would be unable to migrate to and invade into the blood supply produced by the tumour to disseminate and move around the body spreading to other organs[1,6,7]. The final

steps in metastasis are extravasation, where cells leave the bloodstream, and colonisation, where these cells take up residence elsewhere in the body to form a secondary tumour. It is these secondary tumours that form in vital organs that often cause high rates of cancer mortality and not the primary tumours.[6,8,9] Fortunately, as tumour cells remain similar to the cells of the organ that they originate from many tumour cells, once disseminated, will not survive in the circulation or will remain dormant in the secondary organ they metastasised to. However, a small proportion of tumour cells obtain additional mutations that give them the ability to survive in the hostile environment of the distant organ and to proliferate there, overwhelming the organ itself.[9,10]

Due to the high genetic instability of cancer cells, many subpopulations originate within a tumour in response to altering environmental cues which can include specific therapeutic interventions. This characteristic of tumour population dynamics makes drug discovery difficult. Since specific therapeutic interventions can lead to the expansion of drug resistant subpopulations, new and innovative ways to combat tumour growth need to be found.[11–13] Strategies such as combination therapy to compensate for drug resistant subpopulation expansion, as well as treatments harnessing the body's cancer defence system, have a chance of circumventing the evolutionary advantage of tumours.[11–13]

1.1.2 Cancer prevalence

In 2014 the World Health Organization released a world cancer report stating that there was 8.2 million cancer related deaths in 2012.[14] The updated world cancer report released in 2020 noted that this number had increased to 9.6 million deaths in 2018, making cancer the second leading cause of mortality in the world.[14,15] The 2014 report also revealed that 14 million new cases were reported in 2012 and an additional 32.6 million people had been diagnosed in the 5 years previous to the report, who were living with cancer at the time.[14,16] In 2018 this number had increased to 18.1 million new cases worldwide.[15]

There has been an increase of 19-23% in survival rates over the past few decades. However, while this is a positive statistic, it is cancer type specific with some cancers such as pancreatic cancer still without any improved treatment options. It has also been predicted that new cases will increase to 27 million new cases by 2040. This may indicate that even though treatments may improve, cancer burdens will continue to increase.[15,16] Survival rates vary significantly across cancer types with lung cancer having the lowest survival rates closely followed by liver cancer. Cancers like breast, colorectal, and prostate cancer have higher survival rates when detected early. However, this depends on age and geographical location.[15]

Breast cancer represents 12% of all newly diagnosed cancers throughout the world, ranking it as the second most occurring cancer in the world after lung cancer, with 1.7 million new cases in 2012, and 2.1 million new cases in 2018.[15,16] It is the most commonly diagnosed cancer in women accounting for 25% of all cancer cases and is the leading cause for cancer mortality in women with over 520 000 deaths in 2012 and 670 000 deaths in 2018.[14,15] Breast cancer, like most other cancers, had seen a decrease in mortality over the past decade, but this trend seems to be reversing in recent years.[16,17]

According to statistics released in South Africa in the National Cancer Registry in 2014, southern African women have a 1 in 9 lifetime risk of being diagnosed with some form of cancer and a 1 in 27 chance of that cancer being found in the breast. Breast cancer accounts for approximately 21.78% of all cancers that are found in South African women.[18] Approximately 60% of breast cancer deaths have been shown to occur in developing countries, and this is believed to be due to 10% of women being diagnosed with breast cancer where metastasis has already occurred at the time of diagnosis.[16,19,20] If breast cancer is detected in the early stages before the cancer has metastasised then the tumour can often be contained and treated; however that is not always the case in developing countries where clinics and treatment can be in short supply.[18,19]

1.2 BREAST CANCER

1.2.1 Breast cancer classification by the presence of hormone receptors

Breast cancer types are commonly differentiated based on the expression or overexpression of three receptors (Table I). These are oestrogen receptor alpha (ER), progesterone receptor (PR), and human epidermal growth factor receptor 2 (HER2).[21–23] Breast cancer cells expressing these receptors depend on ligand-binding to the receptors to initiate signalling pathways that will allow the cell to survive and proliferate.[21–23]

Table I. Four breast cancer sub-types based on hormonal receptor status[24–26]

Sub-Type	Luminal A	Luminal B	HER2+	Basal-Like/ Triple Negative
Receptor status	ER+ /PR+/HER2-	ER+/PR+/HER2+	ER-/PR-/HER2+	ER-/PR-/HER2-
Prevalence	30-70%	10-20%	5-15%	15-20%
Current Treatment	Chemotherapy Endocrine Therapy	Chemotherapy Endocrine Therapy Immunotherapy	Chemotherapy Immunotherapy	Poor Response Chemotherapy Radiation
Metastases	Bone	Bone, Liver	Bone, Brain, Liver	Lung, Brain, Lymph, Bone

Table I describes four breast cancer sub-types based on receptor status. Luminal A breast cancer is the most prevalent type of breast cancer (30-70%) and is hormone receptor positive (ER+ and PR+) but does not have an amplification of HER2. Luminal A cancers generally have the best prognosis because hormone therapies have been shown to be very effective. Oestrogen binding to ERα can be inhibited with tamoxifen, while aromatase inhibitors reduce the production of steroid hormones including oestrogen, limiting the activation of the receptor and in this way starving the tumour cell of survival and growth promoting signals.[24–28]

Luminal B breast cancers are similar to the Luminal A sub-type in that this cancer also expresses the hormone receptors and therefore can be treated using the same hormone/endocrine therapies as luminal A subtype tumours. This sub-type, which is characterised by overexpressed HER2, only represents 10-20% of diagnosed breast cancers and is a less common

sub-type of breast cancer. However, these tumours are more aggressive than Luminal A tumours which are correlated with the increased HER2 expression. Luminal B cancers are usually treated with Trastuzumab (Herceptin), which is an antibody that targets HER2 thereby inhibiting its ability to bind to its ligand, Epidermal Growth Factor (EGF) resulting in reduced growth. The prognosis with patients with HER2+ cancers is lower than HER2- and this is due to the treatment not being as effective as ER hormone therapies. Breast cancers that are HER2+ have been found to favour liver metastases. HER2 positive breast tumours do not express hormone receptors but do have amplified HER2. This tumour type is quite rare, making up 5-15% of cases. Since there are no hormone receptors, endocrine therapies such as tamoxifen are ineffective but Trastuzumab (Fig. 1) will still be effective against the HER2 receptor. In many cases traditional chemotherapy is also commonly used.[24,27,29,30]

The fourth sub-type of breast cancer is the triple-negative or basal-like type. TNBCs have no expression of the steroid receptors, ER and PR, while also lacking the amplification of the HER2 gene. Since the most common and effective treatments target these receptors in one way or another, TNBC remains problematic with chemotherapy or radiation remaining as the only viable treatment options for patients (Fig. 1).[20–23,31–33] This cancer subtype has a higher rate of metastasis, mostly towards the lungs, but can also be found in the brain, distant lymph nodes, and in the bone.[29,34]

These categories indicate that breast cancer is indeed not one disease but a collection of diseases. Further stratification of tumours has been achieved using gene alteration panels which have helped determine better treatment options and prognosis.

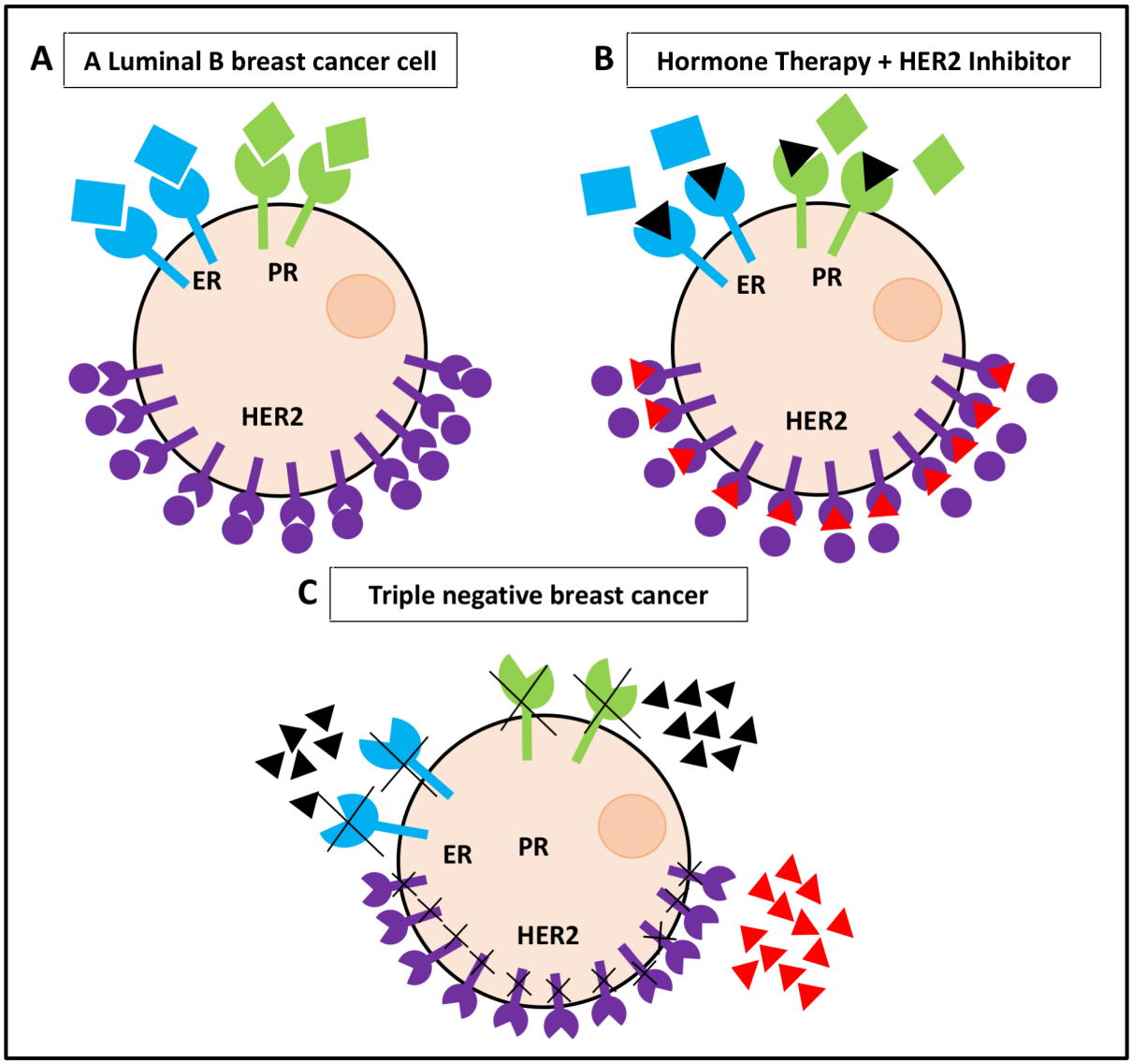

Figure 1. Triple negative breast cancer resistance to hormone therapy

Schematic diagram showing the progression of treatment in different types of breast cancer cells. (A) Luminal B breast cancer cells express oestrogen receptors (blue), progesterone receptors (green), and an amplification of human epidermal growth factor receptor 2 (purple), which causes the breast cancer cells to multiply and grow. (B) Hormone therapy (black) and HER2 inhibitors (red) can be used in most breast cancer cases where the receptors are present on the surface to potentially stop these signals, to slow or halt cell growth, so that surgery can be used to remove the tumour. (C) Triple negative breast cancers do not express these receptors and are thus unaffected by the hormone therapy treatments and HER2 inhibitors, leaving chemotherapy as the only viable option to combat cell growth. (Figure generated by T. Jurgens using Microsoft® PowerPoint for Mac Version (2018).

1.2.2 Breast cancer in Africa

TNBCs makes up 15% of all breast cancers globally and 17-22% of breast cancers in Southern African Women.[16,35] While TNBC accounts for only 22% of breast cancers diagnosed in South African women these tumours progress more rapidly, are more aggressive, and occur more readily in younger women.[35,36] Without improved therapies, specifically targeting TNBC tumours, the mortality rate among premenopausal breast cancer patients will continue to remain high.

Of particular interest is the poor prognosis of breast cancer (especially TNBC) patients in Africa, where survival rates do not exceed 60%. The high mortality rates are often attributed to the lack of access to treatment options, especially in rural towns throughout Africa. A compounding issue is the lack of availability of oncology specialists and current ground-breaking treatments. Without access to radiotherapy, surgery, and cancer drugs, the outlook is bleak. This varies throughout the continent, and there have been strides to improve the situation, but as it currently stands in many less developed areas of the world cancer is identified later in life or too late in the progression of the disease, leading to the higher mortality rates.[20,35,37]

Unfortunately, these are not the only issues that African women face with regards to an increase in mortality rates from breast cancer. It has been shown in several different studies that women of African descent have a genetic predisposition to BRCA-1 mutation related cancers, which have been shown to be more aggressive with low prognosis.[35,36,38] There is currently a drive to obtain more information regarding South African women; however, this is a slow process, and cancer research often takes a backseat to bigger issues that the country faces like HIV infection rates and poverty.[36]

1.3 TUMOUR BIOLOGY

1.3.1 Cell adhesion of tumour cells in primary epithelial tumours and during metastasis

Tumours are a mixture of different subpopulations of cancerous cells and associated non-cancerous cells including fibroblasts, endothelial cells, and immune cells. These associated cells are essential in the survival of the tumour as they provide the supply of oxygen and nutrients, growth factors and hormones, and assist in remodelling the local extracellular matrix (ECM). Such cells are attracted to the tumour through the expression of attractants by the tumour.[39,40] The regulation of the ECM plays an integral part in the survival of tumour cells, and the promotion of motility of tumour cells and can therefore play a role in metastasis. However, it is important to note that many tumour cells within a carcinoma will attach to one another via cell-cell adhesion structures.[40,41]

The make-up of the ECM is very versatile and depends on which organ system it is a part of, but the ECM always has the following primary components: collagen, proteoglycans, laminin, and fibronectin.[42] The ECM typically supports tissue architecture ensuring the correct orientation and positioning of cells so that they can function as needed, at the same time these connections to cells provide activation sites for signal transduction and migration of cells.[5,8,40,41] In cancerous conditions the ECM is frequently altered, and this leads to changes in the communication between the microenvironment and the cells within the tumour. These changes cause an increase in cell migration, increased growth via a change in growth factor signalling pathways, and an invasion of the basement membrane.[30–32]

1.3.2 Cell adhesion molecules (CAMs) important for the tumour progression

As mentioned above, the ECM plays a vital role in cancer progression via cell migration and metastasis. Cells use cell adhesion molecules (CAMs) to attach and interact with neighbouring cells or the ECM. CAMs are not only important for adhesion but through their engagement with essential ligands, they can regulate many cellular functions, including cell growth and survival.

When these regulatory signals are lost or become obsolete uncontrolled growth and metastasis can occur. [6,41,43,44]

CAMs can be categorised into four groups: (1) the integrin family consisting of beta (ß) domains which bind to different alpha (α) subunits, (2) cadherins which are calcium dependent transmembrane glycoproteins, (3) selectins or single chain transmembrane glycoproteins that bind to sugar and carbohydrate molecules, and (4) the immunoglobulin (Ig) superfamily containing either variable or constant IgG domains which includes antibodies and many different types of receptors.[45,46]

The schematic in Figure 2 describes two of the adhesion interactions epithelial cells can establish to form discrete tissues. The integrin heterodimers consist of α and ß subunits expressed from different genes (light and dark green subunits, Fig. 2). In humans 18 α subunits can be found, with only 8 ß subunits, these subunits form up to 24 different heterodimers. The ß subunits are able to bind to multiple α subunits allowing the integrin to bind to several ligands.[47,48] Each integrin molecule has a 'head' and two 'tail' structure, where the large head holds all the ligand binding sites and the tails penetrates the cytoplasm.

These integrin heterodimers span the cell membrane attaching each cell to the ECM in both static and soluble form (purple in Fig. 2). The integrins bind to several different ligands, and this binding will depend on the type of subunits that constitutes the integrin.[49–51] Binding of some integrins occurs through the recognition of the RGD sequence (and other ligand-specific amino acid sequences) present on ligands such as fibronectin. Integrins mediate the physical interaction between the intracellular actin cytoskeleton and the ECM, acting as dynamic anchors for the generation of tension that is needed to regulate cell shape. This involves the regulation of the assembly of protein complexes required for cell adhesion and regulating the signalling pathways (e.g. MAPK/ERK) and recruiting focal adhesion kinases (FAK) needed to control these complexes.[50–53] Integrin expression can determine the behaviour of cells. For instance, expression of α6ß4 allows the formation of hemidesmosomes which are found in the

basal layer of stratified epithelia anchoring the cells to the basal lamina. In contrast, expression of α3ß1 binding to fibronectin allows fibroblast binding and migration within the stroma.[54,55] Tumour cells need to be able to change their integrin expression profile to be successful at invading stroma from the epithelial niche the originated from.[45,55,56]

Cadherins, on the other hand (blue in Fig. 2) are single-pass transmembrane glycoproteins that form cis homodimers. These molecules then form trans-bonds to the same cadherin type on a neighbouring cell (Fig. 2). The majority of the structure of cadherin is extracellular and contains 5 tandem repeats which contain binding sites for calcium. The rest of the cadherin molecule consists of a small cytoplasmic tail, which binds to catenin (ß catenin and p120 catenin), and finally a transmembrane section that connects these two sections. Proteins like ß catenin attach to cadherins and link to the actin cytoskeleton similarly to integrins to mediate cell shape.[57–61]

There are many groups of cadherin, all of which have differing locations and functions, but overall cadherins are found in adherens junctions connecting cells to each other. Cadherins are involved in several calcium dependent processes, including adhesion, tension, protein signalling, mechanical cytoskeletal scaffolding, while cadherin expression is regulated during the process of epithelial to mesenchymal transition (EMT).[58] This process allows for the switching of epithelial cells to a more fibroblast-like morphology allowing for cell migration. E-cadherin, which is the adhesive protein in epithelial cells is downregulated after the methylation of cadherin promotors while N-cadherin expression is upregulated. This switch pre-empts the morphology changes observed during EMT. In tumourigenesis, EMT is an essential step in the switch to metastatically competent cells by increasing cell migration and invasion.[57,58]

Many of the signalling pathways and cell interactions facilitated by integrins and cadherins overlap as both cell adhesion molecules have a variety of functions. There is an adhesive network crosstalk that connects all the adhesion molecules within the tumour

microenvironment. It has also been shown that integrin moderated signalling pathways govern many cell to cell and cell to ECM interactions, including those of cadherin.[46,62] These processes and interactions indicate the vital role that the tumour microenvironment and specifically the ECM plays in tumour progression.

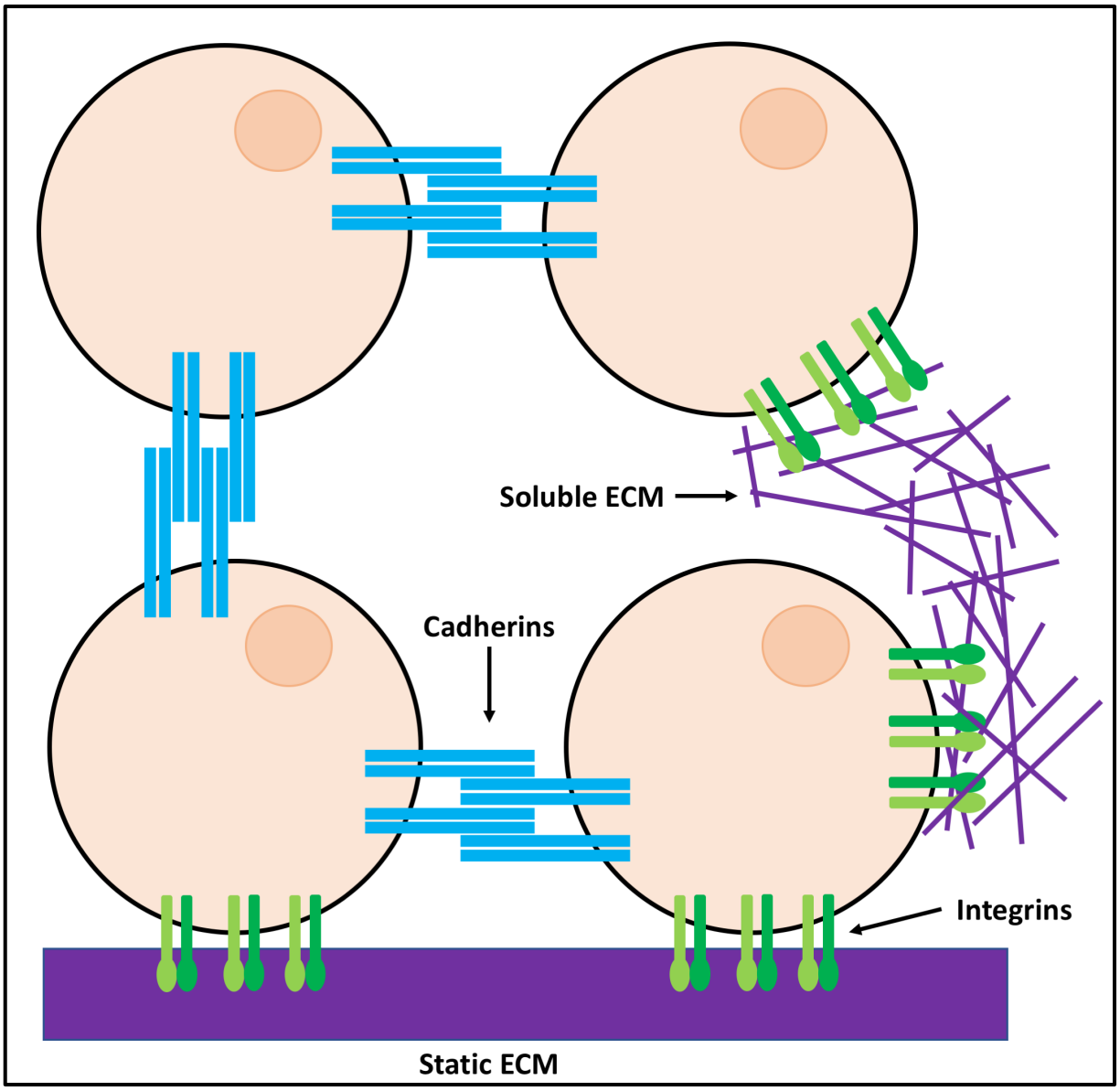

Figure 2. Cell adhesion molecules for the interactions between cells, and between cells and the extracellular matrix.

Schematic diagram illustrating the cell adhesion molecules involved in cellular interactions. Integrins (green) bind and interact with several components of the extracellular matrix (purple), while cadherins (part of adherens junctions) bind cells to neighbouring cells by connecting to fellow cadherins (blue). (Figure generated by T. Jurgens using Microsoft® PowerPoint for Mac (2018). Adapted from Wary, 2005)

1.3.3 Oxygen gradients in tumours

Cells grown in culture are typically exposed to 21% oxygen which is called normoxia. This is a misnomer as oxygen levels in most normal tissues range between 3% and 7.4% while it is lower in most tumours between 0.3% and 4.2%.[63] This reduction in oxygen levels in tumours is mostly a result of delayed innervation by the vasculature.[64,65] Along with this lack of vasculature, tumour blood flow is often lower, and oxygen is utilised at a quicker rate. This lack of adequate oxygen triggers specific gene expression profiles in cells which allow them to withstand the effects of a deprivation of oxygen, known as hypoxia.[66]

Cells (normal and cancerous) respond to hypoxia by upregulating the expression of hypoxia inducible factor 1 – alpha (HIF-1α), which in turn changes several processes in the cell, including metabolic pathways. This allows the cells to survive in a hypoxic environment. For example, vascular endothelial growth factor (VEGF) is activated, stimulating endothelial cell division and vasculature formation. This process is proangiogenic and serves to increase blood flow to the tumour. Other genes upregulated by HIF-1α include carbonic anhydrase IX (CAIX).[67–69] A number of these genes are involved in the upregulation of glycolysis as cells need to shift from oxidative phosphorylation to glycolysis to generate ATP in an oxygen deprived environment. Pyruvate is diverted towards lactate and away from oxidative phosphorylation, repressing mitochondrial respiration. This process aims to protect cells from oxidative damage and make respiration more efficient.[70] This movement towards glycolysis also creates an acidic environment. CAIX, a cell surface glycoprotein commonly found to be overexpressed on the cell surface of cancer cells under hypoxic conditions, is essential for regulating the internal pH in normal cells by capturing carbon dioxide (CO_2) and water to break down carbonic acid to protons and bicarbonate ions.[71,72] In this way CAIX regulates the pH of the tumour microenvironment. CAIX is upregulated by the activation of HIF-1α to assist with the acidosis within the tumour microenvironment.

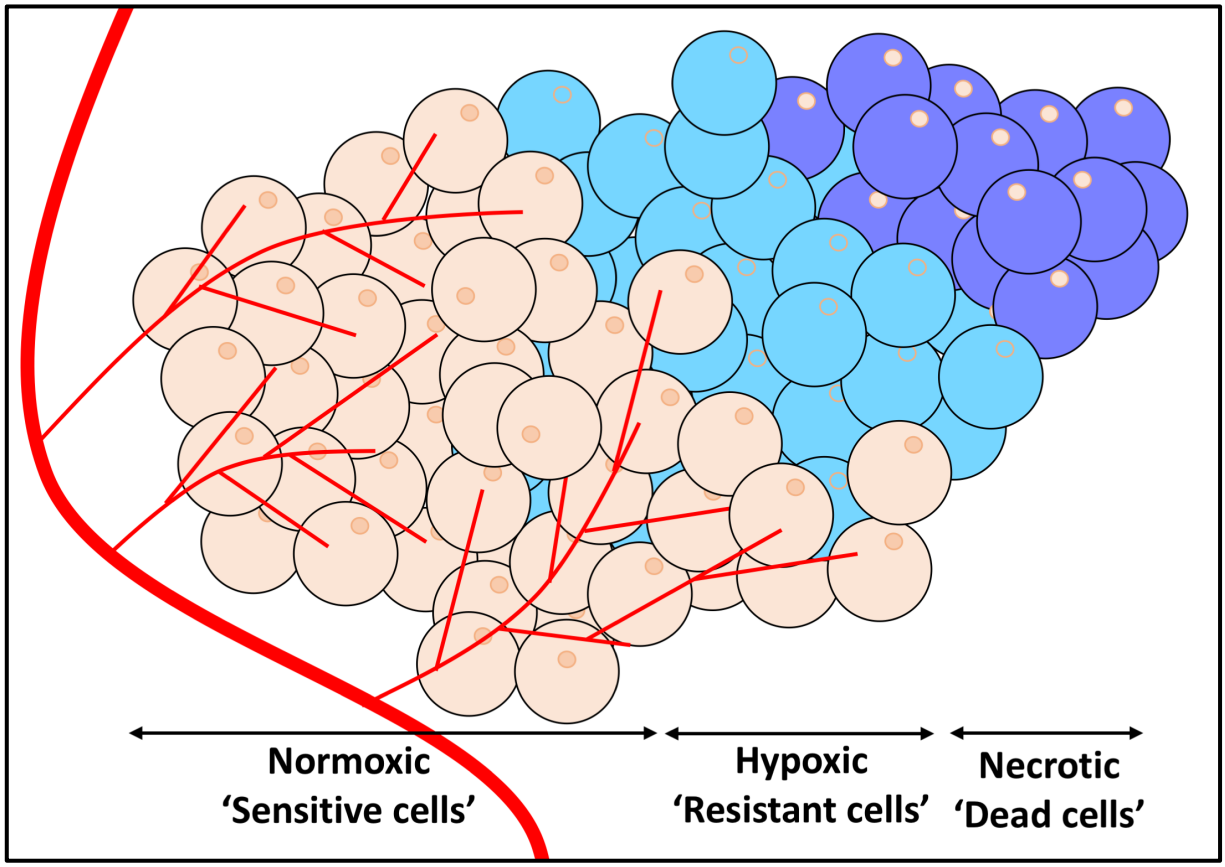

Figure 3. Oxygen levels throughout a solid tumour.

This schematic diagram shows the differing nutrient oxygen levels that are found throughout a solid tumour, with the blood supply depicted as blood vessel in red. The solid tumour contains normoxic cells on the outer edges which have been found to be 'sensitive' to chemotherapeutics (peach cells). There is then a layer of cells that receive minimal nutrients (light blue cells) and can possibly be 'resistant' to drugs due to their hypoxic nature, followed by a small group of cells (purple cells) which are necrotic or 'dead' due to the lack of nutrients (Figure generated by T. Jurgens using Microsoft® PowerPoint for Mac (2018). Adapted from Thomas et al., 2013).

The schematic diagram in Figure 3 depicts the spread of hypoxia throughout a solid tumour as a gradient with high oxygen at the edge and close to the vasculature with low oxygen deeper in the tumour and further away from the vasculature. Three regions can be identified. The cells on the outer edges of the tumour operate under a physoxic (normal physiological oxygen level) environment where sufficient nutrients and oxygen are delivered, and these cells are more sensitive to treatments. These normal cells are based very close to the tumour blood supply (vasculature shown in red, Fig. 3). Cells near the middle of the tumour depicted in light blue in Figure 3 are hypoxic receiving little or no oxygen and have very high expression levels of HIF-1α. There is a gradient of HIF-1α moving towards the middle of a tumour. It is often these

hypoxic cells that are resistant to radiotherapy due to a lack of oxygen-free radicals needed for deoxyribonucleic acid (DNA) damage and resistant to chemotherapy due to the adaptation of cells towards hypoxia as well as the diffusion rate and distance of the cells from the outside. In areas far removed from the vasculature in the centre of the tumour, here in Figure 3 depicted by purple cells, the environment is so harsh that cells cannot survive at all and become necrotic. Here there are no nutrients and a severe lack of oxygen causing cells to die (Fig. 3). This combination of hypoxic cells with a necrotic core is often correlated with a poor prognosis in cancer patients.[65,73–75]

1.4 USING THREE-DIMENSIONAL (3D) CULTURING SYSTEMS AS A METHOD TO IMPROVE DRUG DISCOVERY

1.4.1 Overview of the drug discovery process

The drug discovery and development process tends to follow a set pattern. In the last few decades, the advance of automation has allowed increased throughput in initial screening of compounds, but the rest of the pipeline has remained similar for a long time. Drug discovery is preceded by preclinical basic biology identifying proteins that are either often found to be deregulated in cancer or proteins that are essential in pathways that are deregulated in cancer. These proteins, especially if they are enzymes, make what is colloquially known as druggable targets. With the advent of supercomputing and the crystal structures of many proteins *in silico*, drug selection can be performed first or large compound libraries can be screened for suitable lead compounds.[76–78]

In the preclinical stage identifying potential compounds is done using different *in vitro* assays. These assays are performed to determine drug efficacy in inhibiting cancer cell growth. Current cancer research relies predominantly on *in vitro* assays performed using two-dimensional (2D) monolayer cells, which are usually cultured in tissue culture plates or flasks.[79,80] These assays will give an indication of the potential efficacy of the compound against specific tumours.[81,82] However, this system remains greatly artificial and therefore results from such assays do not extrapolate well to *in vivo* success. After several of rounds of modification and testing of lead

compounds a group of final compounds can be further tested in *in vivo* model systems such as rodents.[81,82] It is well known that at this stage a large majority of compounds will be rejected for either having no effect or for causing severe side effects.

Compounds that survive the pre-clinical stages will now enter clinical testing through 4 stages of human trials. This stage of testing is by far the most expensive, time consuming, and laborious part of drug discovery and yet the vast majority of compounds do not successfully pass through these trials. Phase I clinical trials involve testing the drug in healthy individuals on a small scale to determine the optimal dose of the drug being tested. Here the dose of the most efficacious drug with the least side effects will move forward to Phase II clinical trials.[83,84] Phase II and phase III trials are then performed in increasing populations of patients with the disease being treated by the drug to determine safety and efficacy of the drug. During phase III studies the drug is usually compared to existing medications where investigators need to prove that the drug is at least as safe and effective as drugs already on the market.[83] Phase IV clinical trials are performed after a drug has been approved, usually to treat a different disease or population. As of March 2020, there are over 334 421 clinical trials ongoing in 210 countries, 2761 of which are happening in South Africa (www.clinicaltrials.gov).

Reasons for drug failure in these trials include unforeseen side effects in humans and most importantly, low or no efficacy in humans. Thus, a limitation within the development pipeline is the accuracy achieved during screening and preclinical development. The use of cell lines in an environment that is far removed from the *in vivo* condition causes large differences in biology, while the use of animal models also has drawbacks due to different biology's between these models and humans. Research is therefore ongoing to improve the *in vitro* models used in lead compound identification screens to better mimic the *in vivo* environment and biology to improve the prediction strength of screening for compounds with potential anticancer capabilities.[83,85,86]

1.4.2 The use of classical 2D cell culture systems for drug discovery

2D cell culture was first identified as a potential technique to study cell processes in the early 1900s by Harrison, and it very quickly became a standard methodology for drug discovery.[87,88] The first cancer cell used in cell culture were HeLa cells, obtained in 1951 by Gey and colleagues.[88,89] This is a cell line that is still commonly used in the cancer research industry, even though the cells have since mutated and cross contamination has occurred between different cell lines.[90] These methods have since been improved and adapted, cell culture libraries have been developed with established cell lines from various organisms and various cancers that have been carefully categorised and can be used for a variety of different studies.

In initial drug screening, these cancer cell lines are employed in cell proliferation, cell survival, and cell cycle assays to determine if compounds can inhibit these parameters. 2D cell culture has allowed for intensive automation enabling the screening of hundreds of thousands of compounds efficiently. The drawback is that cancer cells do not naturally grow in isolation and in 2D *in vivo* but rather within a three-dimensional (3D), complex environment. Thus, the predictive power of these screens is limited.

While there have been countless advances in science through the utilisation of these 2D cell culture systems, it remains a highly artificial environment where the cells often lose diverse phenotypes and many biomechanical functions including cell differentiation and cell morphology.[81,82] The main issue with growing cells on a surface is that there is a complete lack of tumour microenvironment in 2D cell culture models. This system lacks the architecture and tumour microenvironment found in *in vivo* systems. It has also clearly been shown that the interactions between tumour cells and the tumour microenvironment (discussed above in section 1.3) are vital for many cancer processes including signal transduction, cell migration, and cell proliferation to occur.[11,82,91,92] There is still a place in research for 2D cell culture, however, more advanced methods within the cell culture realm are required for the evolution of the drug discovery industry. These drawbacks cannot be ignored, and cell culture systems need to mimic the situation occurring in real time in the human body.

1.4.3 The biology of 3D cell culture systems and using 3D cell culture as an improved drug discovery tool

The use of 3D cancer cell systems has in the past decade gained popularity among cancer researchers, attempting to bridge the gap between *in vitro* and *in vivo* assays.[82] This 3D system is achieved when cancer cells are grown as a 3D multi-layered entity rather than as 2D monolayers *in* vitro (Fig. 4).[82,93,94]

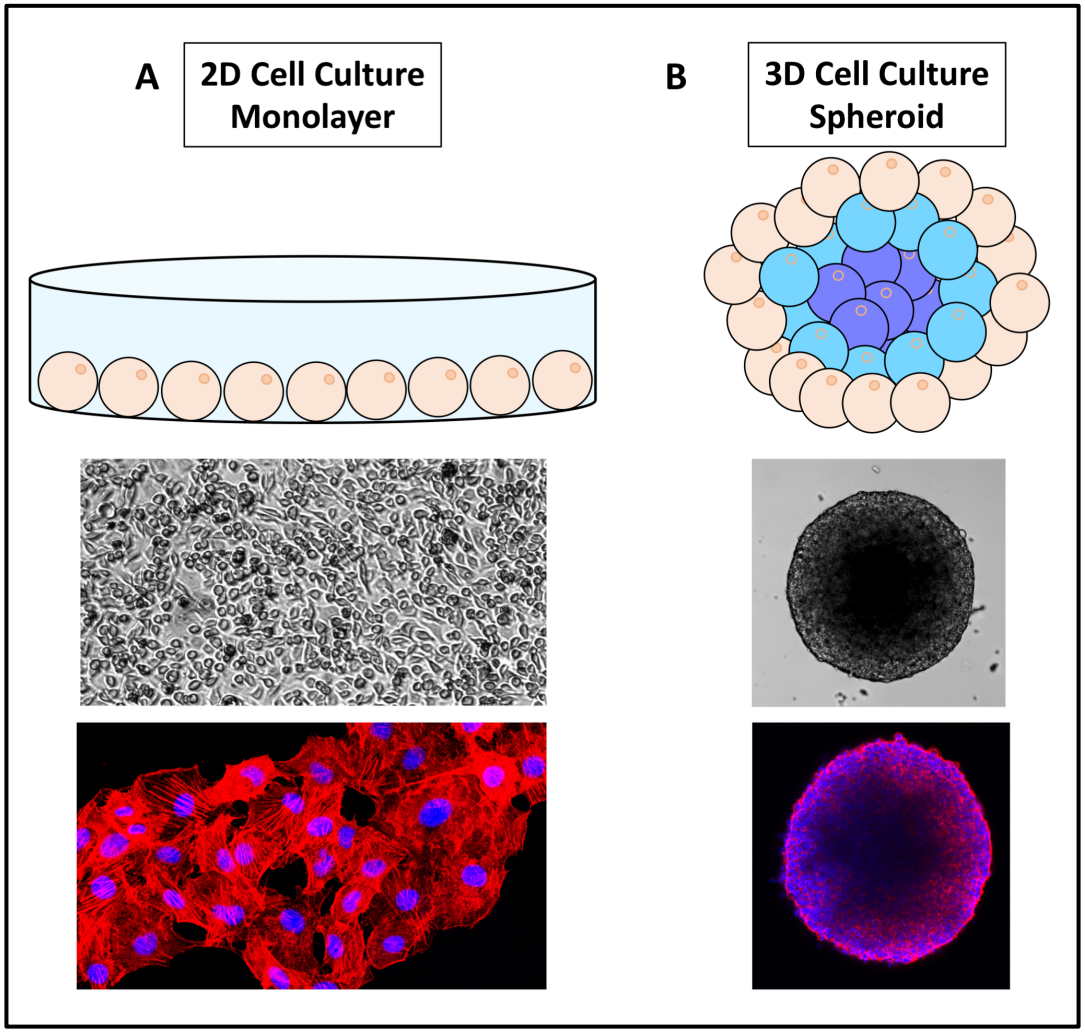

Figure 4. Two cell culture techniques currently used to study the effects of potential therapeutic agents.

Schematic diagrams, light microscopy images, and confocal microscopy images depicting the different cell culture techniques used in drug discovery. (A) 2D cell culture, where the growth of cells in a monolayer is performed using tissue culture treated plastic flasks. This has been the most commonly used technique in cancer research, and (B) cells grown in a spheroid using 3D cell culture, which is becoming more prevalent in drug discovery studies (Figure generated by T. Jurgens using Microsoft® PowerPoint for Mac (2018), light and confocal images were obtained by T. Jurgens using a Zeiss Axiovert CFL40 microscope and a Zeiss LSM 510 Meta confocal microscope respectively).

Figure 4 shows the complexity of a 3D spheroid next to monolayer cell culture within a cell culture dish. Both Figure 4A and 4B describe the different culturing methods in a schematic diagram, displaying the cell architecture in a light microscopy image, and showing the extent of actin cytoskeleton organisation in a confocal microscopy image.

In Figure 4A, the cells are grown as a 2D cell culture monolayer. These cells only interact in a one-dimensional plane with the plastic and directly neighbouring cells. An example of these cells is seen in Figure 4A, where in both the light and confocal microscopy images the cells can be seen interacting with one another in a single plane only. Cells that grow in this manner lack the ECM and 3D organization of *in vivo* tumours and studies have shown that there is only a faint or undetectable expression of ECM proteins.[95,96]

The schematic in Figure 4B, on the other hand, shows how cells aggregate to form a collection of cells as a 3D spheroid, creating an environment where cells interact with neighbouring cells in 3 planes and do not interact with a rigid surface. This methodology of cell culture more closely relates to the multi-layered 3D architecture one expects to find in tumours. The presence of cell-cell junctions (including tight junctions) is vital in physical communications. Cells growing in such close proximity have cell signalling pathways similar those seen in solid tumours. These communication pathways have an effect on cell signalling, cell morphology, and cell proliferation that is different to that of cells grown in monolayer. [82,97,98]

Cells grown in 3D have chemical gradients and hypoxic areas as seen in solid tumours. The internal structures present in a 3D structure of several layers of cells provides the presence of hypoxic and necrotic layers helping to mimic phenomena like chemoresistance. The gene expression of cells in 3D cell culture is more similar to the clinical expression profiles of tumours as well. This is especially important when looking at genes that are overexpressed in certain cancers that cause cells to invade and metastasize throughout the body. [82,94,96]

Overall these are all important aspects of cancer research to consider during drug discovery. The potential for cells grown in a lab to be similar to *in vivo* systems brings the research for drug discovery one step closer to understanding the effects and responses that cancer cells have to the drugs.[82,94,97,98]

1.4.4 3D cell culture systems currently utilised in drug development

To facilitate efficient drug discovery, it is important to use a method that allows for high throughput analysis. In this regard, high throughput includes the ability to generate very similar size and shape spheroids, ease of handling of such spheroids, amenability to automated handling, and reproducible responses to specific inputs. Also, the identification of cell lines that are amenable to spheroid formation is essential. There are several different methods available to induce the formation of spheroids. These include, but are not limited to, using low attachment plates, generating low attachment surfaces with agarose,[45] scaffolding or hydrogels, suspension cultures like bioreactors, magnetic levitation, and the hanging drop method.[11,45,94,99] Many of these methods, while forming reproducible spheroids, are laborious and expensive.[100–102]

Expensive methods make use of devices which continuously move and keep the cells in suspension to prevent adherence, including spinners and bioreactors. While these methods have been shown to produce spheroids on a larger scale, they require equipment that is not always readily available in laboratories and do not produce consistent spheroid sizes. Alternatively, cells can be cultured within a gel substrate like Matrigel, alginate, or collagen. This method provides the cells with a 3D scaffold within which it can form a spheroid. Unfortunately, the components of these gels are often non-defined with batch to batch variation, are expensive, and produce inconsistent spheroids. Although not amenable to high throughput screening, this system is beneficial for directed biological investigation. However, this system is very costly to reproduce, and spheroids are difficult to analyse as they are embedded in the scaffolding. [100–102]

Simpler methods include the hanging drop method and low attachment plates. The hanging drop method is where cells are suspended in a drop of cell culture medium on a culture plate which is inverted, preventing any adhesion from occurring. While this method is very successful in creating consistent spheroids, it still had many drawbacks including the droplet falling off the plate, treatment with a compound proving to be very difficult, and the length of time cells can be cultured is limited. Creating a zero-attachment environment for cells forcing them to self-adhere using adherens junctions to form 3D spheroids can be done using low attachment round bottomed plates. Unfortunately, these plates can also be very costly. Alternatively using agarose, a relatively inexpensive reagent in a flat tissue culture plate (both usually readily available in cell culture laboratories) also creates a low attachment scenario.[100–102]

Thus, 3D cell culture using agarose was identified as a cheap, reproducible method that we could use to implement in our lab for the formation of spheroids. This methodology was based on a paper published in 2009 by Friedrich and colleagues[94], which described the process of using agarose to coat flat bottomed wells to create this zero-attachment environment. This paper also described the seeding of spheroids, drug treatment, image collection, as well as the calculations to determine the spheroid volume. Several cancer cell lines were analysed, and the size and shape were described.[100,102,103]

1.5 CHEMOTHERAPEUTICS IN THE TREATMENT OF CANCER

1.5.1 Current and classic chemotherapy drugs

Cancer cells are abnormally dividing cells without homeostatic control to limit their proliferative potential.[2,4] Chemotherapy treatments have been used since the 1800s, where physicians were using chemicals like mercury and nitric acid to treat cancers internally and externally.[104–106] Cancer research and treatments have greatly advanced since those days, but the theory behind halting the processes causing cells to rapidly grow still remains. Chemotherapy treatment is a general group of therapies that aim to address the first five traits described by Hanahan and Weinberg: (1) evasion of apoptosis, (2) growth signals from the cancer cells, (3) lack of anti-growth signals from surrounding cells, (4) the induction of

angiogenesis, and (5) unlimited proliferative ability and immortality.[2,4] These treatments use different mechanisms but are all used with the same goal in mind, that of stopping excessive cell growth. Chemotherapy drugs have, over time, been loosely classified into several groups, which often overlap and change, these have been described in Table II below:

Table II: Examples of Chemotherapeutic agents[107–113]

Classification of chemotherapeutic agents	General Mechanism	Examples
Alkylating Agents	Stops cell replication at various cell cycle phases	Cisplatin, carboplatin, and chlorambucil
Plant Alkaloids	Stop cell division during the cell cycle	Taxanes (Paclitaxel) and Vinca alkaloids (Vinblastine)
Antitumour Antibiotics	Affect DNA synthesis or break up DNA strands	Anthracyclines (Doxorubicin) and Chromomycins (Dactinomycin)
Antimetabolites	Mimic components and proteins using in cell mechanism	Folic acid antagonists (Methotrexate) and Pyrimidine antagonists (5-Fluorouracil and Gemcitabine)
Topoisomerase Inhibitors	Inhibit the correct manipulation of the DNA structure	Irinotecan (Topoisomerase I Inhibitor) and Amacrine (Topoisomerase II Inhibitor)
Miscellaneous	Specific to the drug	RNA reductase (Hydroxyurea), Enzymes (Asparaginase) and Retinoids (Bexarotene)

Unfortunately, as these treatments target fast growing cells, this means that a significant side effect of these is their effect on normal cells found in the body that by their nature are fast growing. These cells include blood cells and hair follicles. While chemotherapy may be effective in killing cancer cells, the side effects experienced by patients are often severe and include immunosuppression, hair loss, organ damage, and gastro-intestinal distress.[114–116] Much research is currently ongoing to adapt or modify known chemotherapeutics to be more precise and prevent the type of side effects described.

1.5.2 Antimitotic agents and the mitotic spindle

Cell division is dependent on the separation of all chromosomes in an orderly fashion to have an exact copy of the genome in each half of the dividing cell before the cell itself is divided during cytokinesis. This process of mitosis is a complex, multistep program with several checkpoints. During the cell cycle cells remain in interphase for the majority of time during the two growth phases and the synthesis phase. Cells respond to growth factors that initiate a proliferative pathway to become ready for cell division by synthesising mRNAs and proteins necessary for mitosis in the G_1 phase, once the cell is ready the S phase takes place where duplication of the chromosomes occurs, and DNA within the cell becomes tetraploid (4n). These cells rest shortly in the G_2 phase where the DNA replication is checked and monitored, preparing for mitosis, before finally progressing into the Mitosis (M phase), where chromosomes within the cell condense moving through prophase, prometaphase, metaphase, anaphase, and telophase (Figure 5). The chromosomes and cytoplasm are split into two during cytokinesis producing 2 daughter diploid (2n) cells.[113,117]

Antimitotic agents like taxanes will block cell cycle progression during mitosis specifically between metaphase and anaphase where the spindle assembly checkpoint or mitotic checkpoint occurs. This occurs because the compound can stabilise or destabilise the dynamic microtubule network, resulting in a disrupted mitotic spindle causing mitotic arrest (Fig. 5B). During mitosis, the microtubule network, made up of alpha and beta tubulin heterodimers, arranges into the mitotic spindle. This process is needed to generate the spindle fibres that will attach to the chromosomes via the kinetochores to separate the chromatids. A coupling of the kinetochores of each chromosome to the microtubules of the mitotic spindle microtubules occurs allowing the chromosomes to be correctly aligned to ensure even segregation into the two daughter cells.[118,119]

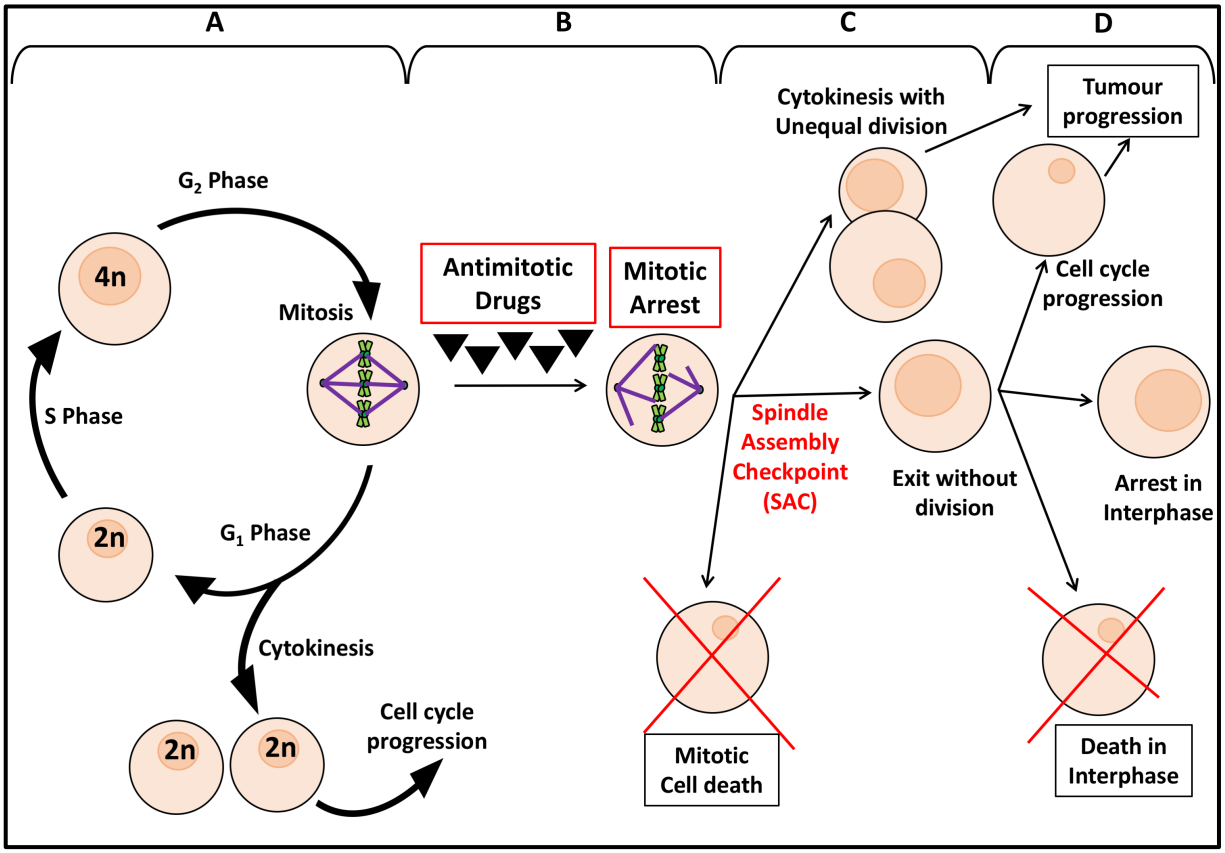

Figure 5. Antimitotic chemotherapeutic agents cause mitotic arrest in cells undergoing mitosis.

(A) Normal cell kinetics include G1 Phase, G2 Phase, S Phase, and Mitosis. (B) Antimitotic drugs cause mitotic arrest, which causes a range of different effects in the hopes to stop the cell cycle and cause cell death (C), this is not always the case and cell can continue where unequal division occurs or cells may exit the cell cycle without any division. (D) Alternatively, once exited without division the cells may join the cell cycle once again increasing the tumour progression, or cells may arrest or die in interphase (Figure generated by T. Jurgens using Microsoft® PowerPoint for Mac (2018). Adapted from Gascoigne et al., 2009; Marzo et al.,2013, and Weaver et al., 2014).

Interference in the integrity or function of the mitotic spindle is closely monitored by cellular sentinels which upon discovery of interference will initiate mitotic arrest and, if unresolved, will lead to apoptosis.[120] This monitoring is called the spindle assembly checkpoint (SAC) (Fig. 5C), several checkpoints take place throughout the cell cycle and specifically during mitosis and thus the SAC is of particular interest as it is used as a target for cancer therapeutics. Vinca alkaloids prevent the formation of the microtubules which destabilises the spindle. These antimitotic agents like vinblastin bind to tubulin during the S Phase inducing microtubule depolarisation.[119–121] Taxanes like paclitaxel, on the other hand, stabilise the microtubules

preventing disassembly. This stops the cell cycle at the G_2-M border preventing the normal function of the mitotic spindles and thus preventing correct orientation of the chromosomes.[118,119]

Chronic activation of the SAC causes the cells to undergo mitotic arrest (Fig. 5B) where the cells are retained in prometaphase leading to eventual apoptosis.[122,123] Some cells will exit mitosis without undergoing cell division, while others will undergo abnormal division (Fig. 5D). While the compounds will effectively arrest a large proportion of cells within a tumour, some cells will adapt by removing the SAC checkpoint and allowing cell division to take place even in poorly aligned or divided cells. This leads to chemoresistance and recurrence of the tumour (Fig. 5D).[117,119,124,125]

1.6 OESTROGEN METABOLITES AND DERIVATIVES AS POTENTIAL ANTIMITOTIC COMPOUNDS

1.6.1 2-Methoxyestradiol (2ME) as an anticancer compound

It has long been postulated that some of the metabolites of oestrogen may be toxic to cells. 2-methoxyestradiol (2ME) is such an endogenous metabolite of the oestrogenic hormone 17β-estradiol that is produced in trace amounts in the human body. 2ME is produced during the metabolism of oestradiol, which is mediated by Cytochrome P450 enzymes. 17β-estradiol is converted into estrone by the process of oxidation. Subsequently, the A-ring of the estrone is then hydroxylated, forming two catechol oestrogens: 2-hydroxyestrone and 4-hydroxyestrone. These metabolites are processed further with one of the reactions being methylation producing 2ME.[126–128]

Countless studies have been performed on 2ME to show that it has antimitotic, antiangiogenic, and pro-apoptotic properties *in vitro* in an array of different cancer types including lung, ovarian, breast, and prostate cancer cell lines, and *in vivo* animal studies on melanoma, breast, and lung cancers. With all this promising data, several phase I and II clinical trials were performed with patients with prostate and breast cancer. However, 2ME did not have an effect

on tumour progression of tumour load, and it was shown to be due to the low bioavailability of 2ME as it was rapidly metabolised to 2-methoxyestrone. This is perhaps not surprising as it is a natural metabolite and thus further metabolism may be expected even though data on this is currently unavailable. This is undesirable in a chemotherapeutic as the compound would be metabolised before it can function correctly.[123,126,129–131]

2ME is recognised as an angiogenesis inhibitor which is thought to occur through the inhibition of HIF-1α and subsequent inhibited VEGF expression. 2ME was also shown to influence anti-apoptotic signalling through the induction of B-cell lymphoma 2 (Blc-2) phosphorylation. 2ME also has anti-mitotic activity in cancer cells through its destabilisation of the mitotic spindle. 2ME is able to bind to the colchicine binding site within the microtubules, preventing polymerisation of tubulin and thus blocking cell division at the G_2/M border of the cell cycle leading to mitotic death.[132–134]

1.6.2 Designing improved 2ME derivatives

As a cancer therapeutic, the rapid hepatic clearance and degradation of 2ME is an undesirable characteristic, but different studies have over the last decade attempted to improve the bioavailability of 2ME. This has been done with the addition of sulfamates, as these can move through the liver bypassing first pass metabolism. Sulfamoyl moieties bind to and inhibit carbonic anhydrases which are present at high levels on the cell surface of erythrocytes. This allows the sulfamoylated compound to bind to these cells and pass through the liver without being absorbed. The most notable derivate is STX140, which has successfully progressed towards clinical trials after exhibiting antiproliferative and antimitotic results *in vitro* and *in vivo*. [135,136]

Several derivatives of 2ME were designed in the cancer biology group at the University of Pretoria with the help of *in silico* design. This was done in the hopes of finding a lead compound that would retain the antimitotic effects of the 2ME molecule through binding to the colchicine binding motif, but attempting to increase the bioavailability through the addition of a sulfamoyl

group to prevent absorption in the liver.[137,138] Different adaptations of 2ME were designed including replacing the 2-methoxy group with an ethyl group to prevent metabolic processing and modifying the D ring to improve the targeting of compound and increase its affinity for the colchicine binding domain of tubulin.[137]

These compounds were tested using 2D cell cultures of different cancer cell lines, including breast, oesophageal, cervical, and epithelial cancer cells. These studies showed that all the sulfamoylated compounds displayed cytostatic characteristics inhibiting cell proliferation while the compounds without a sulfamoyl moiety were no longer able to inhibit cell proliferation.[139–143]

1.6.3 2ME derivatives characteristics

The sulfamoyl moiety added to the oestradiol derivatives have been shown to be potent CAIX inhibitors.[129,138,144] Many cells within a tumour exist in a nutrient poor and low oxygen environment. The cells respond by shifting their metabolism to anaerobic glycolysis which generates lactic acid. Lactic acid and CO_2 generated by glycolysis lower the pH intracellularly, which is detrimental to the cells. Therefore, cells adapt to this environment by overexpressing CA, including CAIX that can convert CO_2 and hydrogen ions and remove it from the cell. [71,145]

In this study, the effects of four 2ME derivatives previously designed and synthesised are compared. These four compounds were chosen as they were closely related to each other allowing the identification of the contribution of specific chemical characteristics of the compounds to their efficacy.[139] 2-Ethyl-estra-1,3,5(10),15-tetraen-3-ol-17-one (EE-15-one) and 2-Ethyl-3-O-sulfamoyl-estra-1,3,5(10),15-tetraen-3-ol-17-one (ESE-15-one) are identical, except for the addition of the sulfamoyl moiety on the 3' position added to improve bioavailability by missing first pass metabolism (Fig. 6A and C, Red circle).[136] Similarly, 2-Ethylestrone (EE-one) and 2-Ethyl-13-methyl-17-oxo-7,8,9,11,12,13,14,15,16,17-decahydro-6cyclopenta[a]phenanthrane-3 sulfamate (ESE-one) also differ by the addition of the sulfamoyl group (Fig. 6B and D, Red circle)[136].

The second modification within this group of compounds is a change at the D ring in EE-15-one and ESE-15-one (Fig. 6A and C, blue box), where both compounds have a double bond present. This alteration was added to improve the affinity of the compounds for the colchicine binding domain.[136] EE-15-one and EE-one retained the original D ring (Fig. 6B and D). EE-15-one and EE-one (Fig. 6A and B) will be compared to ESE-15-one and ESE-one (Fig. 6C and D) to determine if the addition of the double bond is beneficial to the compound. In the same way, the necessity of the sulfamoyl group will be determined by comparing EE-15-one and ESE-15-one (Fig. 6A and C) to the non-sulfamoylated compounds to EE-one and ESE-one (Fig. 6B and D).

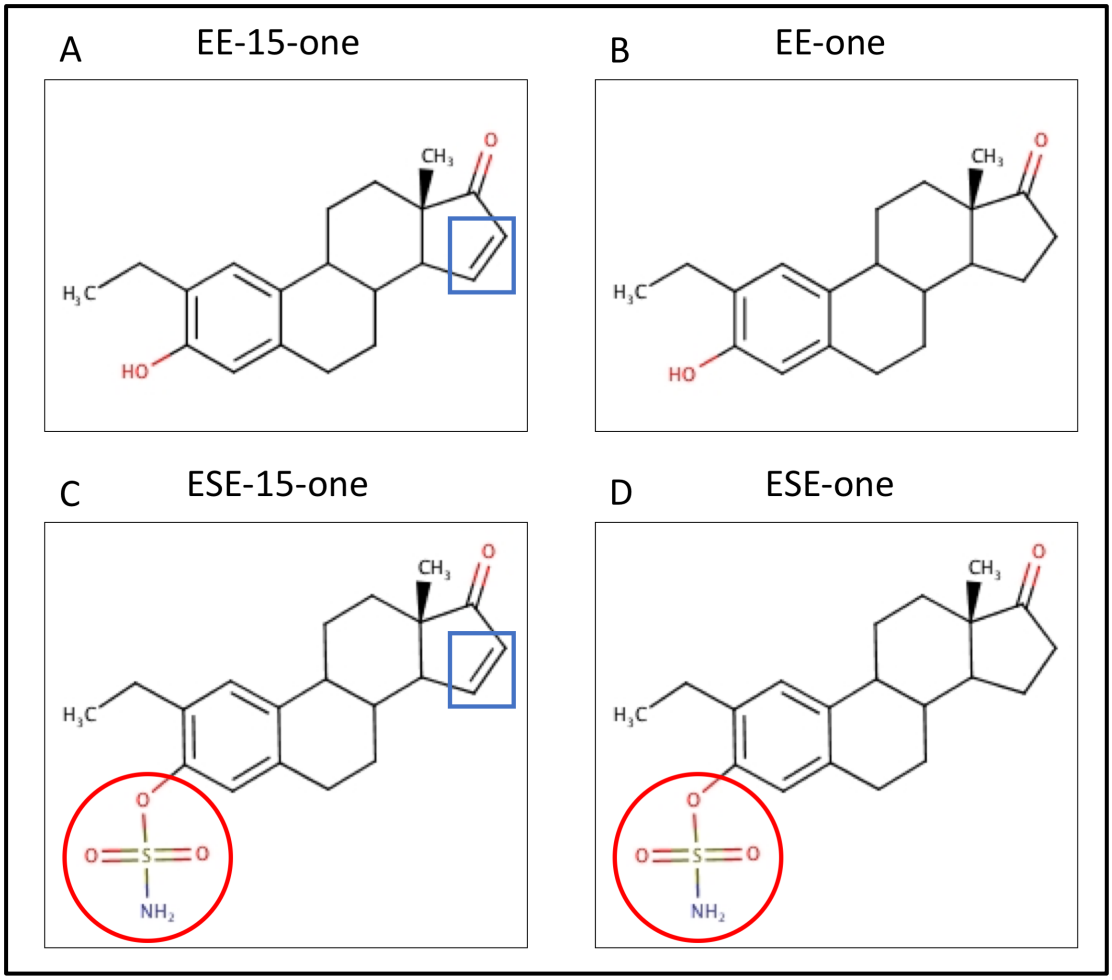

Figure 6. The structural differences of novel oestradiol derivatives used as chemotherapeutics.

Chemical structures of the novel oestradiol derivatives designed by the cancer biology group at the University of Pretoria and synthesised by iThemba Pharmaceuticals (PTY) Ltd. Structures of (A) EE-15-one, (B) EE-one, (C) ESE-15-one, and (D) ESE-one) were created by T. Jurgens using Marvin Sketch version 17.2.27 released on 2007/10/19 (ChemAxon). The blue box indicates the addition of a double bond, and the red circle indicates the addition of a sulfamoyl group.

Initial analysis in breast cancer cells showed that ESE-15-one and 2ME had similar efficacies in inhibiting proliferation and mitosis. Interestingly the paired compound EE-15-one, which does not contain the sulfamoyl moiety, was the only non-sulfamoylated compounds to induce cell loss and did so rapidly and comprehensively. A loss of activity in cancer cell lines was noted in many of the derivates where an ethyl group replaced the 2-methoxy group, but this loss of effect was reversed when the sulfamoyl group was present on the same compounds.[146]

1.7 CONCLUSION

Improved therapies are needed to combat hard-to-treat breast cancer, specifically TNBCs. Chemotherapy is the current treatment used for many cancers. While it has been shown to be successful in an array of different cancer types, the side effects that patients experience due to the impact of the chemotherapy on normal cells can be severe and debilitating. Therefore, there is a continuous drive to identify new compounds that better target cancer cells and have higher efficacy against cancer cells.

Drug discovery and development is undergoing a crisis in that too many drugs are being developed for ever smaller groups of patients with specific cancer types while the pipeline remains the same with enormous time and money investment necessary to get a drug to clinic. A large problem remains the inefficiency of prediction of drug efficacy in preclinical studies. Developing better systems to predict such efficacies will have immediate savings on time and investment as only those compounds with real *in vivo* possibilities are taken further into clinical trials. A significant hurdle is thus developing preclinical models that allow for highly efficient screening of compounds in a setting that recapitulates the cancer environment and structure. Here, the advent of 3D cell culture has started to make a real impact.

In this thesis, we set out to develop an easy, cost-effective 3D cell culture system that can be used to investigate drug efficacy against TNBC cancer cells. We used this system to compare the efficacy of previously developed 2ME derivatives in 2D and 3D culture and will show that there can be significant differences in outcome. We further reveal some of the biology that may be essential to such differences.

1.8 AIMS AND OBJECTIVES

1.8.1 Overall Aim

In this thesis, the aim was to establish a 3D breast cancer spheroid system that can be employed as a cost-effective and time efficient model for the screening of potential anticancer compounds and for the study of cancer cell behaviour in an environment approximating the *in vivo* tumour setting.

1.8.2 Objectives

a) Identify an amenable breast cancer cell line and develop a robust and reproducible *in vitro* 3D breast cancer spheroid model.
b) Assess the ability of the established 3D spheroid system to identify compounds with potential use in inhibiting tumour growth.
c) Investigate the difference in adhesive properties of the established breast cancer spheroids and the corresponding monolayer culture and how this can influence compound efficacy.
d) Ascertain the suitability of this model as a screening tool for potential adverse side-effect of novel anti-malarial compounds.
e) Establish a heterogeneous 3D breast cancer model.

1.9 HYPOTHESIS

The following hypotheses were tested:

- Breast cancer cells can be used to set up a 2D monolayer - 3D spheroid culture model
- Derivatives of the oestrogen metabolite 2-methoxyestradiol are effective in monolayer breast cancer cell cultures and three-dimensional spheroid cultures.
- Three-dimensional spheroid cultures and monolayer cultures make use of different adhesive structures and proteins to adhere.

CHAPTER 2

METHODOLOGY

2 METHODOLOGY

2.1 REAGENTS

M.D. Anderson-metastatic breast-231 (MDA-MB-231 - ATCC: HTB-26), Michigan Cancer Foundation 7 (MCF-7 - ATCC: HTB-22) and breast tumour-20 (BT-20 - ATCC: HTB-19) breast cancer cells were obtained from Cellonex, Separations (Randburg, South Africa [RSA]). Human embryonic kidney 293T (HEK293FT – ATCC PTA-5077) were a kind gift from Dr. Claire Anderson. Dulbecco's modified Eagle's minimal essential medium (DMEM), F-12 Nut Mix (Ham), fetal calf serum (FCS), trypsin- ethylenediaminetetraacetic acid (EDTA), DNA plasmid, lipofectamine, and Opti-MEM Reduced Serum Media were obtained from Gibco, Life Technologies (Johannesburg, RSA). Sterile cell culture flasks, plates, and falcon tubes were obtained from Lasec (Johannesburg, RSA).

Agarose, dimethyl sulphoxide (DMSO), crystal violet, glutaraldehyde, triton X-100, β-mercaptoethanol, colchicine, paclitaxel, propidium iodide (PI); polyethyleneimine (PEI), (P4170), fluorescein diacetate (FDA); (F7378), 4',6-diamidino-2-phenylindole (DAPI); (32670), Fluoromount™ Aqueous Mounting Medium (F4680), Anti-β-Actin antibody (A5441), Phalloidin–Atto 594 (51927), and all general reagents were obtained from Sigma (St. Louis, United States of America [USA]). EE-one, EE-15-one, ESE-15-one, and ESE-one were synthesised and obtained from iThemba Pharmaceuticals (PTY) Ltd. (Modderfontein, RSA). HIF-1α antibody (H-206); (sc-10790) was obtained from Santa Cruz Biotechnology (Texas, USA).

Mini-PROTEAN® TGX Precast Protein Gels (#456-9036), 10x Tris/Glycine/sodium dodecyl sulfate (SDS) running buffer (#1610732), Precision Plus Protein™ All Blue Prestained Proteins Standards Marker (#161-0373), Trans-Blot® Turbo™ Mini PDVF Transfer Packs (#1704156), Clarity™ Western ECL Substrate (#1705061), Goat Anti-rabbit IgG- horseradish peroxidase (HRP) Conjugate (#706515), and Goat Anti-mouse IgG-HRP Conjugate (#1706516) were obtained from Bio-Rad (California, USA). NuPAGE™ LDS Sample Buffer (4x) (NP007) was obtained from Thermo Fisher Scientific (Texas, USA).

2.2 METHODOLOGY

2.2.1 Cell culture

BT-20 TNBC cells, obtained by Lasfargues and Ozzello in 1958, are a tumourigenic, non-metastatic breast cancer cell line from an advanced, infiltrating, duct-cell carcinoma.[147] These cells have previously been used by a few groups for 3D cell culture.[148–150] The MCF-7 cell line is an ER positive, metastatic breast cancer cell line that was isolated from a pleural effusion from a 69-year old patient in the 1970.[151] The metastatic MDA-MB-231 cells were isolated from the pleural effusion of a 51-year-old with a triple negative breast cancer in 1973.[152] Both MDA-MB-231 and MCF-7 cells have previously been used in 3D cell culture.[45,153–155]

MDA-MB-231 and MCF-7 cells were cultured in DMEM enriched with 10% heat-inactivated FCS and 2 mM L-glutamine. BT-20 cells were grown in a 1:1 mix of DMEM and Ham's F12 Nut Mix medium supplemented with 10 % FCS and containing 2 mM L-glutamine, and sodium pyruvate. Cells were maintained in normoxic conditions at 37°C with 21% O_2, and 5% CO_2 in a humidified incubator. For experiments concerning hypoxia cells were moved to a humidified incubator with an oxygen level of 1% at a temperature of 37°C with 5% CO_2 for the duration of the experiment until termination.

2.2.2 Spheroid formation

Cell culture plates (96-well) were coated with 1% (w/v) agarose made up in serum-free growth medium to prevent adherence. Cells (2 x 10^4) were seeded into each well and left to self-assemble over 4 days, as described by Friedrich *et al.*[94] On day 4 the medium was replaced, and spheroids were exposed to 0.5% (v/v) DMSO (vehicle control) or compound for 72 hours. The medium in each well was replaced on day 7 and every second day thereafter. Images were taken on day 4, 7, and 15 prior to feeding at 5x or 10x magnification, using a Zeiss Axiovert CFL40 fluorescent microscope and Zeiss Axiovert MRm monochrome camera (Zeiss; Oberkochen, Germany).

2.2.3 Spheroid volume determination

Spheroid volume was determined using three formulas[156], shape factor (1), spherical volume (2), and shape factor corrected volume (3). Area and perimeter were measured using ImageJ software[157].

$$\boldsymbol{\phi} = \frac{\boldsymbol{\Pi} \times \sqrt{\frac{\boldsymbol{4A}}{\boldsymbol{\Pi}}}}{\boldsymbol{P}} \quad \textbf{... (1)}$$

$$\boldsymbol{V} = \frac{\boldsymbol{4\Pi}}{\boldsymbol{3}} \left(\frac{\boldsymbol{P}}{\boldsymbol{\Pi}}\right)^{\boldsymbol{3}} \quad \textbf{... (2)}$$

$$\boldsymbol{V'} = \boldsymbol{\phi V} \quad \textbf{... (3)}$$

Data is representative of between 10 and 70 independent repeats, depending on the experiment (see figure legends for details). Sample size was determined using continuous outcome equivalence and superiority power calculations,[158,159,160] where an equivalence limit of 10, 95% power, and a 0.025 level of significance were used. The highest standard deviation between the comparing samples was used. Thereafter statistical significance was determined using one-way ANOVA followed by Tukey's multiple comparisons test comparing each treatment to the vehicle control at each time point. This was done using GraphPad Prism version 7.00 for Mac, GraphPad Software, La Jolla California USA, www.graphpad.com.

Table III. Sample size determination from power calculation for comparisons to DMSO treatment.

Compound	Equivalence to DMSO treatment		Superiority to DMSO treatment	
	Day 7	Day 15	Day 7	Day 15
EE-15-one (5 µM)	8	21	1245	341
ESE-15-one (1 µM)	8	21	3	2
ESE-one (1 µM)	19	21	3	2
Paclitaxel (500 nM)	12	21	3	1
Colchicine (500 nM)	10	21	10	2

Table IV. Sample size determined from power calculations for comparison to paclitaxel and colchicine

Compound	Superiority to Paclitaxel treatment		Superiority to Colchicine treatment	
	Day 7	Day 15	Day 7	Day 15
EE-15-one (5 μM)	4	341	14	1
ESE-15-one (1 μM)	1056	1	3	2
ESE-one (1 μM)	783	12	14	128
Paclitaxel (500 nM)			19	11
Colchicine (500 nM)	23	11		

2.2.4 Cell viability

Crystal violet staining was used to determine cell number. The DNA of fixed cells were stained with the triphenylmethane cationic dye, crystal violet, which allows for rapid, accurate, and reproducible quantification of cell numbers. Crystal violet allows for the quantification of cell numbers in monolayer cultures as a function of the absorbance of the dye taken up by the cells.[161]

Cells plated in monolayers were assessed for viability using a crystal violet assay. Cells were seeded into 96-well plates at a density of 1 x 10^4 cells/well (BT-20) or 5 x 10^3 cells/well (MDA-MB-231 and MCF-7) and allowed to adhere overnight. Cells that were exposed to hypoxic conditions were moved to a humidified incubator with an oxygen level of 1% for 7 hours before treatment. Cells were then exposed to a concentration range of each test compound for 72 hours, cells exposed to 0.5% (v/v) DMSO were used as a vehicle control.

Cells were then fixed with 1% glutaraldehyde for 15 minutes at room temperature. Once the glutaraldehyde was discarded the cells were stained with 0.1% (w/v) crystal violet for 30 minutes at room temperature. Wells were washed thoroughly with ddH_2O and allowed to dry. Quantification was performed by solubilising the absorbed dye into a solution of 0.2% (v/v) Triton X-100 in ddH_2O for 30 minutes at room temperature and determining optical density at 570 nm using an EL_x800 Universal Microplate Reader (Bio-Tek Instruments Inc., Vermont, USA). All values were normalised to cells grown in medium only, with no vehicle control or

compound. Experiments were done in three independent repeats and graphs represent the mean with error bars indicating standard error of the mean (s.e.m). One-way ANOVA, followed by Dunnett's multiple comparisons test, comparing each concentration to untreated cells, as well as nonlinear regression analysis to determine IC_{50} was performed using GraphPad Prism version 7.00 for Mac, GraphPad Software, La Jolla California USA, www.graphpad.com.

2.2.5 Live/dead staining

Spheroids exposed to the compounds for 72 hours were collected in a microcentrifuge tube by gravity and the supernatant was removed. Spheroids were washed with phosphate-buffered saline (PBS) and then stained using 8 µg/ml FDA, 20 µg/ml PI, and 2 µg/ml DAPI made up in serum-free medium for 5 minutes in the dark at room temperature. The sample was washed with PBS and visualised using fluorescence microscopy on a Zeiss Axiovert CFL40 fluorescent microscope at 10x magnification (Zeiss; Oberkochen, Germany).

2.2.6 Confocal microscopy

Monolayer cells were seeded on glass coverslips and incubated over- night to attach and spread. Subsequently, cells were exposed to 5 µM EE-15-one or DMSO for different times before they were fixed in 2% (w/v) paraformaldehyde for 20 min, washed with 1× PBS, permeabilised with 0.2% (v/v) triton X-100 for 5 min, and washed with 1× PBS. Coverslips were subsequently blocked with 2% (w/v) bovine serum albumin (BSA) in 1× PBS for 1 h, incubated with primary antibodies against FAK for 1 hat RT. Coverslips were washed once more with 1× PBS, and incubated with the secondary antibodies DAPI, and fluorescently conjugated phalloidin for 1 h at RT. After washing with 1× PBS, coverslips were mounted in mounting fluid. Slides were examined using a Zeiss LSM800 Meta confocal microscope furnished with a 63× magnification oil objective.

Spheroids were grown and exposed to compounds as described above. Several spheroids were carefully moved into a microcentrifuge tube, collected by gravity, and fixed using 4 % paraformaldehyde for 30 minutes. The spheroids were washed with PBS and then

permeabilised with 0.2% Triton X-100 for 15 minutes. Blocking was done using 2 % bovine serum albumin (BSA) in PBS for 1 hour. Spheroids were then stained using fluorescently conjugated phalloidin and DAPI for 2 hours and washed with PBS. Spheroids were mounted on microscope slides with 1 mm silicon borders to avoid compression using mounting fluid and covered with square coverslips. Slides were examined using a 20x magnification objective on a Zeiss LSM 510 Meta confocal microscope (Zeiss; Oberkochen, Germany).

Fluorescence excitation/emission pairs are expressed in each legend as the excitation wavelength/emission wavelength designated nm.

2.2.7 Calcium chelation

Spheroids were seeded and grown for four days and separated into two groups, a test group and a control group. All the spheroids were then exposed to 2 mM ethylene glycol-bis (β-aminoethyl ether)-N,N,N',N'-tetra acetic acid (EGTA) in a 2:1 molar ratio to the available calcium available in the growth medium to chelate the calcium (0.9 mM), for 24 hours. Calcium chloride ($CaCl_2$) was added to the control group in a 2:1 molecular ratio (4 mM) to replace the calcium removed by the EGTA. Light microscopy images were taken on the day the EGTA was added, as well as 24 and 72 hours later at 5x magnification, using a Zeiss Axiovert CFL40 fluorescent microscope and Zeiss Axiovert MRm monochrome camera (Zeiss; Oberkochen, Germany).

BT-20 cells were seeded as a monolayer in 6-well plates at a density of 2.5 x 10^5 cells/well and left to adhere overnight. These cells were treated with EGTA and $CaCl_2$ as above and light microscopy images were obtained before treatment and 24 hours after treatment. Cells treated with EGTA for 24 hours were exposed to 4 hours of excess of $CaCl_2$. Experiments were done in triplicate.

A time study was performed over 6 hours using spheroids treated with EGTA (2 mM). After 3 hours of EGTA exposure $CaCl_2$ was added in intervals of 1 hour. At each time-point the

spheroids were fixed, permeabilised and stained using phalloidin (1:400) and 2 µg/ml DAPI. The spheroids were mounted as described above and visualised using the 20x magnification objective on a Zeiss LSM 510 Meta confocal microscope (Zeiss; Oberkochen, Germany).

2.2.8 Cell Rounding

To quantify the number of cells that round up after expo- sure to the compounds, cells were seeded in 24 well plates (5 × 104/well) and incubated overnight to attach and spread. Cells were exposed to the compounds after having been photographed and were subsequently photographed at indicated timepoints. At least three images were captured per well and three wells per condition were used in each experiment. Photos were taken at 10× magnification using a Zeiss Primovert microscope and a Zeiss Axiocam ERc5s camera (Zeiss, Oberkochen, Germany).

2.2.9 Transfection and infection

HEK293FT cells were seeded to a density of $5x10^5$ cells per 6-well. A mix of 570 ng VSV-G, 1100 ng CMV gag-pol, 2300 pLKO was made in 100 µL of Opti-MEM reduced serum Media, 12.5 µL of PEI was added and incubated at room temperature for 20 minutes. This mixture was then added to cells and left overnight. Medium was replaced with regular DMEM containing Serum. Virus was harvested by removing the medium and passing it through a 0.45 µm filter.

MDA-MB-231 cells were trypsinised and seeded to a density of $2.5x10^5$ cells per well in a 6 well plate and left to adhere and grow confluent overnight. Virus was added to the cells and following day were sorted using flow cytometry to select fluorescent cells. This was performed several times to choose a pure colony.

2.2.10 Co-culture spheroid formation

Fluorescently labelled MDA-MB-231 breast cancer cells were cultured with unlabelled BT-20 in several ratios in a 96-well plate. Briefly, cell suspensions of the two cell lines were added to agarose-coated plates. Cells were incubated for four days, after which each spheroid was be analysed with the Zeiss Axiovert CFL40 fluorescent microscope and Zeiss Axiovert MRm monochrome camera (Zeiss, Oberkochen, Germany) with a 5x magnification. The co-culture was moved to a live imaging container in the Zeiss 510 META confocal laser microscope (Oberkochen, Germany) to determine the effect of the cells over several hours and overnight.

CHAPTER 3

RESULTS

3 RESULTS

3.1 DEVELOPMENT OF A ROBUST AND REPRODUCIBLE *IN VITRO* 3D BREAST CANCER MODEL

3.1.1 Identification of an amenable cell line and establishment of a spheroid generation protocol

Monolayer cell culture is often used in the study of drug efficacy in cancer cells even though this methodology has inherent limitations as far as efficacy prediction is concerned. To improve the predictive strength of *in vitro* cell cultures for potentially useful lead compounds we sought to develop a more complex, 3D cancer cell culture system made up of TNBC breast cancer cells.[82,162–164] 3D cell culture systems more closely recreate many characteristics of epithelial tumours, especially their 3D architecture, which may play a role in drug delivery and uptake.[94] Several 3D models are currently being utilised in cancer studies around the world,[165–168] but many of these methodologies suffer from one or more drawbacks including prohibitive cost, low reproducibility of spheroids, and high labour intensity.[11,94,99]

To introduce a reliable, robust, and cost-effective 3D culturing system a technique was developed based on low attachment tissue culture plates. This method, described in detail below, makes use of agarose to generate a low attachment surface in 96-well plates into which cells could be plated. This would prevent their attachment to the plastic directing cells to aggregate and form attachments to neighbouring cells. The use of agarose, a readily available reagent in most laboratories, instead of using commercially available low attachment plates, was specifically chosen to reduce the cost of the plates used, as general tissue culture treated 96-well plates are readily available in many cell culture laboratories. Making use of this system we analysed three breast cancer cell lines for their ability to form spheroids within a low attachment environment. To assess their utility for drug screening purposes several characteristics including reproducibility, growth, and shape were analysed.

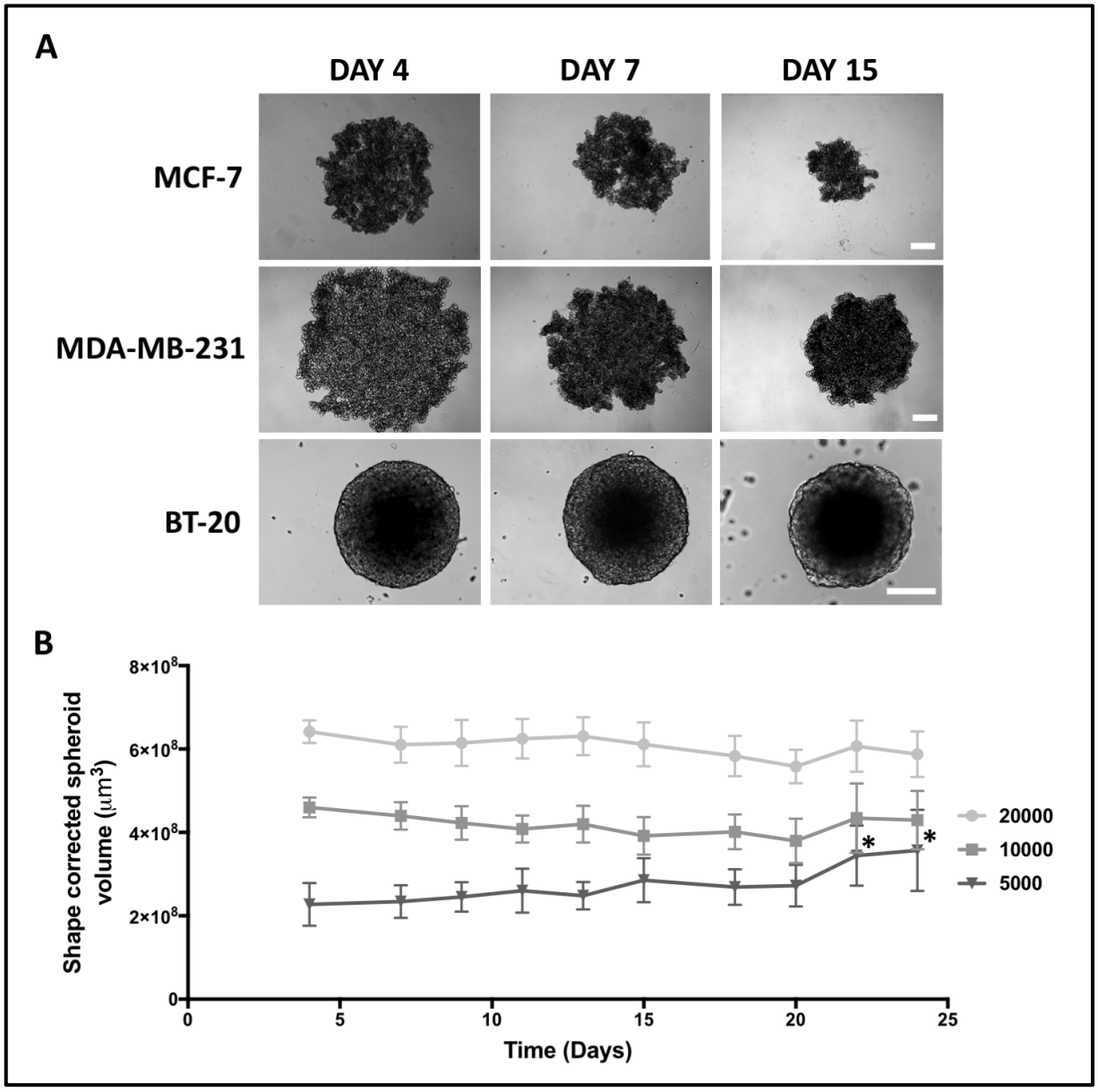

Figure 7. BT-20 breast cancer cells form consistent spheroids in 3D cell culture unlike MDA-MB-231 and MCF-7 breast cancer cells.

(A) MCF-7, MDA-MB-231, and BT-20 cells (2 x 10^4) were seeded into wells coated with 1% agarose and allowed to form spheroids over 4 days. Light microscopy images were taken at day 4, 7, and 15 using a Zeiss Axiovert CFL40 at 5x (MCF-7 and MDA-MB-231) and 10x (BT-20) magnifications (scale bars = 200 μm). (B) The relationship between seeding cell number and spheroid size of BT-20 cells was determined by seeding 5000, 10 000, or 20 000 cells per well and imaging 10 spheroids of each size on the indicated days. Spheroid volumes were calculated, and mean volume is shown with error bars representing standard deviation. Significant differences are indicated with an asterisk (*P<0.001).

The breast cancer cell lines MCF-7 (oestrogen receptor positive), MDA-MB-231 (TNBC, metastatic), and BT-20 (TNBC, non-metastatic) were analysed for spheroid forming capabilities.

Cells were seeded at a density of 2 x 10^4 cells per well in 200 μl of normal growth medium in 96-well plates previously coated with 1% agarose in serum-free medium and were incubated for 4 days to allow the cells to aggregate. After 4 days 100 μl of medium in each well was carefully removed and replaced with fresh medium. Thereafter, medium was refreshed every 48 hours by replacing 100 μl of old medium with fresh medium until 15 days after seeding. To visualise the spheroids, light microscopy images were taken on day 4, 7, and 15. A total magnification of 50x was used with a Zeiss Axiovert microscope for MDA-MB-231 and MCF-7 spheroids and a total magnification of 100x using a Zeiss Axiovert microscope and a 10x objective for BT-20 spheroids. Images of each spheroid were analysed qualitatively for spheroid shape, density, and consistency over time (Fig. 7A).

After 4 days, MCF-7 and MDA-MB-231 cells both formed loosely associated aggregates with MDA-MB-231 aggregates covering a larger area compared to MCF-7 cells. Thereafter, over the next several days, these spheroids compacted significantly while retaining their uneven edge, even after 15 days. BT-20 cells, on the other hand, formed compact spherical spheroids even after 4 days of growth with a lighter outer region along the perimeter of the spheroid and a dark dense interior. No significant further compaction of the spheroid was observed after 7 or 15 days. The spheroids retained a smooth outer edge. After 15 days the dense core became more defined suggesting some differentiation between the outer region and the core of the spheroid or indicating possible necrosis of the inner cells. This dense core was completely absent in the spheroids formed from MCF-7 and MDA-MB-231 cells. Therefore, from these initial studies BT-20 cells were selected as most appropriate for further development of the spheroid culture. To establish useful parameters for spheroid formation of the BT-20 3D spheroid culture system, we assessed the effect of seeding different cell numbers on spheroid formation and reproducibility. 5 x 10^3, 1 x 10^4, or 2 x 10^4 cells were seeded in 1% agarose covered 96-well plates and images were taken of each spheroid four days after seeding and every two days until day 24. From these images the spheroid volume was quantified using the area and circumference measured in Image J[157] and thereafter using the equations described in detail in the methodology section.

Briefly, the area and circumference of each spheroid was used to calculate the shape factor, which is an estimation of the roundness of the spheroid. This value is multiplied with the spherical volume to obtain a shape corrected spheroid volume.[156,157,169] These values were calculated for each spheroid at every time-point and were plotted on a curve to allow comparison of volume of the spheroids generated from the different seeding numbers (Fig. 7B). From this data it is clear that spheroids grown from 5 x 10^3 cells increased significantly in size from an average size of 2.5 x 10^8 μm^3 ± 5.1 x 10^7 μm^3 to 3.6 x 10^8 μm^3 ± 9.7 x 10^7 μm^3 between day 4 and day 24 (* P<0.001; Fig. 7B). Spheroids that were initially seeded with 1 x 10^4 cells had an average volume of 4.2 x 10^8 μm^3 ± 4.7 x 10^7 μm^3 over the 20 days of images with no significant changes in volume (ns P=0.779; Fig. 8B). Similarly, spheroids formed from 2 x 10^4 cells also remained consistent in volume over the 20 days at an approximate volume of 6 x 10^8 μm^3 ± 4.8 x 10^7 μm^3 (ns P=0.090; Fig. 7B). This data suggests that the spheroid size of BT-20 spheroids does not vary significantly over time when 1 x 10^4 or 2 x 10^4 cells are initially seeded. Additionally, the data suggests that after spheroid aggregation no significant compaction or spheroid volume increase occurs. This will make analysis in further experiments based on spheroid volume possible as any changes in volume can be attributed to the impact of an intervention on spheroid bound cell survival, cell proliferation or cell adhesion. It also suggests that cells remain viable over long periods of time although we did not test whether these cells could once again grow in 2D. For further experimentation 2 x 10^4 cells were seeded per well.

The reproducibility of spheroid size and shape are essential features for the use of spheroids in high throughput and quantitative data collection such as during compound screening applications. To test whether BT-20 spheroids form reproducible spheroids the variability of spheroid size and shape of 70 BT-20 spheroids was measured. Spheroids were seeded at a density of 2 x 10^4 cells/well and grown for 15 days with light microscopy images taken at 4, 7, and 15 days (Fig. 8A). The volume of each spheroid was calculated from the circumference and area input into the equations in Figure 8B-D.[157,169]

Shape factor, the first calculation used, indicates the roundness of the spheroid with 1.0 indicating a perfectly symmetrical shape.[156] Shape factor plays an important role in the calculation of the volume of the spheroids as it offers a refinement of volume calculations based on theoretical spheres. Box plots of the shape factors obtained using the calculation in Figure 9B show that the spheroids at day 4 and 7 had high values ranging between 0.97 and 0.99 with minimal variation found between each spheroid (Day 4: 0.987 ± 0.006 and Day 7: 0.986 ± 0.008, Fig. 8B). After 15 days the average shape factor remained high at 0.982 with a somewhat increased, but statistically insignificant variation of 0.013. Overall, BT-20 cells reproducibly formed almost perfectly round spheroids for up to 11 days after formation.

The second value needed for the volume calculations of each spheroid was the spherical volume. Each spheroid volume was calculated and represented as a box plot at each time point (Day 4, 7, and 15) measured using the equation shown in Figure 8C. The spherical volume once again remained consistent over the 15 days, as can be seen in the box plots in Figure 8C. The spheroids measured at an average volume of 6.6×10^8 μm^3 ± 6.8×10^7 μm^3 at the initial analysis at day 4 and a very similar average volume of 6.6×10^8 μm^3 ± 5.8×10^7 μm^3 at day 7, three days later. There was a slight increase in variation, at day 15 (6.6×10^8 μm^3 ± 8.2×10^7 μm^3), which was also seen with the shape factor, but the average volume was exactly the same as the spheroids at day 4 and day 7. This is the second indication that we noted of consistency in volume and shape of the BT-20 spheroids.

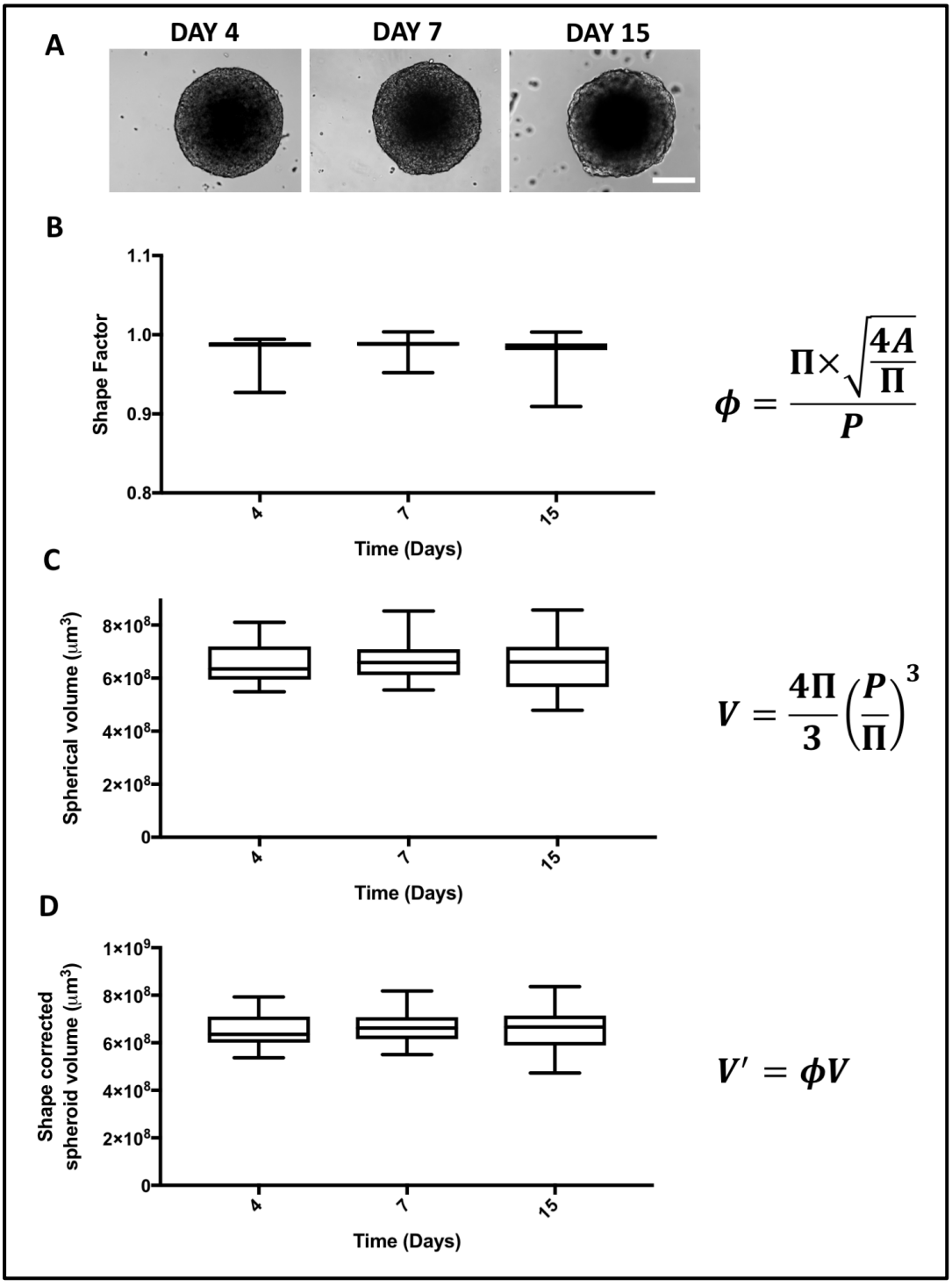

Figure 8. BT-20 cells aggregate reproducibly into similar shaped and sized spheroids.

To analyse reproducibility of spheroid formation 70 spheroids were generated and analysed at different timepoints. (A) Light microscopy images were taken of each spheroid at day 4, 7, and 15 using a Zeiss Axiovert CFL40 microscope at 10x magnification (scale bar = 200 μm). The area and perimeter of the spheroids was measured using Image J and three formulas were used to determine volume (B-D). The box plots indicating shape factor (B), spherical volume (C), and shape corrected spheroid volume (D) are representative of 70 spheroids for each time-point. No significant differences were observed between the different time points (ns P>0.999).

Finally, the spherical volume and shape factor were combined to produce a volume value that could be used to estimate the size of each spheroid. This volume is corrected to the shape factor to account for any variation in the physical spherical shape of the spheroid (the equation used is shown in Figure 8D). Calculations of the corrected volume of all spheroids, as seen in Table V, show that spheroid volume remains similar or even the same with no significant change or variance over the 11 days where images were obtained and analysed. Ultimately there was no statistically significant difference in corrected spheroid volume between day 4 and day 7 (ns *P*=0.675), or day 4 and day 15 (ns *P*=0.849) (values listed in Table V) indicating that BT-20 cells consistently formed near-identically shaped spheroids of very similar shape and size over the space of 15 days. Interestingly at day 7 the spheroids showed the least amount of variability. As this is often the time point after treatment with compounds (72 hours), this would be a beneficial characteristic of this system.

Table V. Spheroid volume of BT20 spheroids corrected by shape factor over time.

Time Point	Mean	SD	P-value
Day 4	$6.6 \times 10^8\ \mu m^3$	$6.8 \times 10^7\ \mu m^3$	Day 4 vs 7: 0.68
Day 7	$6.6 \times 10^8\ \mu m^3$	$5.8 \times 10^7\ \mu m^3$	Day 7 vs 15: 0.95
Day 15	$6.6 \times 10^8\ \mu m^3$	$8.2 \times 10^7\ \mu m^3$	Day 5 vs 15: 0.85

From this data it is clear that BT-20 cells form reproducible spheroids with little to no compaction or substantial cell growth over 15 days. Therefore, spheroid volume corrected with shape factor using the equations described in Figure 8B-D could be used as a reliable methodology to quantify any changes in volume caused by the treatment of spheroids of any compound being tested using this 3D system.

3.1.2 Establishment of a link between spheroid volume and cell proliferation

While spheroid volume may not provide insight into individual cell responses to compounds it does give insight into the effects of compounds on the balance of cell proliferation and cell death. To determine if we can correlate volume changes to changes in cell proliferation or cell death as visualised by fluorescein diacetate (FDA) and propidium iodide (PI), BT-20 spheroids were treated with two known chemotherapeutics, paclitaxel or colchicine. Both these compounds have previously been shown to decrease proliferation in breast cancer cells.[170–172] BT-20 cells were seeded at a density of 2 x 10^4 cells/well into 96-well plates coated with agarose and treated with vehicle control or drug after 4 days up to 15 days with replacement of half the medium volume every two days. Light microscopy images were taken at 4, 7, and 15 days in the presence of vehicle (negative control) or paclitaxel/colchicine (positive control) (Fig. 9A and 9B). Corrected spheroid volume was calculated as described above.

Spheroid volume is determined by the balance of cell proliferation and cell death. To visualise this balance, spheroids were co-stained for fluorescein diacetate (FDA) and propidium iodide (PI). FDA is converted by cellular esterases into the green fluorescent metabolite fluorescein, which can be visualised by fluorescence microscopy and indicates the presence of living cells.[173–175] PI on the other hand can only enter apoptotic cells once the membrane integrity has been compromised where it will concentrate to become visible as a red fluorescent colour when visualised with fluorescence microscopy.[173,176,177] Using these two dyes together for live/dead staining both living and dead cells can be specifically identified within the structure of the spheroid. To visualise each cell, 4',6-diamidino-2-phenylindole (DAPI) was also added to the staining mixture, which stains the DNA within the nucleus of all cells, both living and dead, allowing the identification of each single cell within a spheroid. This dye also gives an indication of the size of the spheroid.

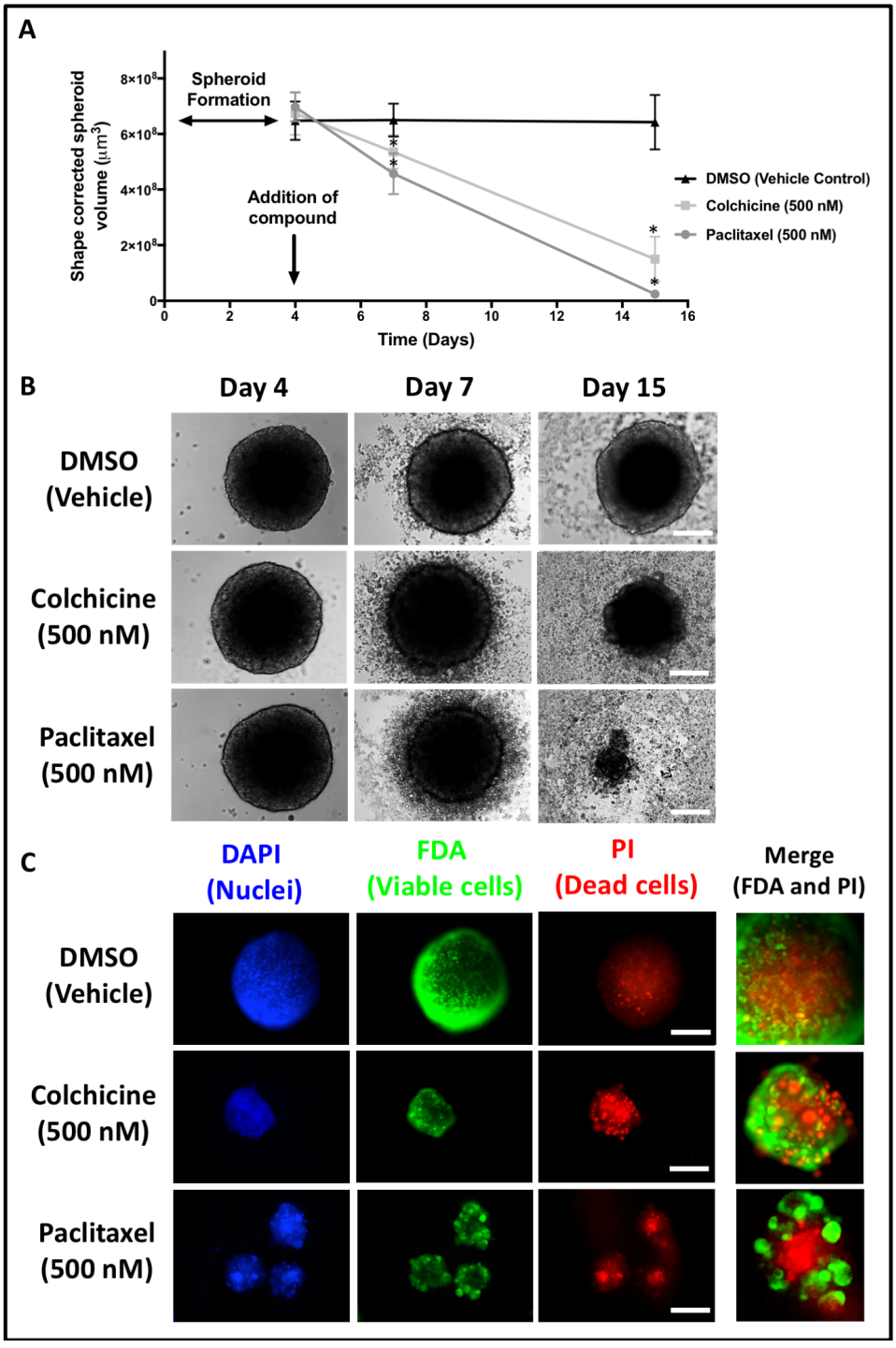

Figure 9. Establishing a link between spheroid volume and cell viability within spheroids.

BT-20 cells ($2x10^4$) were seeded into wells coated with 1% agarose and spheroids were allowed to form for 4 days. The spheroids were exposed to 500 nM colchicine or 500 nM paclitaxel for 72 hours. (B) Light microscopy images were taken at day 4, 7, and 15 using a Zeiss Axiovert CFL40 at 10x magnification (scale bar = 200 µm). Spheroid volumes were measured over 15 days (A). Significant differences are indicated with an asterisk (*P<0.001). After 15 days from seeding the spheroids were stained with DAPI (blue), FDA (green), and PI (red). Spheroids were visualised using a Zeiss Axiovert CFL40 fluorescent microscope and a Zeiss Axiovert MRm monochrome camera at 10x magnification (scale bar = 200 µm).

The spheroids at day 15 were very carefully removed from each well and placed together in a microcentrifuge tube. The spheroids were stained with a mixture of FDA/PI/DAPI in the dark at room temperature. The spheroids were rinsed with PBS and placed in a 24-well plate to be visualised using fluorescence microscopy. The images were obtained at a magnification of 10x using a Zeiss Axiovert CFL40 fluorescent microscope were qualitatively compared (Fig. 9C).

Spheroids exposed to DMSO (Fig. 9A and B) remained similar in size over the 15 days measured (Day 4: 6.7 x10^8 µm^3 ± 9.5 x 10^7 µm^3 vs Day 7: 6.7 x10^8 µm^3 ± 8.2 x 10^7 µm^3 vs Day 15: 6.6 x10^8 µm^3 ± 9.8 x 10^7 µm^3, ns P>0.999). Spheroids exposed to the DMSO vehicle control had intense FDA fluorescence around the edges of the spheroid with lower intensity fluorescence in the middle, although individual bright foci could be seen throughout the spheroid. There were low levels of PI staining. A few bright spots were observed throughout the spheroids potentially representing apoptotic cells (Fig. 9C). The magnified merged images in Figure 9C shows the pronounced FDA staining in the DMSO vehicle control treated spheroids. It must be noted that fluorescence microscopy does not provide information regarding all cells within the spheroid, and rather only the cells on the surface which is a limiting factor in this scenario.

Exposure to 500 nM paclitaxel resulted in a significant decrease in BT-20 spheroid volume after 72 hours to 66% of the control spheroid volume (Fig. 9A and 9B). The images of the spheroids in Figure 9 show that the smooth perimeter that is seen in the DMSO treated spheroids was lost with the exposure to paclitaxel and loose cells had started to amass around the spheroid, seemingly coming off of the spheroid and floating around in the medium (72h – DMSO vehicle control: 6.7 x10^8 µm^3 ± 8.2 x 10^7 µm^3 vs paclitaxel treated spheroid: 4.6 x10^8 µm^3 ± 7.3 x 10^7 µm^3, * P<0.001). After 15 days many of the spheroids exposed to 500 nM paclitaxel had completely disintegrated making accurate measurements difficult as the variation was very large over the sample size but remaining spheroids were on average 3% of the original spheroid volume (DMSO: 6.6 x10^8 µm^3 ± 9.8 x 10^7 µm^3 vs paclitaxel 2.4 x10^7 µm^3 ± 8.5 x 10^6 µm^3, * P<0.001; Fig. 9A and 9B). The staining of spheroids exposed to paclitaxel with FDA and PI showed bright and concentrated PI staining in the middle of the spheroid indicating that these

cells are not viable. Larger cells extending from the edge of the spheroids are still positive for FDA and negative for PI suggesting that some viable cells still remain, but these are only found on the periphery of the spheroid.

Similar to paclitaxel, colchicine exposure also caused spheroids to lose their smooth perimeter with the appearance of loose cells appearing around the spheroid after 7 days. A reduction of 20% of the spheroid volume after 3 days of exposure to 500 nM of colchicine was measured (DMSO vehicle control: 6.7 $x10^8$ μm^3 ± 8.2 x 10^7 μm^3 vs colchicine treated spheroid: 5.4 $x10^8$ μm^3 ± 6.6 x 10^7 μm^3, * P<0.001; Fig. 9A and 9B). A further 8 days of exposure to colchicine resulted in the volume of spheroids to be significantly reduced by 77% compared to control spheroids (Day 15 – DMSO control spheroids: 6.6 $x10^8$ μm^3 ± 9.8 x 10^7 μm^3 vs colchicine treated spheroids: 1.5 $x10^8$ μm^3 ± 7.7 x 10^7 μm^3; * P<0.001; Fig. 11B and Fig 12). The loss of cells in colchicine treated spheroids was less pronounced when compared to the spheroids treated with paclitaxel, however it is noticeable that the loss in smooth perimeter edge was still seen after treatment with colchicine (Fig. 9B).

Spheroids exposed to 500 nM colchicine presented with distinct PI staining throughout the spheroid, concentrating in the centre of the spheroid (Fig. 9C). While some FDA staining was present it is limited to individual cells on the periphery of the spheroid while the PI positive centre of the spheroid extends to the edge of the spheroid compared to the vehicle control. From this data we can conclude that the decrease in spheroid volume after exposure to paclitaxel and colchicine, is associated with increased PI and decreased FDA staining suggesting that the reduction in volume observed is due to increased cell death and decreased cell proliferation within the spheroids.

3.2 IDENTIFYING COMPOUNDS WITH POTENTIAL ANTI-PROLIFERATIVE ACTIVITY IN A BREAST CANCER 3D CELL MODEL.

3.2.1 Assessing anti-proliferative effects of novel compounds in a 2D monolayer culture

It is well known that some tumours can be resistant to chemotherapeutic compounds that have previously been found to be effective when tested on cells in 2D *in vitro* cultures. This resistance can be induced by the architecture of 3D tissue, reduction in nutrient or oxygen supply, and an array of other factors uniquely present in *in vivo* settings but lacking in *in vitro* monolayer cultures.[81,82,97,98] We hypothesised that the 3D cell cultures of BT-20 breast cancer cells induce chemoresistance to some anticancer compounds. To test this hypothesis, a number of compounds were analysed for their effect on the cell survival of BT-20 cells grown as 2D monolayers or grown into 3D spheroids. Cells were exposed to four novel compounds. Four of these compounds were 2ME derivatives described in Figure 6: EE-one, EE-15-one, ESE-15-one, and ESE-one. These compounds have previously been shown to inhibit cell proliferation in monolayer cell cultures. A new derivative of the oestradiol 3,17-O,O-bis-sulfamate (E2bisMATE), STX1972, was also tested as it was shown to inhibit mitosis in cancer cell lines.[178,179] As controls paclitaxel and colchicine were tested as it is assumed that there would be no resistance to these drug in 2D or 3D as is shown in the previous experiment.

Dose-response curves of 2D cell cultures of BT-20 cells were generated for each compound (Fig. 10A-D). Cells were grown as 2D monolayers in 96-well plates and exposed to increasing concentrations of compound. Concentration ranges were based on published values and all values were normalised to DMSO vehicle treated cells. The exposure of BT-20 cells grown in monolayer to paclitaxel induced a significant, near complete, loss of cells (95%) after 72 hours of exposure at low nanomolar concentrations (* P<0.001). An E_{max} of 50 nM was calculated along with a EC_{50} of 25 nM in line with previous reports of paclitaxel treatments (Fig. 10A)[180–183]. Colchicine had a similar effect compared to paclitaxel with the low nanomolar concentration of 100 nM of colchicine causing an 81.73% loss of cells (Fig. 10B; * P<0.001). This effect plateaued thereafter with no increase in cell loss. For colchicine an EC_{50} of 60 nM was calculated, which is in accordance with published data.[184–188]

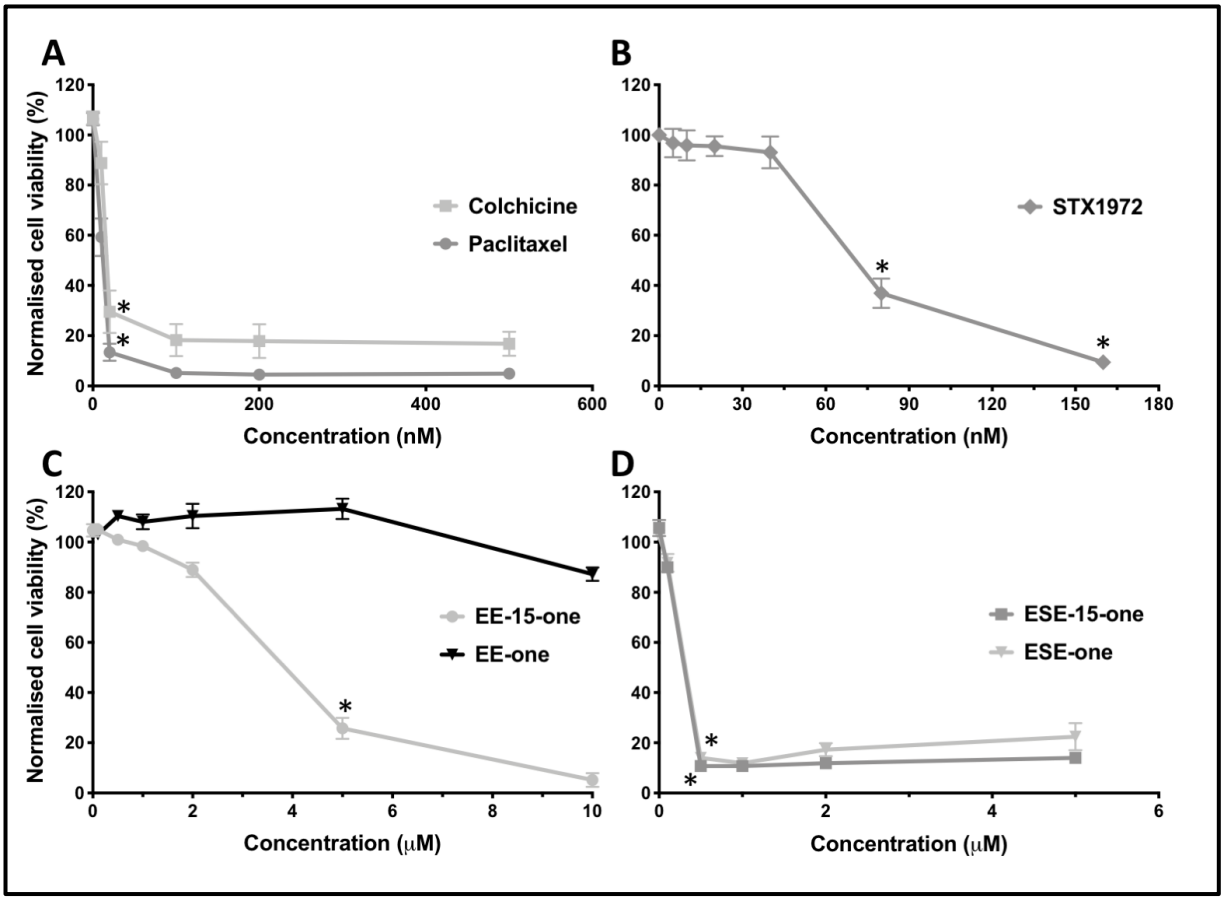

Figure 10. Response curves of BT-20 monolayer cells treated with two classic chemotherapeutics and five novel compounds.

Cell viability of BT-20 cells grown in monolayers exposed to paclitaxel (A), colchicine (B), EE-15-one and EE-one (C), and ESE-15-one and ESE-one (D), were measured using crystal violet staining. BT-20 cells (1 x 10^4 cells/well) were seeded and allowed to adhere overnight after which cells were exposed to the indicated range of concentrations of each compound for 72 hours. Cells were fixed and stained with crystal violet and solubilised with triton X-100. Optical density was measured at 570 nm using an EL_x800 Universal Microplate reader. Graphs represent the average of three independent repeats, error bars indicate s.e.m (*P<0.001).

STX1972 was added to cells in nanomolar concentrations (Fig. 10B). While low nanomolar concentrations did not affect cell survival, treatment with 80 nM of the compound resulted in a 62% decrease in cell viability while at 160 nM exposure only 10% of cells remained viable. This indicates that in 2D STX1972 has an anti-proliferative effect on these cancer cells in the nanomolar range with an EC50 of 70.54 nM.

Exposure of BT-20 cells to the non-sulfamoylated compound EE-one led to a small and statistically insignificant 13% reduction (ns $P>0.999$) in cell number at 10 µM with no difference in cell survival seen at lower concentrations (Fig. 10C). Exposure to the non-sulfamoylated compound EE-15-one, which only differs from EE-one by one double bond (Fig. 7A and B), caused a substantial reduction in cell number with a maximal effect measured at 7 µM and an EC_{50} of 3.49 µM after 72 hours (Fig. 10C). At 5 µM a loss of 78.9% of BT-20 cells was seen compared to vehicle treated cells (* $P<0.001$), while at 10 µM, almost no cells remained (Fig. 10C).

The sulfamoylated compounds ESE-15-one and ESE-one (Fig. 7C and D, respectively) were assessed in BT-20 cells grown in monolayers through exposure for 72 hours. ESE-15-one exposure led to significant inhibition (* $P<0.001$) of cell proliferation reaching an E_{max} of 1.4 µM, while an EC_{50} of 0.70 µM was calculated (Fig. 10D). ESE-one exposure also led to a significant reduction (* $P<0.001$) in cell number as well with an E_{max} of 1.1 µM and an EC_{50} of 0.55 µM (Fig. 10D). The cell loss caused by these two sulfamoylated compounds occurred at a lower concentration (1 µM) compared to the effect seen after exposure to 5 µM EE-15-one, the non-sulfamoylated compound. Therefore, BT-20 cell survival in a 2D environment is severely inhibited by the antiproliferative agents, paclitaxel and colchicine, at nanomolar concentrations after 72 hours. These cells are also responsive to STX1972, both sulfamoylated 2ME analogues, ESE-15-one and ESE-one), as well as the non-sulfamoylated 2ME derivative EE-15-one albeit at higher micromolar concentrations.

3.2.2 Assessing the effects of potential anticancer compounds in the 3D breast cancer model

The five compounds tested in 2D were now tested in the 3D spheroid culture system to determine whether 3D cell culture conditions altered the sensitivity of the cells to the different compounds. BT-20 cells were seeded at a density of 2 x 10^4 cells/well into 96-well plates coated with agarose and grown for 15 days with light microscopy images taken at 4, 7, and 15 days (Fig. 11A). All compounds were added at day for by replacement of half the medium with compound containing medium. Afterwards, half the medium volume was replaced every second day. Corrected spheroid volumes were calculated as described above. The effects of the DMSO vehicle control and positive (colchicine and paclitaxel) controls in the BT-20 spheroids were established above and images are included here as comparison (Fig. 11A and 11B).

Spheroids were exposed to 1 µM of ESE-15-one and 1 µM of ESE-one. Images taken after 72 hours show that both compounds caused the loss of the smooth edge of the spheroids as seen in the positive control conditions, with loose cells accumulating around the spheroid (Fig. 11A). The initial decrease in size was also similar to that seen in paclitaxel and colchicine treated spheroids. Both 1 µM ESE-one and 1 µM ESE-15-one treatments resulted in significant decreases in the BT-20 spheroid volume after 72 hours. ESE-15-one treated spheroids were 31% smaller than spheroids at day 4 (treatment day 0) (Day 4: 6.6 x10^8 µm^3 ± 4.5 x 10^7 µm^3 vs Day 7: 4.5 x10^8 µm^3 ± 5.2 x 10^7 µm^3, * *P*<0.001; Fig. 11C), while ESE-one treated spheroids were reduced by 37% compared to the same paired spheroids at day 4 (Day 4: 6.9 x10^8 µm^3 ± 1.4 x 10^7 µm^3 vs Day 7: 4.4 x10^8 µm^3 ± 9.82x 10^7 µm^3, * *P*<0.001; Fig. 11C). After 8 days of exposure, the effect of both compounds was even more pronounced with ESE-15-one treatment leading to a further 25% reduction in the volume of the spheroids, leaving only 43% of each spheroid (Day 7: 4.5 x10^8 µm^3 ± 5.2 x 10^7 µm^3 vs Day 15: 2.8 x10^8 µm^3 ± 3.8 x 10^7 µm^3, * *P*<0.001). ESE-one exposure also reduced the spheroid volume, in this case even more effectively than ESE-15-one, by 84% after 11 days of exposure (Day 4: 6.6 x10^8 µm^3 ± 9.8 x 10^7 µm^3 vs Day 15: 1.2 x10^8 µm^3 ± 5.7 x 10^7 µm^3, * *P*<0.001).

STX1972 exposure resulted in a spheroid volume decrease of 12% 4 days post exposure to 100 nM of STX1972 (Fig. 11A and 11C). This decrease, however, was not statistically significant (Fig. 11C) and visually there was very little difference in the size of spheroid, with the spheroid edge remaining completely intact (fig 11A). After 15 days spheroid volume had increased but with no significant difference between vehicle treated and STX1972 exposed spheroids (Actual volumes; Day 4: 6.3×10^8 μm^3 ± 1.1×10^7 μm^3 vs Day 7: 5.5×10^8 μm^3 ± 1.3×10^7 μm^3 vs Day 7: 5.7×10^8 μm^3 ± 1.4×10^7 μm^3 ns $p>0.999$). Therefore, the data suggests that unlike the large effect observed in 2D culture (Fig. 10B), a nanomolar concentration of this compound has no effect on cell survival or proliferation in 3D as the spheroids remain the same size appearing very similar to the negative control.

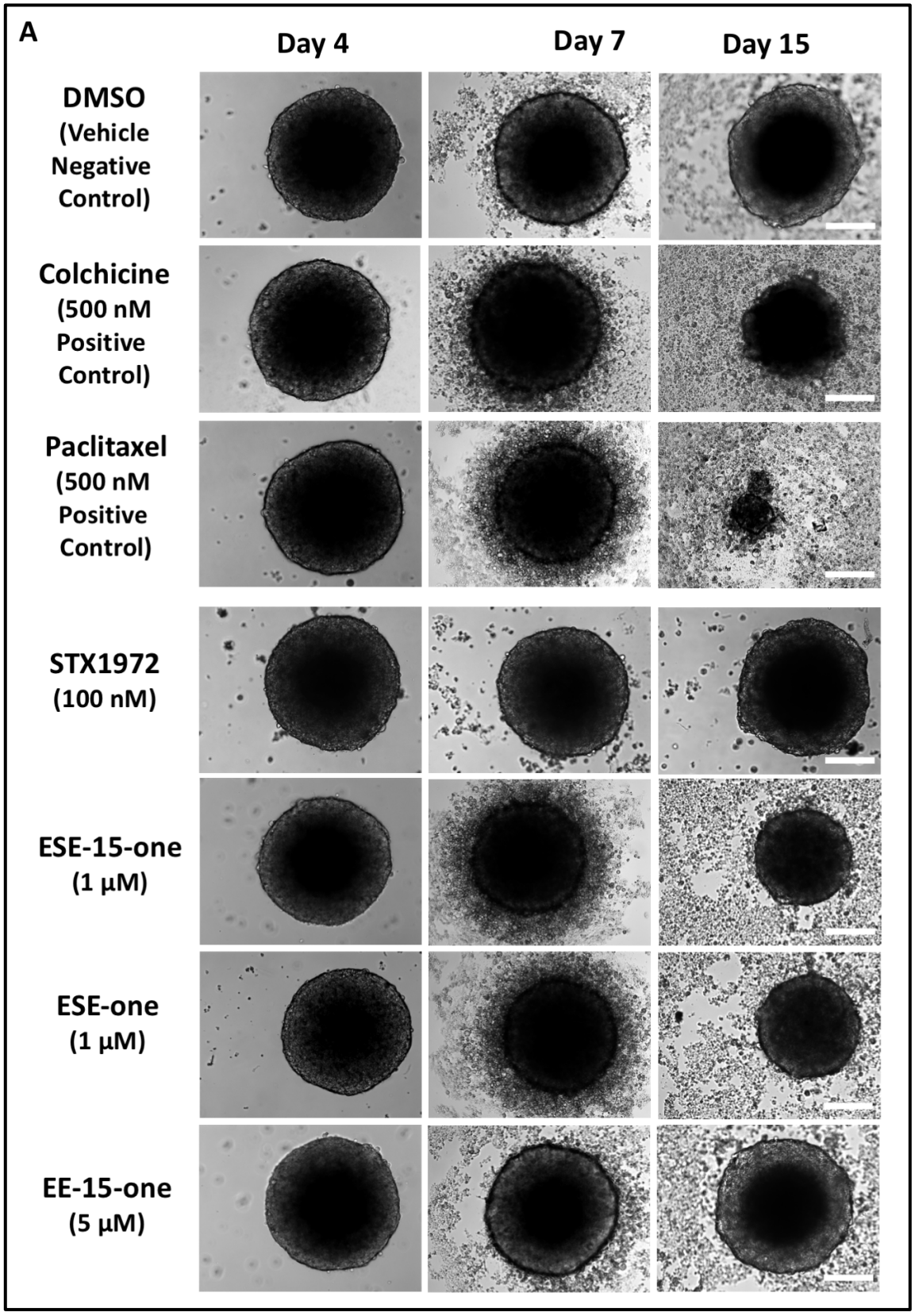

Figure 11. BT-20 spheroids response to different anticancer compounds. (Part 1)

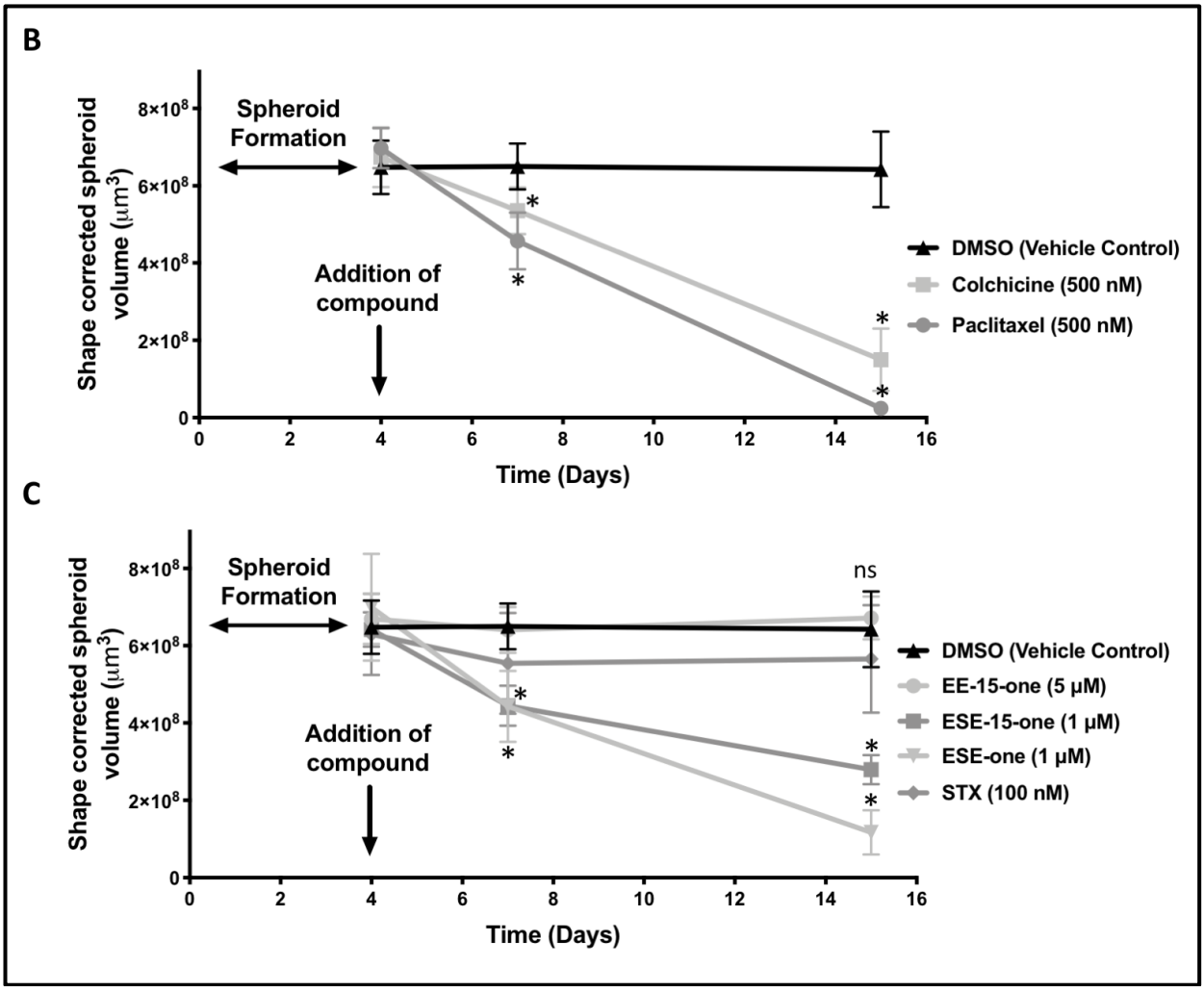

Figure 11. BT-20 spheroids response to different anticancer compounds. (Part 2)

BT-20 cells (2 x 10^4) were seeded into wells coated with 1% agarose and left to form spheroids over 4 days. The spheroids were exposed to 5 µM EE-15-one, 1 µM ESE-15-one, 1 µM ESE-15-one (A), and 500 nM colchicine and 500 nM paclitaxel (B) for 72 hours. Light microscopy images were taken at day 4, 7, and 15 using a Zeiss Axiovert CFL40 at 10x magnification (scale bar = 100 µm). Spheroid volumes were measured over 15 days. Each point is representative of 50 independent repeats, error bars indicate standard deviation (*P<0.001). BT-20 cells (2 x 10^4) were seeded into wells coated with 1% agarose and left to form spheroids over 4 days. The spheroids were exposed to 5 µM EE-15-one, 1 µM ESE-15-one, 1 µM ESE-15-one, and 500 nM colchicine and 500 nM paclitaxel for 72 hours. Light microscopy images were taken at day 4, 7, and 15 using a Zeiss Axiovert CFL40 at 10x magnification (scale bar = 100 µm). Spheroid volumes were measured over 15 days.

BT-20 spheroids exposed to 5 µM EE-15-one, the non-sulfamoylated compound, remained intact with a discrete spheroid edge after 72 hours (Fig. 11A), also appearing similar to DMSO vehicle control spheroids. No visible effects were observed at day 7. Concomitantly, spheroid volume remained similar between day 4, day 7, and day 15 (Day 4: 6.6 x10^8 µm^3 ± 6.5 x 10^7 µm^3 vs Day 7: 6.4 x10^8 µm^3 ± 6.0 x 10^7 µm^3 vs Day: 15 6.7 x10^8 µm^3 ± 5.8 x 10^7 µm^3, ns P>0.999),

(Fig. 11C). The spheroid sizes at each timepoints were visibly the same as each DMSO treated spheroid (Fig. 11A) and quantitatively the same volume (Fig. 11C). This is suggestive that EE-15-one does not induce any effects on BT-20 cells grown in 3D. Once again this is an interesting observation considering the pronounced effects of 75% cell loss seen at this concentration in 2D monolayer experiments after 72 hours (Fig. 10C). It is therefore possible that BT-20 cells become resistant to the compound when grown as a 3D spheroid, or the mechanism of action is rendered void in a 3D scenario. To measure if BT-20 cells are completely refractive towards EE-15-one we tested higher concentrations of the compound against BT-20 spheroids.

Spheroids were exposed to 10 µM or 20 µM EE-15-one for 72 hours similarly to the above experiments. Spheroid volume was measured at day 7 and day 15 after replacing half of the medium in each well. Spheroids exposed to 10 µM or 20 µM EE-15-one did not change significantly in size after 7 days as can be seen in the graph in Figure 12A as well as the light microscopy images in Figure 12B (10 µM: Day 4: 5.2 $x10^8$ μm^3 ± 3.3 x 10^7 μm^3 vs Day 7: 5.1 $x10^8$ μm^3 ± 3.3 x 10^7 μm^3 vs Day 15: 5.4 $x10^8$ μm^3 ± 3.4 x 10^7 μm^3, ns P>0.999 and 20 µM: Day 4: 5.1 $x10^8$ μm^3 ± 6.2 x 10^7 μm^3 vs Day 7: 5.0 $x10^8$ μm^3 ± 3.4 x 10^7 μm^3 vs Day: 15 5.4 $x10^8$ μm^3 ± 2.6 x 10^7 μm^3, ns P>0.999). There was a minor increase in size noted when the spheroids were measured at day 15, compared to spheroids measured right after exposure to the different concentrations of EE-15-one at day 4, i.e. baseline, but this minor increase was not statistically significant nor noticeable on the images in Figure 12B.

The images of spheroids exposed to varying concentrations of EE-15-one in Figure 13B show well-rounded spheroids with smooth defined edges similar to the control spheroids only exposed to the vehicle DMSO. At day 7 a few cells dying or falling off the spheroids were observed but these did not change the size of the spheroid and following ‘wash-out’ when half the spheroid medium was replaced with new fresh medium this effect completely disappeared, returning the spheroids to the original defined shape.

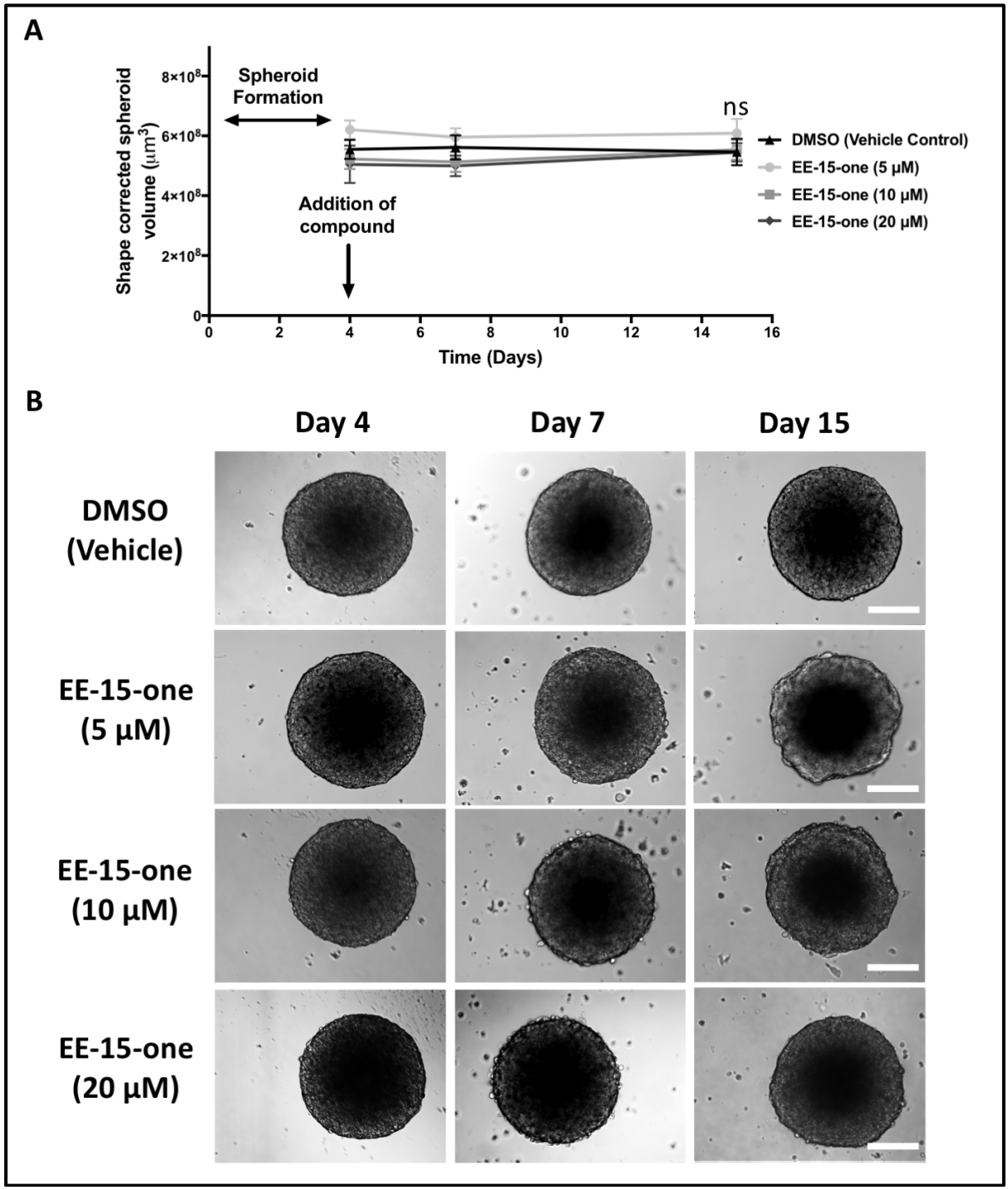

Figure 12. Different concentrations of EE-15-one have no effect on spheroid growth.

(A) BT-20 cells ($2x10^4$) were seeded into wells coated with 1% agarose and left to form spheroids over 4 days. The spheroids were exposed to 5 µM, 10 µM, and 20 µM of EE-15-one for 72 hours. The area and circumference of each spheroid was measured using Image J and several formulas were used to determine volume. The volume of BT-20 spheroids exposed to DMSO and EE-15-one were measured over 15 days. Each point is representative of 20 independent repeats, error bars indicate standard deviation. (B) Light microscopy images were taken at day 4, 7, and 15 using a Zeiss Axiovert CFL40 fluorescent microscope and a Zeiss Axiovert MRm monochrome camera at 10x magnification (scale bar = 100µM).

This cumulative evidence (Fig. 10-12) suggests that the 2ME derivatives that were tested during this study, excluding EE-one, induce a loss of cells at micromolar concentrations when these were grown as 2D cell cultures. This is unlike paclitaxel and colchicine, which act at nanomolar concentrations inducing a near-complete loss of cells. Both paclitaxel and colchicine caused a significant loss of spheroid volume at nanomolar concentrations suggesting that BT-20 cells grown as spheroids may not become resistant to these compounds although further dose response assays would have to be performed to confirm this. Similarly, ESE-15-one and ESE-one led to a decrease in cells whether grown in monolayers or in the 3D system, suggesting that these compounds act independently of the architecture of the cell culture used. While the compounds induced complete cell loss at 1 μM in 2D the effect was somewhat more muted in spheroids suggesting that some resistance to the compounds may occur from the method of cell culture utilised during testing. In contrast, EE-15-one induced a significant loss of cells in 2D monolayer cell culture at micromolar concentrations but no cell loss was measured in 3D spheroids exposed to the compound suggesting that EE-15-one impacts on a process important for cells grown in 2D but is redundant in cells grown in 3D.

Using the spheroid volume calculations described above we have shown that paclitaxel, colchicine, ESE-15-one, and ESE-one exposure lead to reductions in spheroid volume, which we associate with cell death within the spheroid. As in Figure 9C, we do hypothesise that these compounds are causing cell death within the spheroid, which results in the subsequent reduction in measured spheroid volume. PI/FDA/DAPI live dead staining was thus also used to further investigate the changes in volume seen in Figure 11A.

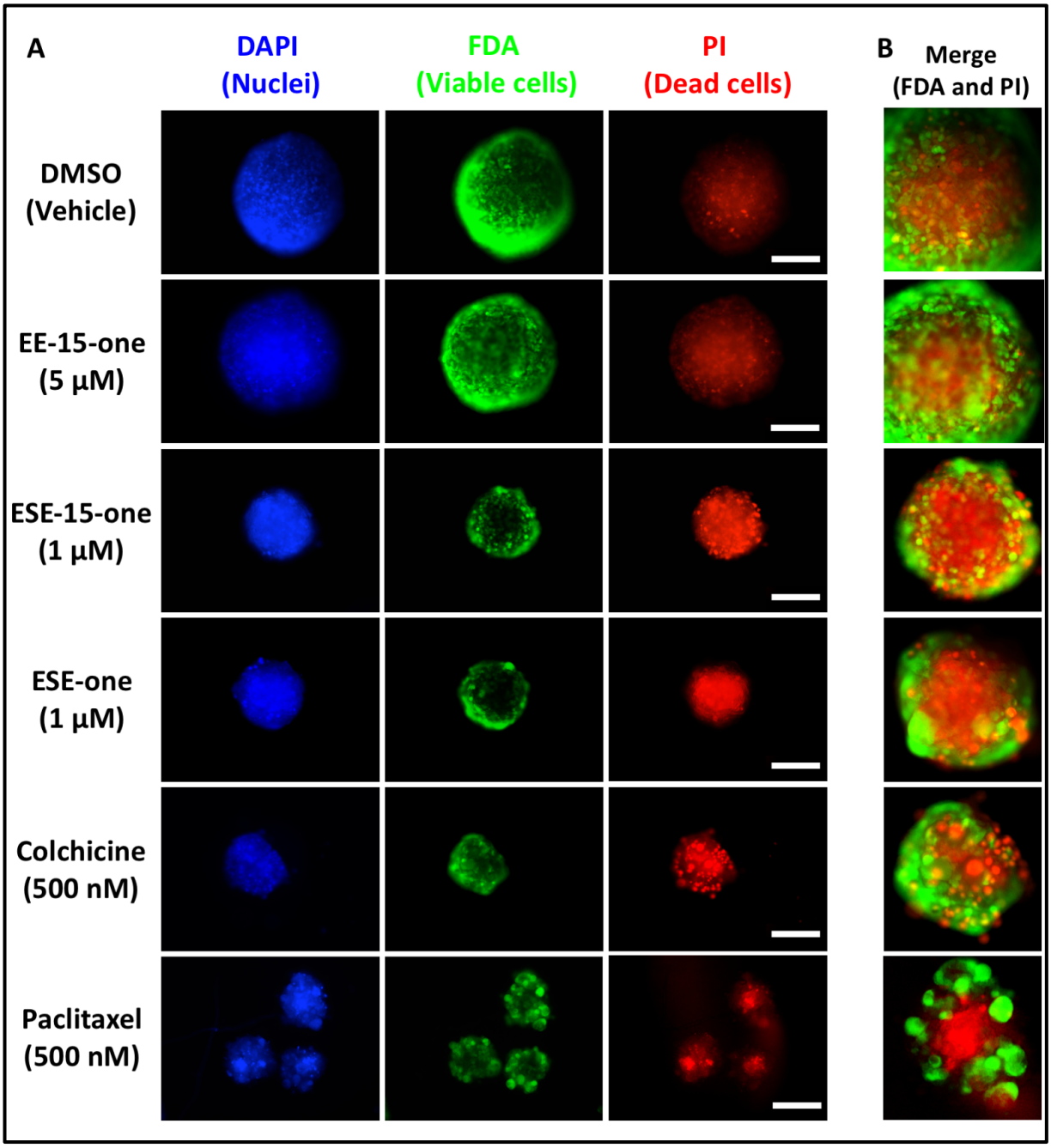

Figure 13. Live/dead staining of BT-20 spheroids exposed to EE-15-one, ESE-15-one, ESE-one, colchicine, and paclitaxel.

BT-20 cells ($2x10^4$) were seeded into wells coated with 1% agarose and spheroids were allowed to form for 4 days. The spheroids were exposed to 5 µM EE-15-one, 1 µM ESE-15-one, 1 µM ESE-one, 500 nM colchicine, and 500 nM paclitaxel for 72 hours. After 15 days from seeding the spheroids were stained with DAPI (blue), FDA (green), and PI (red) for 5 minutes. Spheroids were visualised using a Zeiss Axiovert CFL40 fluorescent microscope and a Zeiss Axiovert MRm monochrome camera at 10x magnification (scale bar = 200 µm). A zoomed in merge image of each spheroid is given in the right-hand column to show the mutual exclusivity of the PI and FDA staining.

To analyse cell viability in spheroids after exposure to compounds, cells were seeded as described before and allowed to form spheroids for four days before they were exposed to each compound at the indicated concentration or alternatively with the DMSO vehicle control for 72 hours. Afterwards, half of the culture medium was replaced every second day until day 15. Fifteen spheroids that were exposed to each of the different compounds were very carefully removed from each well and placed together in a microcentrifuge tube. The spheroids were carefully washed and stained with a mixture of FDA/PI/DAPI for 5 minutes in the dark at room temperature. Afterwards, spheroids were allowed to sink to the bottom of the tube and the staining mixture was removed. The spheroids were rinsed with PBS ensuring that no spheroids were lost and placed in a 24-well plate to be visualised using fluorescence microscopy. The images obtained at a magnification of 10x using a Zeiss Axiovert CFL40 fluorescent microscope were qualitatively compared (Fig. 13).

Spheroids exposed to 5 µM EE-15-one, displayed very similar FDA and PI staining to the DMSO vehicle control treated spheroids. This included intense FDA staining around the edges of the spheroid with less staining in the centre and only low levels of PI staining throughout the spheroid with occasional bright foci (Fig. 13A). The zoomed merged images in Figure 13B show the pronounced FDA staining in both the DMSO vehicle control treated spheroids and the spheroids exposed to 5 µM EE-15-one. The FDA staining was observed along the edge of the spheroid with an increase in PI staining in the centre of the spheroids suggesting that most cells at the edge of the spheroid are viable while there may be a necrotic core of cells in the middle of the spheroid. Spheroids exposed to 1 µM ESE-15-one and 1 µM ESE-one showed FDA staining that was much lower and only visible in a few scattered cells along the edges. The PI staining indicating dead cells was much more pronounced when compared to the vehicle treated cells, with individual clusters of intense red fluorescence clearly visible (Fig. 13). From this data we can conclude that the decrease in spheroid volume after exposure to paclitaxel, colchicine, ESE-15-one, and ESE-one (Fig. 11A-C) is associated with increased PI and decreased FDA staining suggesting that the reduction in volume observed could be due to cell death within the spheroids.

3.3 HYPOXIA IN SPHEROIDS IS NOT RESPONSIBLE FOR THE DIFFERENCE IN EE-15-ONE RESPONSE OF BT-20 CELLS IN 2D VERSUS 3D CULTURE.

3.3.1 Assessing breast cancer cell survival after exposure to novel 2-ME derivatives under hypoxic conditions

The oestradiol derivatives shown to cause a reduction in viability in both 2D monolayer and 3D spheroid cell culture systems (ESE-15-one and ESE-one) were specifically designed to increase the bioavailability compared to the original compound 2ME. 2ME as a natural metabolite of oestrogen is rapidly metabolised and cleared from the body when injected, which led to failure during Phase I trials.[123,129] In an attempt to improve the bioavailability one of the changes to the structure of 2ME was the addition of a primary sulfamoyl group (Fig. 6C and D), which could bind to the carbonic anhydrase IX (CAIX) present on the plasma membrane of red blood cells and by binding would prevent clearing when passing through the liver.[138,144] Since hypoxic cancer cells also have been shown to express high levels of CAIX on their cell surface we postulated that these novel oestradiol derivatives could be targeted to such cancer cells and induce cell death.[138,189–192] To assess whether the hypoxia commonly present in tumours and in spheroids could affect the efficacy of EE-15-one, BT-20 cells in normoxia and hypoxia were treated with the different compounds and cell survival was measured.

BT-20 cancer cells were grown in 2D monolayer cell cultures. The cells were seeded into 96-well plates and placed in a normoxic incubator (21% O_2) and left to adhere overnight as normal. One set of cells (for each experiment) was transferred to a hypoxic incubator (1% O_2) for 7 hours. The other set of cells were left in the normoxic incubator. Both incubators were set at the same temperature (37°C) and CO_2 level (5%). Cells under both conditions were exposed to a concentration range of ESE-15-one, ESE-one, or EE-15-one, and paclitaxel as positive control for 24 hours. Cell number was determined using crystal violet staining and quantification was performed via spectrophotometry. Treated cells were normalised to untreated cells from each condition grown only in medium. EC50 concentrations are tabulated in Table VI.

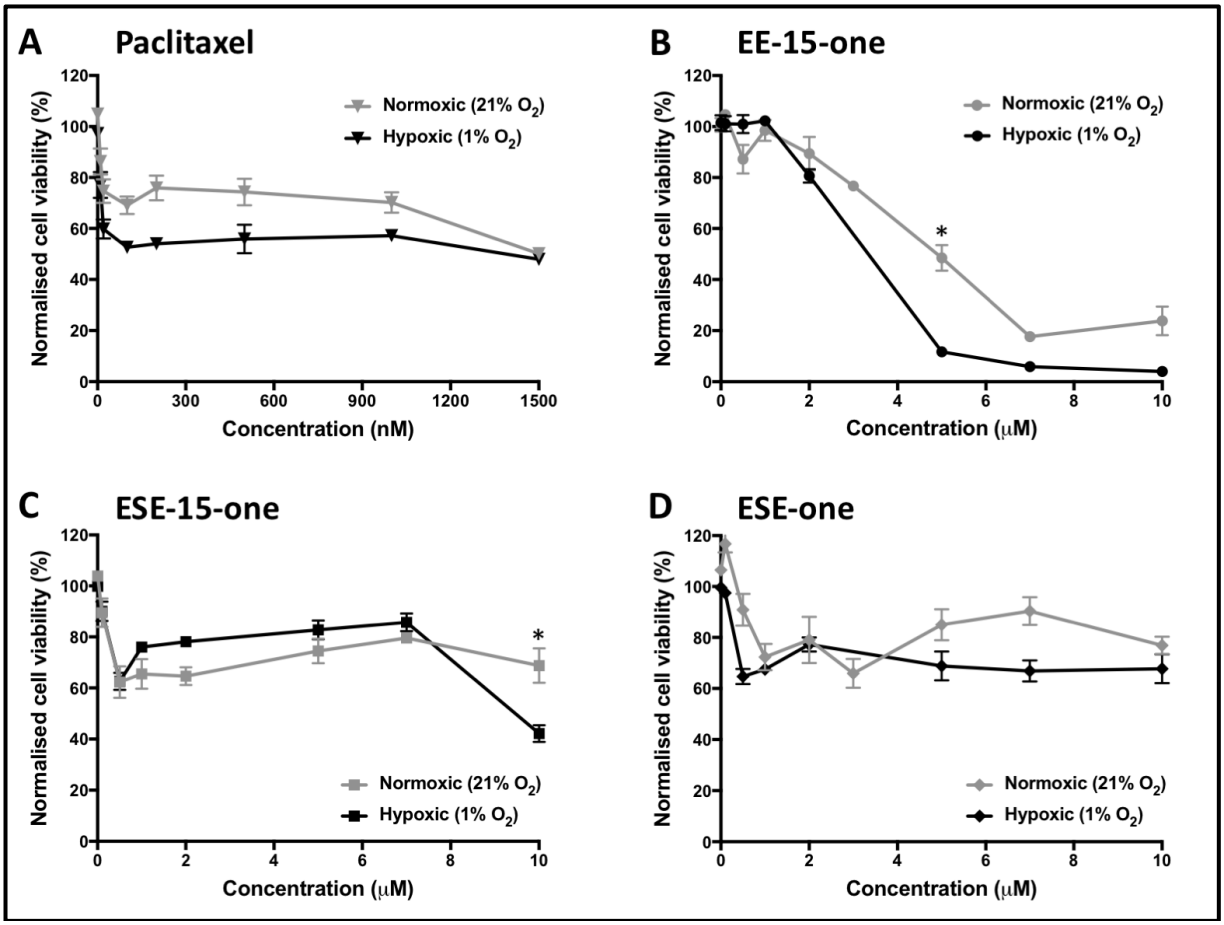

Figure 14. BT-20 exposed to EE-15-one respond differently under normoxic and hypoxic conditions.

BT-20 cells were seeded at a density of 1 x 10^4 cells/well and allowed to adhere overnight. Half the cells were exposed to hypoxic conditions (1% O_2) for 7 hours and exposed to paclitaxel (A), EE-15-one (B), ESE-15-one (C), and ESE-one (D) for 24 hours and fixed, stained with crystal violet and analysed with spectrophotometry. Cells exposed to 0.5% (v/v) DMSO were used as a vehicle control and all wells were normalised to cells only exposed to medium. Experiments were done in three independent repeats and graphs represent the mean with error bars indicating standard error of the mean (s.e.m). Significant differences are indicated with an asterisk (*P<0.001).

Paclitaxel exposure led to a reduction in cell number of maximum 50%. No significant differences in response (ns P>0.999) were measured between cells under normoxic or hypoxic conditions in any of the cell lines (Fig. 14A). This was an interesting finding as we expected to see some difference between the conditions as many cells have been shown to be resistant to the paclitaxel under hypoxic conditions.[193–196] The maximum loss of 50% of cells after paclitaxel treatment is in contrast to the earlier effect measured in BT-20 cells where 98% of cells were lost (Fig. 10A). This was however after 72 hours indicating that cell loss due to

paclitaxel increases over time. Our aim, in only treating cells for 24 hours, was to minimise any effects that prolonged hypoxia may have on the cells.

The effect of ESE-one, ESE-15-one, and EE-15-one were subsequently assessed in monolayer cell cultures (Fig. 14B-D). Treating the cells with increasing concentrations did not result in consistent differences in sensitivity towards the compounds of cells when in hypoxia even though at some data points a small change was observed. Overall, we saw no movement of the curve to the left which would indicate altered sensitivity.

Table VI. IC50 values for BT-20 cells treated with compounds over 24 hours in normoxic or hypoxic conditions.

	BT-20	
	Normoxia	**Hypoxia**
Paclitaxel (nM)	1411	568.9
EE-15-one (μM)	5.47	2.86
ESE-15-one (μM)	11.84	12.95
ESE-one (μM)	22.24	11.11

3.4 THE ADHESIVE PROPERTIES OF MONOLAYER VERSUS SPHEROID CULTURE EXPLAIN THE DIFFERENTIAL EFFECTS OF EE-15-ONE

3.4.1 Cell adhesion of monolayer cells is rapidly diminished by EE-15-one due to loss of focal adhesion formation

Cells attached to the rigid surface of tissue culture plates will form monolayers. These are characterised by flattened cells attached on the basal side to the plastic with some cell-cell adhesion between lateral sides and no attachment on the dorsal side. This type of adhesion scenario is rarely seen *in vivo*. Instead, epithelial cells within the upper layers of stratified epithelia will only attach via cell-cell interactions mediated by cadherins. The rapid loss of cell numbers seen in the crystal violet assays in Figure 10 suggested a possible effect on cell adhesion to the rigid substrate. To determine if the oestradiol derivatives induce cell rounding, cells were plated and then treated with either EE-15-one or ESE-15-one and images taken at different timepoints after addition. Rounded cells were identified and represented as

percentage of total cells (Fig. 15A). There was no significant increase in cell rounding in DMSO control treated cells. Interestingly, there was also no significant increase in cell rounding after treatment with ESE-15-one. In contrast, treatment with EE-15-one resulted in a rapid and large increase in cell rounding with 70% of cells already rounded after 2 hours.

The observed loss in cell adhesion after EE-15-one treatment was further investigated. It is generally understood that cells in monolayers attach to the cell culture plate surface with the help of integrin bearing focal adhesions that attach to the actin cytoskeleton. To visualise focal adhesions, we stained cells fixed with paraformaldehyde with antibodies directed against the focal adhesion constituent, talin. At the same time, a phalloidin stain was used to visualise the actin cytoskeleton (Fig. 15B).

The staining of untreated cells shows large focal adhesions spread throughout the cell and clearly attached to thick actin fibres. However, cells treated for 2 hours with EE-15-one have lost all focal adhesion localisation of talin, have become much less spread with only thin filopedia, and a lack of actin fibres. Importantly, a cytoplasmic staining of talin is observed in the treated cells suggesting the loss of talin from focal adhesions which would pre-empt the uncoupling of focal adhesions from the actin fibres. Together, this data suggests that EE-15-one causes a reduction in cell-to-substrate attachment through the disassembly of focal adhesions and the concomitant loss of cell tension through the dissolution of the actin fibres.

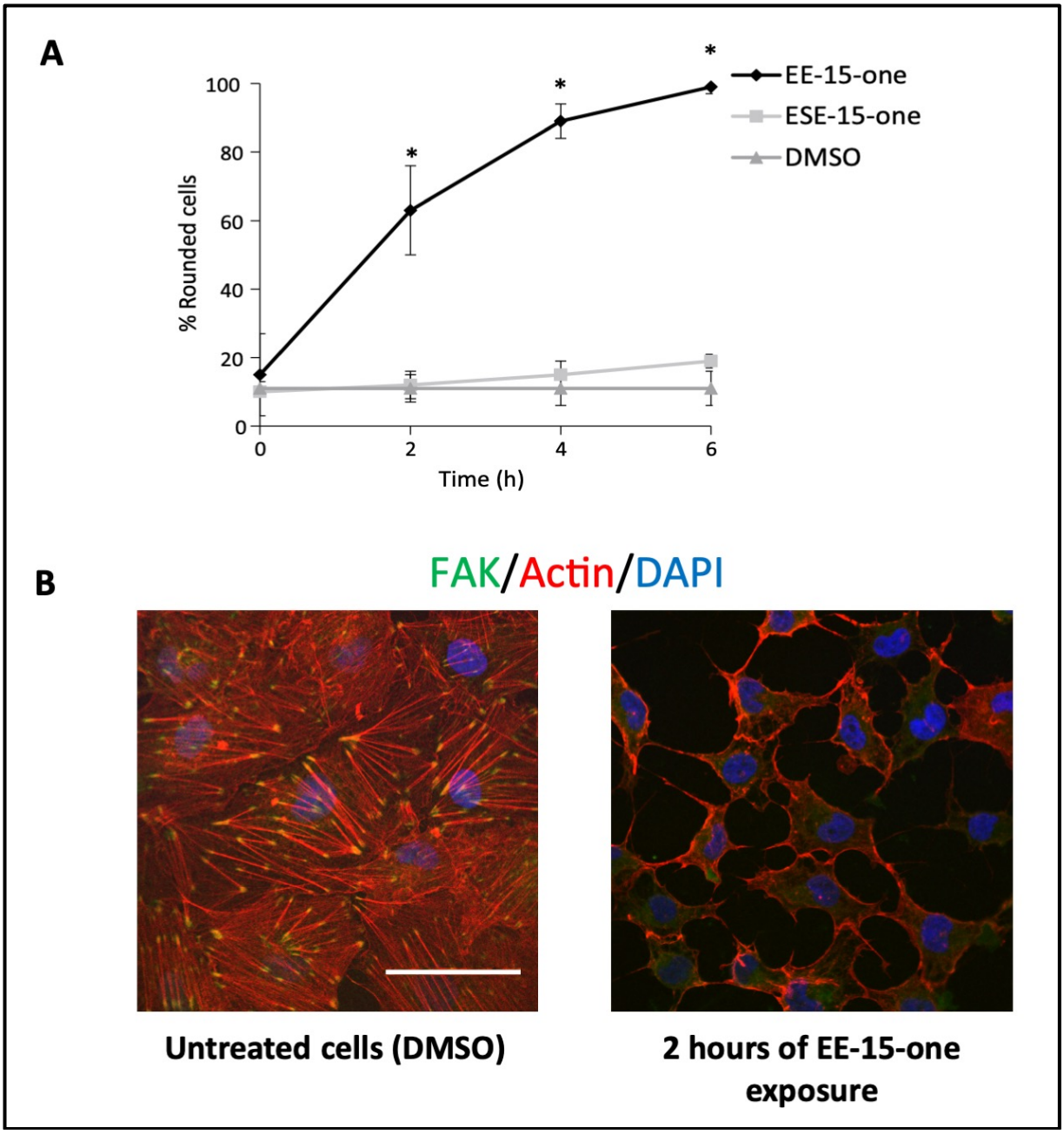

Figure 15. Effects of ESE-15-one and EE-15-one on cell rounding and adhesion complex formation in 2D monolayer cells.

(A) Cell rounding of cells treated with ESE-15-one and EE-15-one was measured 2, 4, and 6 hours after addition. Cells were categorised as rounded or spread using light microscopy and the percentage rounded cells were calculated. (B) Cells were treated for two hours with EE-15-one and fixed in paraformaldehyde before being incubated with anti-talin antibodies and secondary Alexa488 conjugated antibody (494 nm/ 519 nm), and TexasRed conjugated phalloidin (595 nm/ 615 nm).

3.4.2 Spheroids aggregate through the formation of cadherin junctions

Treatment of BT-20 cells with EE-15-one showed an almost binary effect in 2D and 3D with cells losing adhesion rapidly in 2D, while no effect on adhesion occurred in treated spheroids. Therefore, we hypothesised that the difference in effect of EE-15-one is due to differences in cell adhesion when cells are grown in 2D versus 3D. We, and others, show that cells in monolayers attach to the rigid cell culture surface by making use of integrin dependent focal adhesions.[53,197–200] Spheroids, on the other hand, are thought to aggregate through the use of cadherin dependent adherens junctions.[97,201–204]

To determine whether BT-20 cells grown as spheroids aggregate via cadherin dependent adhesions cadherin localisation was first visualised using an antibody directed against all cadherins. Spheroids were fixed with paraformaldehyde and processed for visualisation using a pan cadherin antibody and an Alexa 488 conjugated secondary antibody. Spheroids were imaged using confocal microscopy and visualised on a Zeiss LSM800 Meta confocal microscope.

These results suggest that cells within a spheroid have cadherin localised at the cell-cell borders with distinct staining along the cell periphery of cells within the spheroid was observed with no nuclear and very limited cytoplasmic staining suggesting that cadherin protein is present mostly at the cell-cell boundaries confirming that cadherin is in the correct locale to play its role in cell adhesion (Fig. 16). To ascertain if this cadherin also functioned as the adhesive structure to keep the integrity of the spheroid, cadherin function was modulated. Inhibition of cadherin activity was induced by removing the essential mineral calcium. Cadherins require the presence of calcium ions to interact with neighbouring cadherins to form strong homotypic adhesions between cells.[59–61] Calcium ions (Ca^{2+}) present in the growth medium were removed through chelation by the addition of ethylene glycol-bis(β-aminoethyl ether)-N,N,N',N'-tetraacetic acid (EGTA).[57] Ethylenediaminetetraacetic acid (EDTA) is also often used in the chelation of metals ions, but EDTA has been shown to have a higher affinity for magnesium ions (Mg^{2+}), while EGTA specifically targets Ca^{2+} over Mg^{2+}.[205,206]

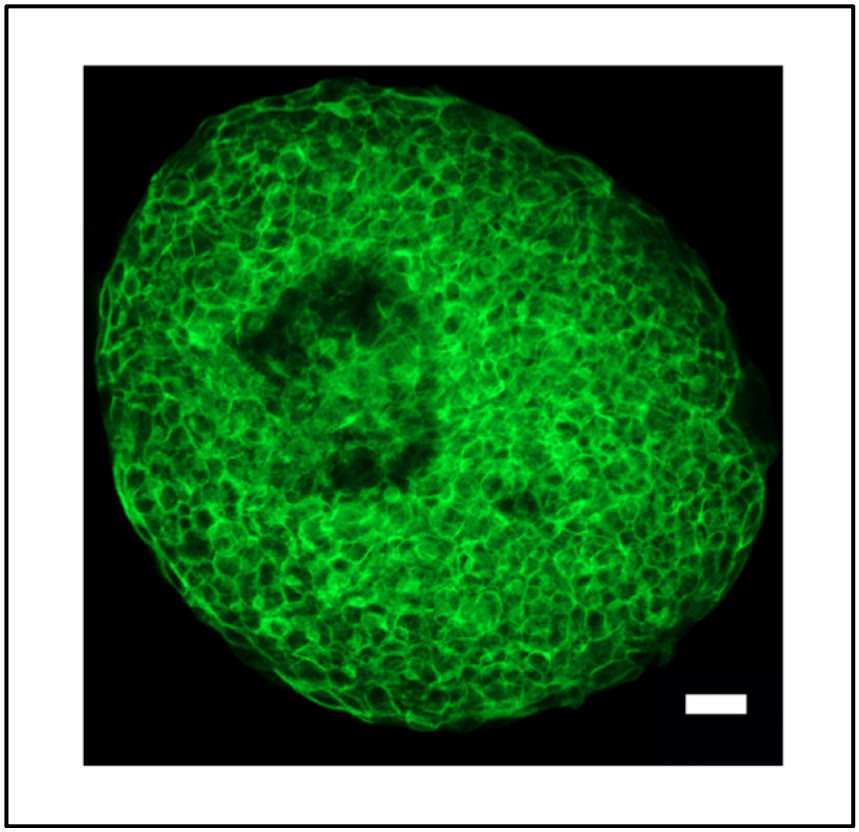

Figure 16. Cadherin localisation in BT-20 spheroids

BT-20 cells ($2x10^4$) were seeded into wells coated with 1% agarose and spheroids were allowed to form for 4 days. Spheroids were fixed with paraformaldehyde and stained with a pan-cadherin antibody and Alexa488 secondary antibody (494 nm/ 519 nm), and images were taken at a 20x magnification on a Zeiss LSM800 Meta confocal microscope (scale bar = 100 µm).

To test whether chelation affects spheroid adhesion, spheroids were grown for 4 days to allow formation and the chelating agent EGTA (2 mM) was added to the medium, alone, or in combination with a molar excess of calcium chloride ($CaCl_2$) for 24 hours (4 mM; 2:1 molar ratio to EGTA) (Fig. 17A). Light microscopy images were obtained 24 hours after each treatment. Untreated spheroids displayed the characteristic defined edge and dark core previously identified in BT-20 spheroids (Fig. 11). After exposure to EGTA for 24 hours the defined edge of spheroids was absent while numerous cells were loosely arranged around the spheroid core (Fig. 17A). The appearance of these spheroids suggests the loss of adhesion between cells resulting in the loss of aggregation. In contrast, spheroids exposed to EGTA in the presence of a molar excess of $CaCl_2$ retained a smooth outer perimeter with spheroids

similar in size to non-exposed spheroids although loose cells were observed around the spheroid (Fig. 17A).

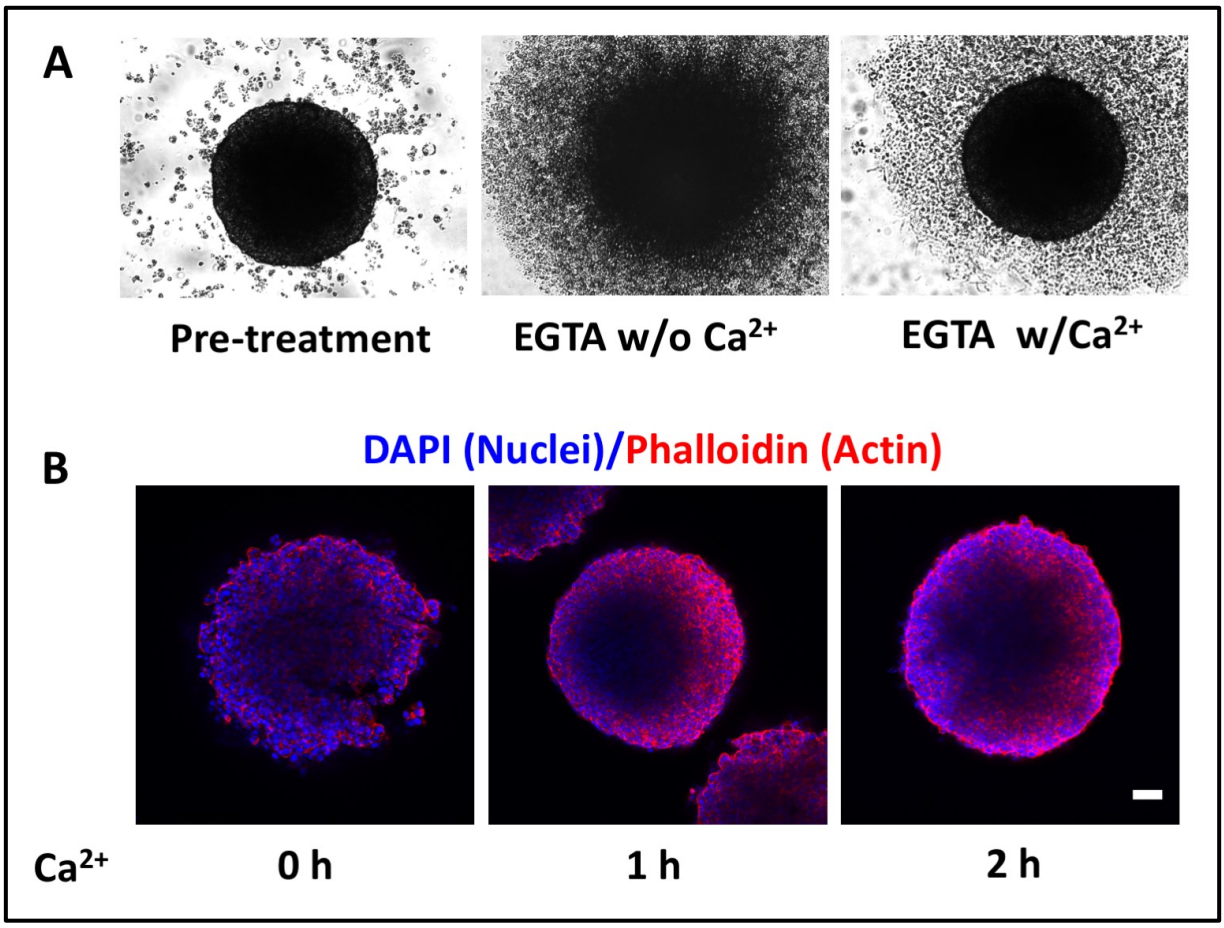

Figure 17. BT-20 spheroids aggregate using calcium dependent adherens junctions.

(A) BT-20 spheroids were exposed to 2 mM EGTA with or without 4 mM $CaCl_2$. Light microscopy images were taken at 0 hours and 24 hours after EGTA treatment. (B) Confocal images were obtained of BT-20 spheroids stained with TexasRed conjugated phalloidin (595 nm/ 615 nm) and DAPI (345 nm/ 455 nm) 0, 1, and 2 h after 4mM $CaCl_2$ was added to spheroids pre-treated with 2 mM EGTA for 3 h, images were taken at a 20x magnification on a Zeiss LSM510 Meta confocal microscope (scale bar = 100 µm).

To confirm that cells within the spheroids were dispersing after treatment with EGTA and to analyse the reversibility of such treatment, cells were stained with the actin fibre dye phalloidin-Atto 665 to display the structure of the spheroid, while nuclei were visualised with DAPI to provide an indication of the location of cells within the spheroid. Spheroids were first treated with EGTA (2mM) for 3 hours and subsequently with a molar excess of calcium ions ($CaCl_2$: 4 mM; 2:1 molar ratio to EGTA) for 1 hour and 2 hours. Spheroids were fixed at each

time point using paraformaldehyde and permeabilised with Triton X-100 after being washed with PBS. All spheroids were processed for confocal microscopy (Fig. 17B). The spheroids were stained with DAPI and fluorescently conjugated phalloidin, washed and mounted on a microscope slide with 1 mm silicon borders to avoid compression.

Spheroids exposed to EGTA for 3 hours showed compromised spheroid integrity since cell-cell distances were increased and the actin cytoskeleton was no longer continuously present along the cell periphery as can be seen in the first confocal image in Figure 16B. Upon introduction of a molar excess of $CaCl_2$, cells became tightly packed and a continuous actin cytoskeleton became visible around each cell (Fig. 17B). This occurred within 1 hour after addition of $CaCl_2$ with only a few areas of spheroid peripheries remaining uneven. After 2 hours all spheroids returned to their original appearance with a smooth perimeter. Therefore, calcium plays an important role in spheroid cell aggregation and its removal leads to a reversible dispersal of cells from the spheroid which can be reversed by reintroducing calcium. Thus, we suggest that BT-20 cells aggregate in spheroids using cadherin mediated adhesion.

To determine if BT-20 cells grown in a 2D monolayer cell culture environment attach through Ca^{2+} dependent cell adhesion using cadherins, cells grown in monolayers (100% confluent to insure all cells were in contact with neighbouring cells) were treated with 2mM EGTA for 24 hours, with or without the addition of 4 mM $CaCl_2$ (Fig. 18A). Untreated control cells and cells exposed to EGTA in combination with a molar excess of $CaCl_2$ formed a continuous monolayer of well-spread cells attached to the substrate and to each other. Cells treated with EGTA alone, on the other hand, were less spread and were no longer attached to each other but still adhered to the plastic of the culture dish (Fig. 18A). This suggests that the cells use a different adhesion mechanism, possibly integrins, to attach to the surface of the culture dish. Conversely, inhibition of cadherin via EGTA resulted in cells detaching from one another but remaining attached to the plate.

The loss of cell-cell adhesion in monolayer cells was found to be reversible. The addition of 4mM $CaCl_2$ after an initial exposure to EGTA reversed the effects allowing cells to spread again and form cell-cell adhesion within 4 hours (Fig. 18B).

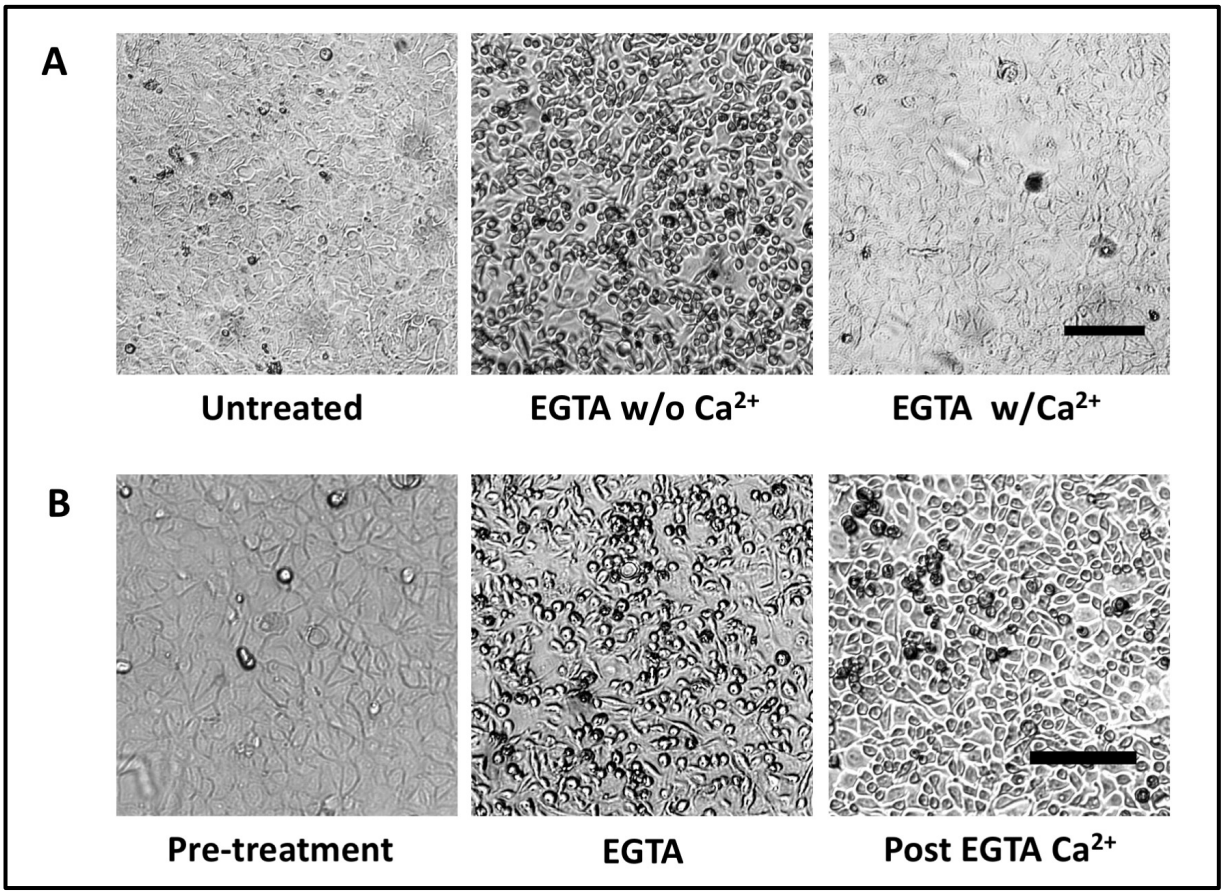

Figure 18. BT-20 monolayer cells adhere via calcium-independent adhesions.

(A) Monolayer BT-20 cells were exposed to 2 mM EGTA for 24 h with or without 4 mM $CaCl_2$. Light microscopy images were taken at 0 h and 24 h after treatment. (B) Monolayer BT-20 cells treated for 24 h with 2 mM EGTA were subsequently exposed to 4 mM $CaCl_2$ for 4 hours. Light microscopy images were taken before exposure, after EGTA exposure and after 4mM $CaCl_2$ addition using a Zeiss Axiovert CFL40 fluorescent microscope at 5x magnification (scale bar = 100 μm).

Together this data suggests that cells grown in 3D as spheroids aggregate through calcium dependent cadherin adhesions while cells grown in monolayer attach to the plastic cell culture flask in a calcium independent manner. Therefore, we hypothesise that the difference in response of cells to EE-15-one is correlated with the absence of integrin mediated adhesion found in BT-20 spheroids.

3.5 INVESTIGATION OF THE POTENTIAL USE OF THE SPHEROID BREAST CANCER MODEL FOR IDENTIFYING POTENTIAL OFF-TARGET EFFECTS TO ASSIST THE DEVELOPMENT OF ANTI-MALARIAL COMPOUNDS

3.5.1 Assessing the effects on cell survival of potential anti-malarial compounds in BT-20 cells grown in monolayers and as spheroids

While the spheroid system can be used to identify effective compounds targeting breast cancer cells, we believe it can also be used as a first pass screen to identify novel compounds targeting non-human organisms such as malaria that may harbour significant non-specific effects in mammalian cells. To test this idea a number of novel compounds designed by Dr. Andre Stander from the Department of Physiology at the University of Pretoria targeting malaria were obtained and tested using this system. These compounds were tested to determine their effect in mammalian cells by using the paired BT-20 2D monolayer and 3D spheroid systems.

Two compounds were obtained for testing, W12 and W41, which are potential lead compounds based on bromodomain inhibitors, which have been shown to potentially stop the growth of several parasites, including the malaria parasite *Plasmodium falciparum*.[207–209] BT-20 cells were seeded into monolayers in a 96-well plate to determine dose response curves for the new anti-malarial and anticancer compounds. The cells were treated for 72 hours with a range of concentrations as well as a DMSO vehicle control. Crystal violet was used to stain the cells that remained as described above and values were normalised to cells with medium only. EC50 values for BT-20 cells exposed to W12 and W41 are listed in Table VII for reference.

Table VII. EC50 values for BT-20 cells treated with anti-malarial compounds over 72 hours.

Compound	EC_{50}
W12 (mM)	24.83
W41 (mM)	53.10

The two anti-malarial compounds, W12 (Fig. 19A) and W41 (Fig. 19B) both affected BT-20 cells grown in 2D at micromolar concentrations. Cells exposed to W12 showed a significant reduction in cell number of 31% when exposed to 10 µM when compared to vehicle control, while further decreases in cell number were measured at 20 µM (49% reduction) and at 30 µM (59% reduction) (Fig. 19A, * $P<0.001$). Similarly, W41 exposure led to a reduction in cell number of 18% at 5 µM and 21% at 10 µM although these changes were not statistically significant. However, the 31% reduction measured at 20 µM and further reductions of 39% at 40 µM and 52% at 60 µM were all significant and indicate that in 2D both these compounds have non-specific, anti-proliferative effects on BT-20 cells at modest micromolar concentrations.

Results obtained in the 2D cell culture system were compared to effects measured in 3D to determine if the original assessments were informative for further development of these compounds. To test whether the anti-malarial compounds did indeed have antiproliferative effects on mammalian cells, BT-20 spheroids were exposed to 20 µM W12 or 20 µM W41. At this concentration, significant decreases in cell viability were observed in 2D cultured cells. BT-20 cells were grown in a 96-well plate coated with 1% agarose for 4 days and treated for 72 hours, light microscopy images were obtained at Day 4, 7, and 15 (Fig. 19A). Shape corrected spheroid volume was calculated with the volumes measured at day 4 normalised to 100%. (Fig. 19B). DMSO was used as a vehicle control. Spheroids exposed to the vehicle control did not significantly change in volume over the 15 days measured (Actual volumes - Day 4: 5.7×10^8 $\mu m^3 \pm 4.2 \times 10^7$ μm^3 vs Day 15: 5.6×10^8 $\mu m^3 \pm 8.1 \times 10^7$ μm^3, ns $p>0.999$).

Spheroids exposed to 20 µM W41 did decrease somewhat in volume (21%) by day 7, but this decrease was statistically insignificant due to variation in spheroid size (Fig. 19B - Actual volumes – Day 4: 6.4×10^8 $\mu m^3 \pm 1.2 \times 10^7$ μm^3 vs Day 7: 5.1×10^8 $\mu m^3 \pm 8.5 \times 10^7$ μm^3, ns $p>0.999$). Spheroid volume did increase after this initial decrease to reach an average of 87% of their original volume with no significant difference in volume between the treated and vehicle control treated spheroids by day 15 (Fig. 19B - Actual volumes Day 15 - DMSO: 5.6 x

10^8 µm^3 ± 8.1 x 10^7 µm^3 vs W41: 5.4 x 10^8 µm^3 ± 4.3 x 10^7 µm^3, ns *P*>0.999). The results suggest that while there may be an initial, small response to W41, no significant decrease in cell number is observed after prolonged growth.

Exposure of BT-20 spheroids to 20 µM of W12 for 72 hours did not have an effect on spheroid volume when compared to vehicle control spheroids (Actual volumes Day 4: 6.4 x 10^8 µm^3 ± 1.2 x 10^7 µm^3 vs Day 7: 6.4 x 10^8 µm^3 ± 1.2 x 10^7 µm^3, ns *P*>0.999). However, at 15 days post exposure, W12 exposed spheroids increased significantly in volume by 28% (Fig. 19A), Absolute values – Day 7 6.4 x 10^8 µm^3 ± 1.2 x 10^7 µm^3 -. Day 15 8.1 x 10^8 µm^3 ± 1.2 x 10^7 µm^3 (Fig. 19B; **P*<0.001). These data contrast the data obtained in 2D where BT-20 cells displayed reduced viability when exposed to 20 µM W12. Therefore, W12 exposure in micromolar concentrations inhibits cell viability in 2D while it leads to increased spheroid volume in 3D cultures. This effect could be potentially dangerous if this compound were to be used as an anti-malarial, as it could cause increased cell growth in human cells.

In summary, our data show that the use of 3D cell cultures of BT-20 spheroids can be used as an effective first pass screen to determine if novel compounds with potential anti proliferative activity will have an impact within 3D tissues or whether their effectiveness in 2D is an artefact of the culture system. At the same time, the spheroid system can also be used to determine the presence of unintended side effects with a much lower false positive rates, which will prevent the unnecessary removal of lead compounds due to off-target effects. The anti-proliferative effects are observed at relatively high concentrations and further experimentation would be needed at lower concentrations if these compounds showed promise in other avenues. It would be advisable to retest these samples on a range of different cell types.

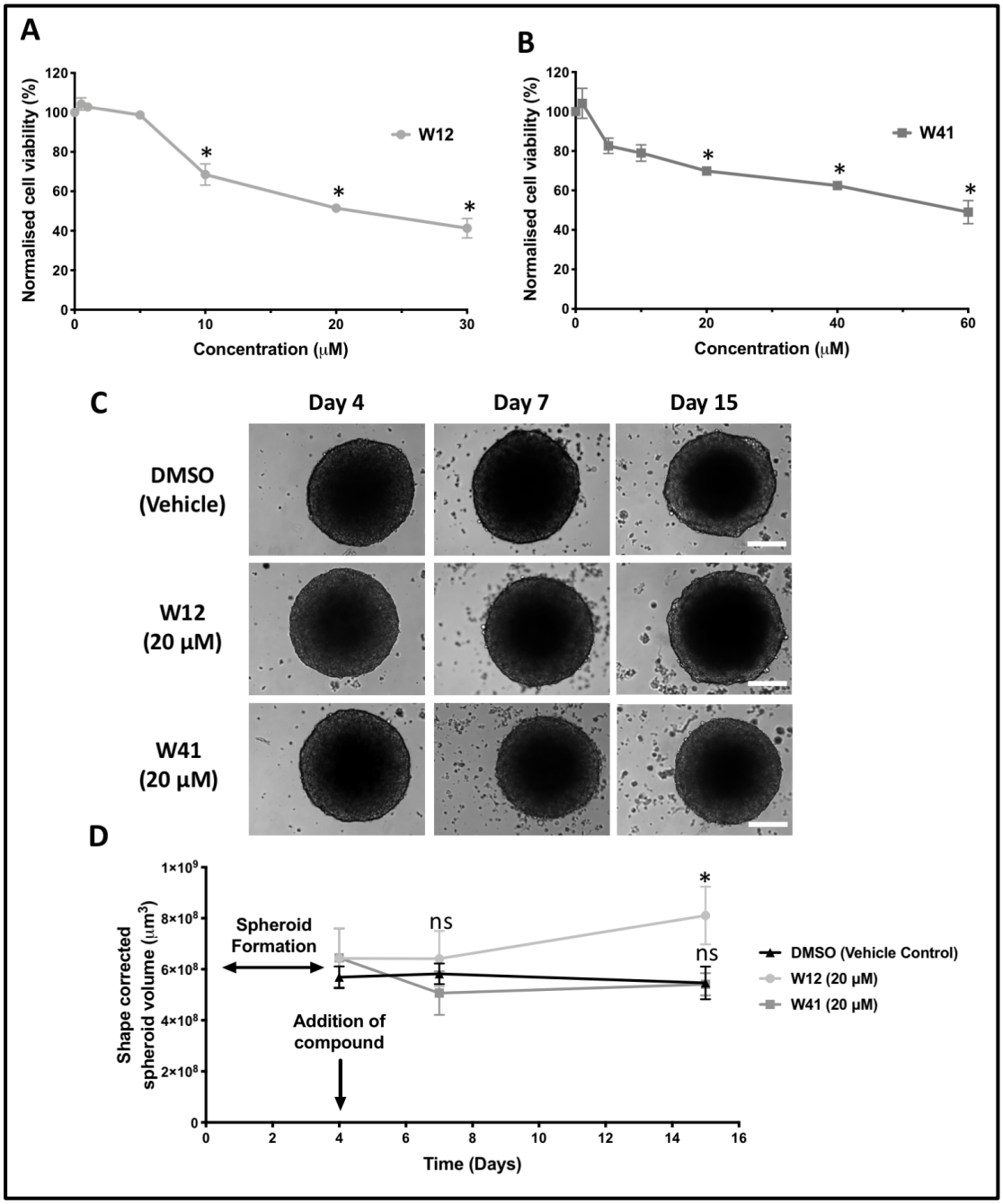

Figure 19. BT-20 cell survival in monolayer after exposure to anti-malarial compounds.

Cell viability of BT-20 cells exposed to W12 (A) and W41 (B) was measured using crystal violet staining. BT-20 cells (1×10^4) were seeded and allowed to adhere overnight. The cells were exposed to a range of concentrations of W12 and W41 for 72 hours. Cells were fixed and stained with crystal violet and solubilised with triton X-100. Optical density was measured at 570 nm using an EL_x800 Universal Microplate reader. Graphs represent the average of three independent repeats, error bars indicate s.e.m Significant differences are indicated with an asterisk (*P<0.001). (C) BT-20 cells (2×10^4) were seeded into wells coated with 1% agarose and left to form spheroids over 4 days. The spheroids were exposed to 20 µM W12 or 20 µM W41 for 72 hours. Light microscopy images were taken at day 4, 7, and 15 using a Zeiss Axiovert CFL40 at 10x magnification (scale bar = 200 µm). (D) Spheroid volumes were measured over 15 days. Each point is representative of 32 independent repeats, error bars indicate standard deviation. Significant differences are indicated with an asterisk (*P<0.001).

3.6 DEVELOPMENT OF A COMPLEX SPHEROID SYSTEM TO INCORPORATE TUMOUR HETEROGENEITY

3.6.1 Development of a co-culture spheroid system of BT-20 and MDA-MB-231 cells

While BT-20 spheroids represent an improvement in terms of recapitulating the *in vivo* tumour environment it remains far removed from the actual *in vivo* conditions. One important issue is the lack of heterogeneity of cancer cells within these spheroids. Breast cancer tumours are heterogeneous *in vivo* due to rapid mutation rates and the establishment of multiple subpopulations within the tumour. To start to address this issue, we were determined to establish a co-culture spheroid system between the non-metastatic BT-20 cell line and the metastatic breast cancer cell line MDA-MB-231 to determine if they would form useful spheroids and to investigate how each cell line would behave.

To distinguish between BT-20 and MDA-MB-231 cells, green fluorescent protein was expressed in MDA-MB-231 cells. A stable cell line was generated by transferring a Green fluorescent protein (GFP) gene into the genome of the cells by lentiviral delivery and integration. Subsequently, positive cells were selected twice by flow cytometry to establish a stable GFP expressing cell line. Attempts to generate a BT-20 cell line stably expressing a red fluorophore were unsuccessful as BT-20 cells seemed to not be amenable to lentiviral infection.

To determine if a co-culture spheroid would form reliably, non-labelled BT-20 cells and GFP expressing MDA-MB-231 cells were trypsinised and resuspended before they were mixed together and plated into the agarose prepared 96 well plates and allowed to form spheroids (Fig. 20A). Cells were mixed in ratios of 1:1, 3:2, 7:3, or 4:1 BT-20 cells to MDA-MB-231 cells before plating (Fig. 20B). Spheroids were allowed to form for 4 days after which they were photographed using a light microscope to assess their formation, shape, and density. After four days spheroids plated in a 1:1 ratio, 3:2 ratio, and 7:3 ratio was inconsistent in shape and roundness with distinct protrusions of cells forming on the surface of the spheroid. Spheroids plated in a 4:1 ratio displayed improved reproducibility and roundness and had little to no

projections of cells forming. It therefore seemed that this ratio gives spheroids with desirable characteristics for further analysis (Fig. 20B).

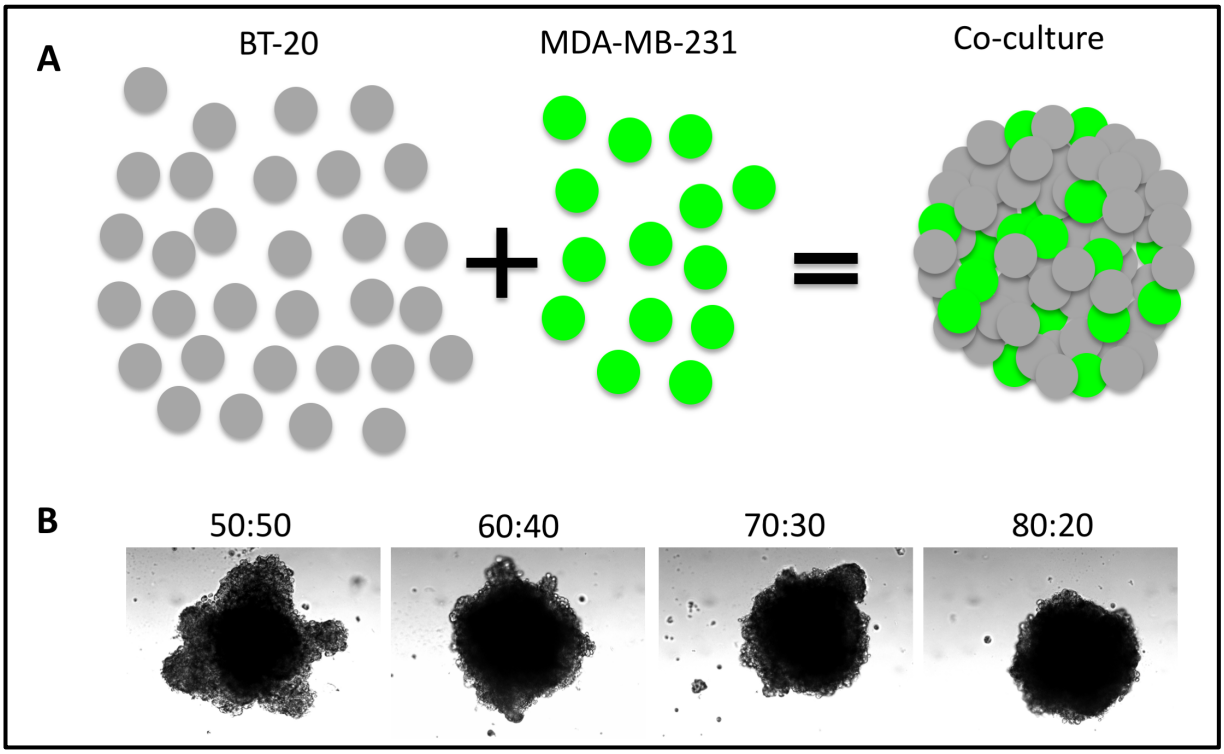

Figure 20. Establishment of a co-culture spheroid culture system.

(A) BT-20 cells were mixed with GFP expressing MDA-MB-231 cells and incubated for four days to form a co-culture spheroid. (B) Several ratios ranging from 50:50 to 80:20 of BT-20 to MDA-MB-231 were tested and images were taken at day 4 using a Zeiss Axiovert CFL40 at 10x magnification.

3.6.2 MDA-MB-231 cell behaviour within the spheroid relates to its migratory ability

To determine if MDA-MB-231 and BT-20 cells would behave differently in spheroid cultures, 4:1 ratio spheroids (BT-20 to MDA-MB-231) were generated with the GFP expressing MDA-MB-231 cell line. These spheroids were transferred to a glass bottomed incubation chamber which allowed for the visualisation of the cells on a Zeiss LSM 800 confocal microscope with temperature control. Spheroids were imaged using the 20X objective and the 488-laser light to visualise the MDA-MB-231 cells while light microscopy images were also taken at the start and end of the live imaging session. The plating of the spheroids onto a glass surface provided a substrate for cells to potentially adhere to and utilise for migration.

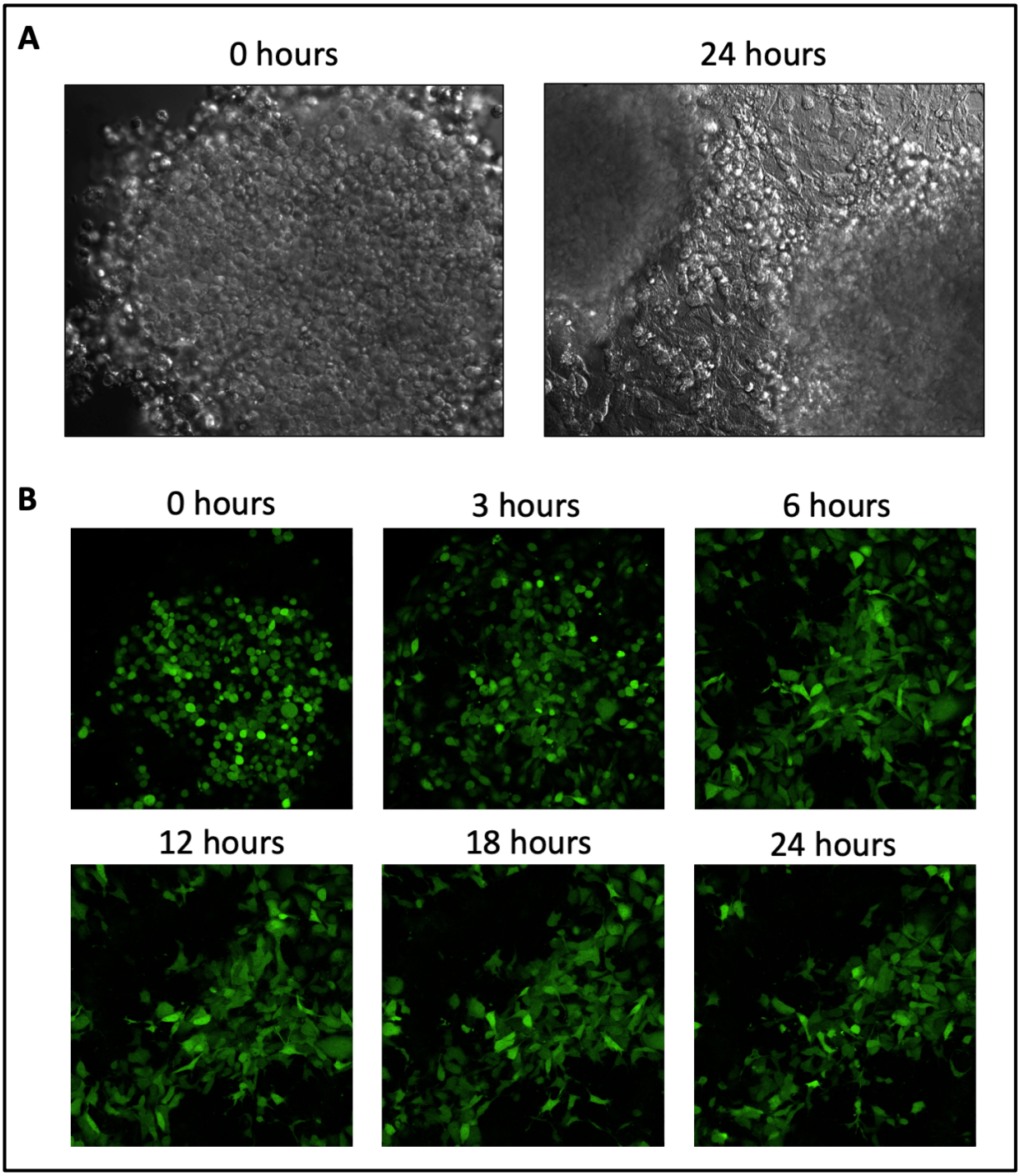

Figure 21. MDA-MB-231 cells migrate out of the co-culture spheroid.

Fluorescently labelled MDA-MB-231 breast cancer cells were cultured with unlabelled BT-20 in an 80:20 ratios in a 96-well plate coated with agarose. Cells were incubated for four days, after which each spheroid was analysed with the Zeiss Axiovert CFL40 fluorescent microscope and Zeiss Axiovert MRm monochrome camera with a 5x magnification. The co-culture was moved to a live imaging container in the Zeiss 510 META confocal laser microscope (Oberkochen, Germany) to determine the effect of the cells over several hours and overnight.

Initial images show spheroids that were round (Fig. 21A, 0 hours) and had a relatively homogenous distribution of MDA-MB-231 cells throughout the spheroid (Fig. 21B, 0 hours). MDA-MB-231 cells also appeared round without any visible protrusions. After 3 hours many MDA-MB-231 cells had become elongated with protrusions and started to migrate away from the spheroid while some remained round. However, by 6 hours all cells were migratory with many cells escaping from the spheroid onto the glass. The light microscopy image after 24 hours reveals that the majority of BT-20 cells (Fig. 21A) were assumed to have remained compact and bound together in the remnants of the spheroid, while most MDA-MB-231 cells had escaped and appeared flat and motile on the glass surface.

While this data remains preliminary it does show that the two cell lines behave very differently with the metastatic MDA-MB-231 cells escaping and migrating away from the spheroid, while it seems that the non-metastatic BT-20 cells remain tightly linked together in the remnants of the spheroid. This could, however, only be confirmed if the BT-20 cells are labelled along with the MDA-MB-231 cells.

CHAPTER 4

DISCUSSION

4 DISCUSSION

4.1 ESTABLISHMENT OF A RELIABLE, COST-EFFECTIVE 3D BREAST CANCER MODEL FOR COMPOUND SCREEN AND DRUG DEVELOPMENT

4.1.1 Drug development and identifying a niche

Drug development is a cash-intensive endeavour with a low success rate and long timeframes between identifying a lead compound and a clinically proven drug reaching the market. This is especially true in cancer drug development because the target is the body's cells. This results in a range of mild to severe side effects, specifically adverse effects, due to the drug's impact on healthy cells. The presence of harmful side effects along with clinical lack of effect on the tumour are common reasons for the termination of clinical trials.[85] While side effects are hard to predict, clinical efficacy should ideally be accurately predicted with *in vitro* models that better recapitulate the *in vivo* tumour setting. To shorten development time and decrease cost, it is therefore essential that initial screening of lead compounds accurately identifies those compounds that are most effective in treating cancer. In the cancer research industry, 2D cell culture has traditionally been used to study the efficacy of lead compounds.[82] However, due to the lack of 3D structure found in these simplified systems, the absence of cohabiting cell types, and the lack of appropriate soluble factors such models often fail to predict the potential cancer-killing ability of lead compounds accurately.[210]

Improving this initial screening capability has been a constant area of research where a large number of different models have been developed over the past several decades. One such model is the cancer spheroid model where cancer cells grown as cell lines are induced to grow into 3D structures. Cancer cell spheroid systems using an array of methodologies have been proven to mimic *in vivo* micro tumour conditions, expressing cell signalling markers typically found in cancer tissue, and exhibiting behaviour observed in primary cancer tissue. These behaviours include increased chemoresistance and reduced cell division rate, as well as the presence of complex tumour microenvironments with the expression of cell adhesion proteins.[85,211,212] For these reasons, spheroids have become an attractive 3D cell culturing

system for use in high throughput screening systems when looking for lead compounds during drug discovery development.

There are several different described protocols for producing spheroids. Each methodology has its strengths, but a variety of weaknesses have also been identified. Such weaknesses include high labour intensity, prohibitive expenses, lack of reproducibility, or the need for specialised and often expensive equipment or culture additives such as bioreactors or manufactured extracellular matrices.[213] The issue with the cost of spheroid culture is especially pressing in the academic research environment in Southern Africa where a lack of funding compels researchers to turn over every penny. It is often in these academic environments that lead compounds are identified, studied and elucidated. Still, in many cases, these compounds do not manage to move forward into the next stages of drug discovery due to the high costs of many of these methodologies.

4.1.2 Choosing BT-20 triple negative breast cancer cells to develop a 3D spheroid model

This prompted us to identify a cell line amenable to spheroid culture at the lowest cost but with the highest reproducibility and ease-of-use, so that it would be useful not only in our research group but could easily be adapted by others as well. To establish this particular cost-effective, reliable, reproducible, and easy-to-use spheroid culture system, we needed to identify a suitable cell line first. We chose to focus on breast cancer cell lines since our research focuses on breast cancer, and these were readily available cell lines that were well characterised. Previous studies showed that MDA-MB-231 cells did not readily form spheroids, while MCF-7 cells formed the best spheroids in hanging drop plates supplemented with cellulose ethers.[154] In this study, we compared the spheroid forming capability in a liquid overlay system of the ER-positive and TNBC metastatic cell lines, MCF-7 and MDA-MB-231, with a TNBC non-metastatic cell line, BT-20.

To remain cost-effective, we aimed to establish a low-cost and straightforward measurement methodology that easily and quickly predicted whether cell survival or growth within a

spheroid was affected by compounds. A prerequisite of such a measurement system was that the spheroids would form in a reproducible manner and be spherical enough to allow for perimeter measurements and thus accurate volume calculations that could be used to deduce effects on cell survival within the spheroid. To test this concept, we grew a large number of BT-20 spheroids from the same initial cell number and measured their volume at different time points as described in the results (Fig. 7B and Fig. 8A-D). Adjusted volumes were calculated from circumference and area measurements taken from light microscopy images using ImageJ analysis software. The volume calculations used were taken from previously published work describing how to calculate volume adjusted for small deviations in the spherical shape of spheroids by Friedrich *and colleagues.*[94,156] These represent a set of simple calculations to determine shape factor, spherical volume, and shape corrected volume.

BT-20 cells were explicitly chosen because, in 2D cell culture, these cells formed tight epithelial islands, which suggested that they may readily form spheroids as well. Qualitatively, BT-20 cells formed very smooth and regular spheroids that appeared to be consistently spherical. Our analysis of the measurements shows that BT-20 spheroids are highly spherical with shape factors above 0.9. Furthermore, these cells form reproducible spheroids that do not change significantly in size over time. The lack of further compaction of the spheroids could potentially be due to the strength of initial adhesion that BT-20 cells generate when aggregating. While the exact mechanism of spheroid formation was not proven during this study, we suggest that BT-20 cells may be able to form strong cadherin based adherens junctions as they aggregate (Fig. 16-17). This would lead to immediate compaction of the spheroid, and no further decrease or increase in size. The lack of volume increase in spheroids suggests that cells within a spheroid may not be as proliferative as they are in monolayer resulting in a balance between cell proliferation and cell death. However, it has to be mentioned that in 2D BT-20 cells have a doubling time of around 60 hours in contrast to MDA-MD-231 cells which doubles every 33 hours.[214] Nonetheless, for screening purposes a lack of rapid compaction or spheroid expansion could be advantageous and BT-20 spheroids certainly show consistency in volume over time. Overall, our expectation that a non-metastatic and non-migratory breast cancer cell

line would form the most compact and reproducible spheroids was met. To our knowledge, there is only one other group working on BT-20 spheroids, and this group are using a similar low adhesion plate for growth of these spheroids, although they have only published two studies to date.[149,215]

In accordance with previous data[103], MDA-MB-231 cells failed to form compact spheroids, instead forming thin flat islands of cells that did not seem to aggregate into a spheroid shape (Fig. 7A). These islands were impossible to measure and were inconsistent in shape and size despite the same number of cells being seeded in each well. It was decided at this point that in this situation, MDA-MB-231 cells were unlikely to be useful for this specific simplified spheroid model.

MCF-7 cells, on the other hand, did form spheroids using this method, but these spheroids were also inconsistent and not spherical, making accurate measurement difficult (Fig. 7A). With this said, when MCF-7 cells were grown for much longer time frames (upwards of 30 days) compact spheroids did eventually form however they were still inconsistent and difficult to measure (data not shown). We postulated that the cells in the MCF-7s spheroids grown for extended periods might be necrotic, although we did not confirm this in any manner and did not pursue this further. We do, however, believe that this cell line has excellent potential for further research. While these spheroids would be potentially difficult to work with in regards to spheroid measurement, these spheroids are easily imaged using confocal microscopy, and it should also be noted that these cells are metastatic. As metastasis is a predominant cause for high cancer mortality rates worldwide, these cells would provide another important aspect for study using spheroid models. It is perhaps this metastatic potential that prevents the cells from forming compact, consistent spheroids using the liquid overlay method. These cells are however widely used for cancer research and have successfully used with different techniques such as the hanging drop method.[156]

Overall the first hypothesis stated in this study was that breast cancer cells could be used to set up a 2D monolayer - 3D spheroid culture model and we believe that while there can be several improvements to the model as it currently stands this hypothesis was confirmed to be true. Breast cancer cells can be used to set up a cell culture model.

4.1.3 Limitations identified with the use of this methodology

Using a 3D spheroid breast cancer cell culture method has the potential to improve the screening of anticancer compounds. Our own data shows that it is better able to eliminate non-effective compounds when compared to screening using 2D monolayer cell culture. However, the method still retains some limitations that we identified, and these should be addressed in further studies. The BT-20 cells, while forming compact spheroids, are non-metastatic and have a low growth rate, which may be beneficial for an initial testing environment but may not be representative of all the types of breast cancers. However, it is a triple negative breast cancer cell line against which there are few current therapies which counts in its favour. Nonetheless, ideally, compounds should be tested on an array of different breast cancer cell lines. We believe that the methodology described in this thesis has the potential to be applied to the growth of spheroids using many different cell lines.

The spheroids were set up using a low attachment surface using agarose, and while this is a cheap and easily available option, this system lacks an external tumour matrix. Matrices such as collagen lattices are known to affect cell behaviour.[216,217] Unfortunately, generating reproducible scaffolds is difficult and time-consuming while others are prohibitively expensive and unrealistic in smaller labs but may be necessary to expand and improve the model. Thus, a drawback of the current model is the lack of extracellular matrix induced signalling.

It is commonly understood that spheroids do form necrotic cores once they pass a volume threshold, which is in line with what is found in many epithelial tumours. The cadherin staining of a BT-20 spheroid suggests that these spheroids also contain a necrotic core although direct proof has not been obtained yet. The measurement methodology used to calculate spheroid

volume, while relatively quick and easy to use, does not discern between loss of live cells or the expulsion of necrotic cells. Better visualisation techniques and identification of live and dead cells will help to better assess effects on proliferation and cell death.

FDA/PI staining was used with fluorescence microscopy to provide information regarding the status of cells before and after drug treatment. Using the standard fixation techniques introduced signal loss from the centre of the spheroid due to the interference of certain proteins and lipids with the emission light of the compounds used. Additionally, the depth light can reach within these spheroids is limited when using standard confocal microscopy thus keeping the interior of the spheroid hidden from view. New methods in clearing of the spheroid along with alternative instrumentation such as two photon technology could reduce this opacity and allow a view throughout the spheroid to allow the visualisation of all cells and their proliferative status. Single cell analysis of the spheroid to ascertain each cell's proliferative status or an overall metabolic health indicator could also be used to determine the spheroids overall health before and after treatment. The proliferation of the spheroids could then be assessed over time. Verified apoptosis testing could provide more insight into the growth rate of the spheroids. These methods can be pursued further to substantiate the model and validate that the loss in cell spheroid volume is directly correlated to increased cell death or reduced cell proliferation.

4.2 BT-20 SPHEROID CULTURE REVEALS SOME COMPOUNDS ARE INEFFECTUAL IN 3D.

4.2.1 Spheroid culture confirms the anti-proliferative effect of sulfamoylated 2-methoxyestradiol derivatives.

It has been established previously that several sulfamoylated derivatives of the oestrogen metabolite 2ME reduce cell proliferation of numerous cancer cell lines by arresting cells at the G2/M border of the cell cycle.[141,146,218,219] Indeed, BT-20 monolayers also responded to these compounds with exposure to the sulfamoylated compounds leading to decreased proliferation and increased cell death (Fig. 10). With the spheroid model in place using the BT-20 cells we were keen to establish whether these compounds were as effective at inhibiting cell division processes in 3D cell culture and if they were able to penetrate multiple cell layers.

Before testing the efficacy of these novel compounds we were keen to determine if commonly used chemotherapeutic agents did affect BT-20 cells similarly in 2D and 3D. This was done to ensure that compounds known to affect tumours *in vivo* also affected spheroids *in vitro*. Indeed, our data shows that paclitaxel and colchicine were both effective in inducing cell death in 2D and 3D cultures of BT-20 cells and FDA/PI staining clearly showed a huge increase in cell death in these treated spheroids. This data suggests that known effective compounds induce cell death in BT-20 cells. Thus, it is possible to make a prediction of potential efficacy of compounds in an *in vivo* setting based on the effect in spheroids.

Subsequently, the sulfamoylated 2ME derivatives were tested on BT-20 spheroids and spheroid volume decreased in line with what was observed in 2D. Furthermore, FDA/PI staining confirmed an increase in apoptotic cells suggesting that these compounds can induce cell death in BT-20 cells regardless of the culture setting. This provides strong evidence that these compounds should be tested in pre-clinical *in vivo* models. It is important to note that even though effects were observed in 2D and 3D they were of a different order than paclitaxel suggesting that the mechanism employed may differ from that of paclitaxel. This is interesting because paclitaxel is known to stabilise microtubules rendering the mitotic spindle assembly impeded.[220,221] Data published by our group previously shows that these compounds have a large effect on microtubule organisation especially on centrosomes.[142,144,146,222] Such

differences may relate to the efficacy and temporal differences seen in cells treated with paclitaxel or 2ME derivatives. Suffice to conclude that the compounds tested were effective in 2D and 3D. Future *in vivo* investigation may reveal whether these compounds are then also effective in preclinical models pointing to an enhanced predictive value of the spheroid system.

4.2.2 The differential effect of the non-sulfamoylated 2ME derivative, EE-15-one, in 2D and 3D indicates the value of a spheroid screening program

From a large panel of compounds designed and generated as derivatives of 2ME, only one compound not modified by the addition of a sulfamoyl moiety had any effect in cancer cell lines.[223] EE-15-one acted differently from the other effective compounds in 2D in that it induced a very rapid loss of cells albeit at micromolar concentrations whereas the sulfamoylated compounds induced only incomplete cell loss after at least 48 h. Indeed, we show here and in a recent publication that unlike the blockage in cell cycle induced by the sulfamoylated derivatives, EE-15-one affects cell adhesion by inhibiting the ability of cells to remain adhered or to adhere to rigid surfaces. This loss in cell-substrate adhesion will result in eventual cell death.[224] Thus, we have identified a compound with an unique mode of action.

When grown in spheroids, epithelial cancer cells aggregate via cadherin dependent adhesion. Alternatively, initial aggregation and subsequent adhesion modulation can involve a mix of adhesion types. This complexity better mimics the tumour microenvironment found *in vivo*.[11,82,91,92] We showed in our experiments that the BT-20 cell spheroids aggregate and attach via cadherin adhesion. Using the calcium chelator EGTA we interrupted cadherin-dependent adhesion by removing the calcium cadherins depend on for adhesion. This led to a rapid dissociation of the spheroid. This effect was reversible, and addition of calcium allowed cells to aggregate once again. Additionally, excess calcium was able to inhibit the effect of the chelator further demonstrating that BT-20 spheroids were kept intact via calcium dependent adhesion. Confocal microscopy confirmed that cadherin was localised at the cell border

between cells within the spheroid. Together, this data suggests that BT-20 cells employ cadherin dependent adhesion to aggregate.

Cells in monolayer lost cell-cell adhesion in the presence of EGTA but remained attached to the substrate, suggesting that cadherin adhesion was lost but cell-substrate adhesion was not affected. This correlates with published data showing that cells grown in monolayers on plastic used integrin adhesion.[225,226] How does this relate to the mechanism of action of EE-15-one? Our data shows that while it is efficacious in 2D spheroid volume is not affected and FDA/PI staining remains similar to control spheroids after exposure to the compound. Our data suggests that there is a correlation between the mode of adhesion employed by the cells and the efficacy of this compound. We currently have no direct proof that EE-15-one directly inhibits cell adhesion although published data from our group shows that within minutes of exposure focal adhesions and the actin cytoskeleton start to disassemble.[224] Direct proof of the dependence on adhesion type could be obtained by plating cells in 2D on tethered cadherin antibodies which would induce cadherin mediated cell-substrate adhesion instead of integrin dependent cell-substrate adhesion and determining if EE-15-one still can induce loss of adhesion.

Nonetheless, our data shows that some compounds will be ineffectual against 3D cultured cells and can indicate that they rely on signals present in 2D culture to affect cell survival. It also gives the opportunity to further dissect such compounds as was done here to show that it influences a particular signalling or adhesive process. EE-15-one, while probably not effective as a cancer treatment, could prove useful in the dissection of integrin dependent signalling research. Its mode of action does suggest, however, some potential to influence the ability of cancer cells to adhere and migrate using integrins which is a process intimately associated with metastasis. Further research may elucidate such a connection and prove that this compound could still have use as an anti-metastatic intervention.

It has been proven in several different types of multicellular spheroids that, depending on the size, the centre of a 3D spheroid has a necrotic core surrounded by hypoxic cells caused by a lack of vasculature.[227–229] The cadherin staining of the BT-20 spheroids using confocal microscopy alludes to this necrotic core being present in these spheroids (Fig. 16). Hypoxia has been suggested to induce protein expression in tumour cells related with chemoresistance and thus the lack of effect seen in spheroids treated with EE-15-one could be due to the induction of chemoresistance brought on by hypoxia. To test if cells could become resistant to EE-15-one when hypoxic, monolayer BT-20 cells were grown in hypoxia or normoxia and treated with a concentration range of EE-15-one (Fig. 11). The dose response curve did was not significantly altered between hypoxia and normoxia suggesting that cells did not become resistant to EE-15-one when hypoxic. Thus, the lack of effect of EE-15-one seen in BT-20 spheroids is not due to the induction of hypoxia related gene expression and induced resistance.

Further analysis of compounds revealed that another compound developed in the group called STX1972 also had a differential effect on cells in 2D and 3D. In 2D STX1972 exposure resulted in diminished cell numbers at nanomolar concentrations. However, no effect on spheroid volume was observed (Fig. 10 and 11). The studies performed for EE-15-one would need to be performed to determine if this compound also affects adhesion although differences in the 2D response suggest a possible different mechanism. If it is shown that adhesion is not the main determinant for STX1972 efficacy in 2D and lack of effect in 3D it would suggest that beyond changes in adhesion mechanism other cell signalling mechanisms differ in 2D and 3D that can affect compound efficacy.

4.3 A RATIONALISATION OF THE USE OF CANCER SPHEROIDS AS SCREENING TOOL FOR POTENTIAL OFF-TARGET EFFECTS OF COMPOUNDS TARGETING PATHOGENS SUCH AS MALARIA.

Testing of compounds for possible side effects is limited. The most commonly used system is testing for hepatotoxicity using a hepatic cell line such as HEPG2 which is a hepatic cancer cell line. Testing of compounds on epithelial cells could reveal potential problems including the induction of cell growth or of cell death which can translate into important adverse effects later on. Furthermore, these cells are easy to grow and are amenable to high throughput testing unlike primary cells or iPSC which can only be maintained at great cost and labour.

In this study, two potential anti-malarial compounds (W12 and W41) were assessed for their effect on cell proliferation and survival of BT-20 cells in 2D and 3D. When testing W12 and W41, in 2D monolayer BT-20 cells, inhibition of cell proliferation was observed at concentrations starting at 5 µM (Fig. 19). In contrast, in spheroids treated with up to 20 µM W41, no effect on spheroid volume was observed (Fig. 19). Thus, W41 has no effect on breast cancer proliferation or survival in 3D at concentrations well above that to be used in vivo. To test whether this is indeed a good predictor of the effect of the compound on primary epithelial cells should be assessed and compared with the spheroid data. W12, at the same exposure of 20 µM, caused a significant increase in spheroid volume compared to the control spheroids. Although this effect was prominent at high concentrations it still could point to a potential adverse effect on cell growth. Further studies should determine if this effect is also seen in primary epithelial cells. However, it is clear that potential adverse effects could be identified with this method.

4.4 CO-CULTURE SPHEROIDS INDICATE THAT METASTATIC CELLS AND NON-METASTATIC CELLS DISPLAY DIFFERENT BEHAVIOUR EVEN IN SPHEROID CULTURES.

The development of complex, heterogeneous spheroids is the ultimate goal to produce a complete *in vitro* recapitulation of the tumour and its microenvironment. To develop this type of *in vitro* tumour model system, it will be essential to mimic the heterogeneous tumour population by co-culturing different breast cancer cell types within one spheroid. This is especially important since it has become clear that there is communication between different cancer subpopulations and this can lead to effects on cell behaviour, including metastasis.[8,44] The establishment of such a complex spheroid system will better mimic the *in vivo* tumour and lead to improved drug discovery and a better understanding of cancer cell biology.

To develop the BT-20 spheroid into a more comprehensive *in vitro* breast cancer tumour test platform, we first introduced another breast cancer cell line into the spheroid. The metastatic MDA-MB-231 cell line was modified by the introduction of a fluorescent GFP protein through lentiviral genomic insertion of an GFP containing expression cassette. This allowed us to discriminate between non-fluorescent BT-20 cells and fluorescent MDA-MB-231 cells. Labelling of the BT-20 cells with another fluorescent protein is still in production and was not ready at the time of writing. Co-culturing these cells as spheroids showed that spheroids similar to BT-20 spheroids were able to form when 20% of the total cell population was MDA-MB-231 cells. Higher ratios of these metastatic cells caused the spheroids to form large protrusions of cells or to fall apart entirely. This may be due to the seemingly diminished epithelial morphology of the MDA-MB-231 cells. Alternatively, it could point to differences in cadherin expression prohibiting efficient cell-cell adhesion between BT-20 and MDA-MB-231 cells. The intriguing finding that MDA-MB-231 cells seem to cluster together within the spheroid after some time seem to reinforce this idea of differential cadherin expression. However, protein expression studies pinpointing the exact cadherin isoforms expressed by either cell line need to be performed to determine if this is a possible reason for this phenomenon.

When such co-culture spheroids were placed on a rigid surface allowing cell-surface interactions, the migratory MDA-MB-231 cells were able to leave the spheroid and migrate in 2D on the plate surface, whereas the BT-20 cells remained in the spheroids. This experiment, while preliminary, points to some interesting possibilities. Firstly, it shows that the two cell lines behave very differently but according to their origins as MDA-MB-231 cells were obtained from a metastatic profusion while BT-20 cells were obtained from a primary tumour. Secondly, it suggests that MDA-MB-231 cells prefer the rigid surface of the culture flask to the adhesive environment of the spheroid. These suggest that both cell lines employ different adhesive strategies which only become apparent in this spheroid co-culture setting. Further research will reveal how these cells interact inside the spheroid and whether they can communicate and influence one another's behaviour. This model system will allow for in depth study of such interactions.

4.5 CONCLUSIONS

In this thesis, I have described a cell line and a methodology with which the first pass screening process for new compounds can be conducted in a 3D spheroid culture system that is both reliable in its consistency and cost-effective. Using this system, I have shown that while some compounds are effective in both 2D monolayer cell cultures and 3D spheroid cultures a substantial number of lead compounds will exhibit anticancer effects at nanomolar or micromolar concentrations within a 2D monolayer system, but in a 3D cell environment these compounds may not have any effect at all. Therefore, while this system has room for improvement, and requires further study with more controls, it has the potential to screen with a stricter degree for potentially effective compounds. This will save time, money, and effort in the drug discovery industry, specifically in smaller laboratory environments. This system was validated using anti-malarials showcasing the potential use in screening non cancer compounds as well, but in future this system will need to be validated against *in vivo* scenarios using several different cell types.

The study shows that for some compounds, the lack of effect in 3D may be due to the adhesion strategy employed by the BT-20 cell line in 2D monolayer cell culture versus 3D spheroid culture. It also shows that there are substantive differences in basic cellular machinery in these two different cell culture systems, which will significantly impact on the response of cells to various lead compounds. This may provide insight into the mechanistic actions of compounds during the drug discovery process.

An initial step was made to generate a complex *in vitro* cancer tumour model that incorporates breast cancer cells with different behaviours. Further development of such a system to include a more advanced tumour microenvironment will allow for much more precise investigation of the complex environment tumours find themselves in. It is necessary to create a model that consists of several cell types, while also containing several components of the microenvironment. The overall aim is to mimic a small tumour and its tumour microenvironment in a laboratory. In this way, the effects of compounds on cancer cells and the surrounding cells can be closely observed. The ultimate goal is to produce a complete *in vitro* recapitulation of the tumour and its microenvironment.

CHAPTER 5

REFERENCES

5 REFERENCES

1. Martin, G. S. Cell signaling and cancer. *Cancer Cell* **4**, 167–74 (2003).
2. Hanahan, D. & Weinberg, R. A. Hallmarks of cancer: the next generation. *Cell* **144**, 646–674 (2011).
3. Vogelstein, B. & Kinzler, K. W. Cancer genes and the pathways they control. *Nat. Med.* **10**, 789–99 (2004).
4. Hanahan, D. & Weinberg, R. A. The Hallmarks of Cancer. *Cell* **100**, 57–70 (2000).
5. Pickup, M. W., Mouw, J. K. & Weaver, V. M. The extracellular matrix modulates the hallmarks of cancer. *EMBO Rep.* **15**, 1243–1253 (2014).
6. Bill, R. & Christofori, G. The relevance of EMT in breast cancer metastasis: Correlation or causality? *FEBS Lett.* **589**, 1577–1587 (2015).
7. Gupta, G. P. & Massagué, J. Cancer metastasis: building a framework. *Cell* **127**, 679–695 (2006).
8. Bogenrieder, T. & Herlyn, M. Axis of evil: molecular mechanisms of cancer metastasis. *Oncogene* **22**, 6524–6536 (2003).
9. de Groot, A. E., Roy, S., Brown, J. S., Pienta, K. J. & Amend, S. R. Revisiting Seed and Soil: Examining the Primary Tumor and Cancer Cell Foraging in Metastasis. *Mol. Cancer Res.* **15**, 361–370 (2017).
10. Wilson, W. R. & Hay, M. P. Targeting hypoxia in cancer therapy. *Nat Rev Cancer* **11**, 393–410 (2011).
11. Lovitt, C., Shelper, T. & Avery, V. Advanced Cell Culture Techniques for Cancer Drug Discovery. *Biology (Basel).* **3**, 345–367 (2014).
12. Kumar, B., Singh, S., Skvortsova, I. & Kumar, V. Promising Targets in Anti-cancer Drug Development: Recent Updates. *Curr. Med. Chem.* **24**, (2017).
13. Zahreddine, H. & Borden, K. L. B. Mechanisms and insights into drug resistance in cancer. *Front. Pharmacol.* **4**, 1–8 (2013).
14. Stewart, B. W. & Wild, C. P. World Cancer Report: World Health Organization (WHO) and International Agency for Research on Cancer (IARC). *GLOBOCAN* (2014). Available at: https://publications.iarc.fr/Non-Series-Publications/World-Cancer-Reports/World-

Cancer-Report-2014. (Accessed: 1st March 2015)

15. Wild, C. P., Weiderpass, E. & BW, S. World Cancer Report Cancer research for cancer prevention. *GLOBOCAN* 1–613 (2020). Available at: https://publications.iarc.fr/Non-Series-Publications/World-Cancer-Reports/World-Cancer-Report-Cancer-Research-For-Cancer-Prevention-2020. (Accessed: 29th March 2020)
16. Ferlay, J. *et al.* Cancer Incidence and Mortality Worldwide: IARC CancerBase No. 11. *GLOBOCAN 2012 v1.0* (2014).
17. Siegel, R. L., Miller, K. D. & Jemal, A. Cancer statistics, 2015. *CA. Cancer J. Clin.* **65**, 5–29 (2015).
18. Signh, E. & Sengayi, M. Cancer in South Africa. 2014. Full Report. *NATIONAL CANCER REGISTRY* 1–38 (2014). Available at: https://www.nicd.ac.za/centres/national-cancer-registry/. (Accessed: 1st March 2015)
19. Redig, A. J. & McAllister, S. S. Breast cancer as a systemic disease: a view of metastasis. *J. Intern. Med.* **274**, 113–126 (2013).
20. Lin, N. U. *et al.* Sites of distant recurrence and clinical outcomes in patients with metastatic triple-negative breast cancer: high incidence of central nervous system metastases. *Cancer* **113**, 2638–2645 (2008).
21. Chavez, K., Garimella, S. & Lipkowitz, S. Triple Negative Breast Cancer Cell Lines: One Tool in the Search for Better Treatment of Triple Negative Breast Cancer. *Breast Dis.* **32**, 35–48 (2010).
22. Anders, C. K. & Carey, L. A. Biology, Metastatic Patterns, and Treatment of Patients with Triple-Negative Breast Cancer. *Clin. Breast Cancer* **9**, S73–S81 (2009).
23. Lehmann, B. D. *et al.* Identification of human triple-negative breast cancer subtypes and preclinical models for selection of targeted therapies. *J. Clin. Invest.* **121**, 2750–2767 (2011).
24. Buzdar, A. U. Endocrine therapy in the treatment of metastatic breast cancer. *Semin. Oncol.* **28**, 291–304 (2001).
25. Freedman, O. C. *et al.* Adjuvant endocrine therapy for early breast cancer: a systematic review of the evidence for the 2014 Cancer Care Ontario systemic therapy guideline.

Curr. Oncol. **22**, S95–S113 (2015).

26. Podo, F. *et al.* Triple-negative breast cancer: Present challenges and new perspectives. *Mol. Oncol.* **4**, 209–229 (2010).
27. Wang, J., Sun, C., Huang, X., Qiu, J. & Yin, Y. Long-term remission of hormone receptor-positive/HER2-positive metastatic breast cancer due to combined treatment with everolimus/trastuzumab/exemestane: A case report. *Oncol. Lett.* **14**, 1725–1730 (2017).
28. Jordan, C. Historical perspective on hormonal therapy of advanced breast cancer. *Clin. Ther.* **24**, 3–16 (2002).
29. Chen, W., Hoffmann, A. D., Liu, H. & Liu, X. Organotropism: new insights into molecular mechanisms of breast cancer metastasis. *npj Precis. Oncol.* **2**, 4 (2018).
30. Ross, J. S. *et al.* The Her-2/neu gene and protein in breast cancer 2003: biomarker and target of therapy. *Oncologist* **8**, 307–325 (2003).
31. Lin, N. U. *et al.* Clinicopathologic features, patterns of recurrence, and survival among women with triple-negative breast cancer in the National Comprehensive Cancer Network. *Cancer* **118**, 5463–5472 (2012).
32. Uscanga-Perales, G. I., Santuario-Facio, S. K. & Ortiz-López, R. Triple negative breast cancer: Deciphering the biology and heterogeneity. *Med. Univ.* **18**, 105–114 (2016).
33. Burstein, M. D. *et al.* Comprehensive genomic analysis identifies novel subtypes and targets of triple-negative breast cancer. *Clin. Cancer Res.* **21**, 1688–1698 (2015).
34. Engebraaten, O., Vollan, H. K. M. & Børresen-Dale, A.-L. Triple-Negative Breast Cancer and the Need for New Therapeutic Targets. *Am. J. Pathol.* **183**, 1064–1074 (2013).
35. Dickens, C. *et al.* Racial comparison of receptor-defined breast cancer in Southern African women: subtype prevalence and age-incidence analysis of nationwide cancer registry data. *Cancer Epidemiol. Biomarkers Prev.* **23**, 2311–2321 (2014).
36. Vanderpuye, V. *et al.* An update on the management of breast cancer in Africa. *Infectious Agents and Cancer* **12**, 1–12 (2017).
37. Feng, B. *et al.* Colorectal cancer migration and invasion initiated by microRNA-106a. *PLoS One* **7**, e43452 (2012).

38. Stark, A. *et al.* African ancestry and higher prevalence of triple-negative breast cancer. *Cancer* **116**, 4926–4932 (2010).
39. Sounni, N. E. & Noel, A. Targeting the Tumor Microenvironment for Cancer Therapy. *Clin. Chem.* **59**, 85–93 (2013).
40. Wang, M. *et al.* Role of tumor microenvironment in tumorigenesis. *J. Cancer* **8**, 761–773 (2017).
41. Walker, C., Mojares, E. & Del Río Hernández, A. Role of Extracellular Matrix in Development and Cancer Progression. *Int. J. Mol. Sci.* **19**, 3028 (2018).
42. Cooke, M. J. *et al.* Enhanced cell attachment using a novel cell culture surface presenting functional domains from extracellular matrix proteins. *Cytotechnology* **56**, 71–79 (2008).
43. Wang, M. *et al.* Role of tumor microenvironment in tumorigenesis. *J. Cancer* **8**, 761–773 (2017).
44. Poltavets, V., Kochetkova, M., Pitson, S. M. & Samuel, M. S. The Role of the Extracellular Matrix and Its Molecular and Cellular Regulators in Cancer Cell Plasticity. *Front. Oncol.* **8**, 431 (2018).
45. Ivascu, A. & Kubbies, M. Diversity of cell-mediated adhesions in breast cancer spheroids. *Int. J. Oncol.* **31**, 1403–1413 (2007).
46. Weber, G. F., Bjerke, M. A. & DeSimone, D. W. Integrins and cadherins join forces to form adhesive networks. *J. Cell Sci.* **124**, 1183–1193 (2011).
47. Takada, Y., Ye, X. & Simon, S. The integrins. *Genome Biol.* **8**, 215 (2007).
48. Campbell, I. D. & Humphries, M. J. Integrin structure, activation, and interactions. *Cold Spring Harb. Perspect. Biol.* **3**, 1–14 (2011).
49. Wary, K. K. Recognizing scientific excellence in the biology of cell adhesion. *Cell Commun. Signal.* **3**, 7 (2005).
50. van der Flier, A. & Sonnenberg, A. Function and interactions of integrins. *Cell Tissue Res.* **305**, 285–298 (2001).
51. Humphries, J. D., Byron, A. & Humphries, M. J. Integrin ligands at a glance. *J. Cell Sci.* **119**, 3901–3903 (2006).

52. Bökel, C. & Brown, N. H. Integrins in development: moving on, responding to, and sticking to the extracellular matrix. *Dev. Cell* **3**, 311–321 (2002).

53. Huttenlocher, A. & Horwitz, A. R. Integrins in cell migration. *Cold Spring Harb. Perspect. Biol.* **3**, 1–16 (2011).

54. Schwarzbauer, J. E. & Sechler, J. L. Fibronectin fibrillogenesis: a paradigm for extracellular matrix assembly. *Curr. Opin. Cell Biol.* **11**, 622–627 (1999).

55. Zou, L., Cao, S., Kang, N., Huebert, R. C. & Shah, V. H. Fibronectin induces endothelial cell migration through β1 integrin and Src-dependent phosphorylation of fibroblast growth factor receptor-1 at tyrosines 653/654 and 766. *J. Biol. Chem.* **287**, 7190–202 (2012).

56. Balcioglu, H. E., van de Water, B. & Danen, E. H. J. Tumor-induced remote ECM network orientation steers angiogenesis. *Sci. Rep.* **6**, 22580 (2016).

57. Kim, S. A., Tai, C.-Y., Mok, L.-P., Mosser, E. A. & Schuman, E. M. Calcium-dependent dynamics of cadherin interactions at cell-cell junctions. *Proc. Natl. Acad. Sci. U. S. A.* **108**, 9857–9862 (2011).

58. Maître, J.-L. & Heisenberg, C.-P. Three functions of cadherins in cell adhesion. *Curr. Biol.* **23**, 626–633 (2013).

59. Pokutta, S., Herrenknecht, K., Kemler, R. & Engel, J. Conformational changes of the recombinant extracellular domain of E-cadherin upon calcium binding. *Eur. J. Biochem.* **223**, 1019–1026 (1994).

60. Perez, T. D. & Nelson, W. J. Cadherin adhesion: mechanisms and molecular interactions. *Handb. Exp. Pharmacol.* **165**, 3–21 (2004).

61. Cailliez, F. & Lavery, R. Cadherin mechanics and complexation: the importance of calcium binding. *Biophys. J.* **89**, 3895–3903 (2005).

62. Zaidel-Bar, R. *et al.* The switchable integrin adhesome. *J. Cell Sci.* **123**, 1385–8 (2010).

63. McKeown, S. R. Defining normoxia, physoxia and hypoxia in tumours—implications for treatment response. *Br. J. Radiol.* **87**, 20130676 (2014).

64. Riffle, S. & Hegde, R. S. Modeling tumor cell adaptations to hypoxia in multicellular tumor spheroids. *J. Exp. Clin. Cancer Res.* **36**, 102 (2017).

65. Chen, J. *et al.* HIF-1α inhibition reverses multidrug resistance in colon cancer cells via downregulation of MDR1/P-glycoprotein. *PLoS One* **9**, e98882 (2014).

66. Marin-Hernandez, A., Gallardo-Perez, J., Ralph, S., Rodriguez-Enriquez, S. & Moreno-Sanchez, R. HIF-1α Modulates Energy Metabolism in Cancer Cells by Inducing Over-Expression of Specific Glycolytic Isoforms. *Mini-Reviews Med. Chem.* **9**, 1084–1101 (2009).

67. Chiche, J. *et al.* Hypoxia-inducible carbonic anhydrase IX and XII promote tumor cell growth by counteracting acidosis through the regulation of the intracellular pH. *Cancer Res.* **69**, 358–368 (2009).

68. Mabjeesh, N. J. *et al.* 2ME2 inhibits tumor growth and angiogenesis by disrupting microtubules and dysregulating HIF. *Cancer Cell* **3**, 363–375 (2003).

69. Simiantonaki, N. *et al.* Hypoxia-induced epithelial VEGF-C/VEGFR-3 upregulation in carcinoma cell lines. *Int. J. Oncol.* **32**, 585–592 (2008).

70. Lee, J.-W., Bae, S.-H., Jeong, J.-W., Kim, S.-H. & Kim, K.-W. Hypoxia-inducible factor (HIF-1)α : its protein stability and biological functions. *Exp. Mol. Med.* **36**, 1–12 (2004).

71. Li, Y. *et al.* Role of hypoxia and EGF on expression, activity, localization and phosphorylation of carbonic anhydrase IX in MDA-MB-231 breast cancer cells. *Biochim. Biophys. Acta* **1813**, 159–167 (2011).

72. Thiry, A., Dogné, J. M., Masereel, B. & Supuran, C. T. Targeting tumor-associated carbonic anhydrase IX in cancer therapy. *Trends Pharmacol. Sci.* **27**, 566–573 (2006).

73. Thomas, S. N. *et al.* Exosomal Proteome Profiling: A Potential Multi-Marker Cellular Phenotyping Tool to Characterize Hypoxia-Induced Radiation Resistance in Breast Cancer. *Proteomes* **1**, 87–108 (2013).

74. Groebe, K. & Mueller-Klieser, W. On the relation between size of necrosis and diameter of tumor spheroids. *Int. J. Radiat. Oncol. Biol. Phys.* **34**, 395–401 (1996).

75. Brahimi-Horn, M. C., Chiche, J. & Pouysségur, J. Hypoxia and cancer. *J. Mol. Med.* **85**, 1301–1307 (2007).

76. Fang, Y. & Eglen, R. M. Three-Dimensional Cell Cultures in Drug Discovery and Development. *SLAS Discovery* **22**, 456–472 (2017).

77. Wadood, A. *et al.* In-silico drug design: An approach which revolutionarised the drug discovery process.OA Drug Design and Delivery. *Drug Des. Deliv.* **1**, 3 (2013).

78. Zahreddine, H. & Borden, K. L. B. Mechanisms and insights into drug resistance in cancer. *Front. Pharmacol.* **4**, 1–8 (2013).

79. Hoarau-Véchot, J. *et al.* Halfway between 2D and Animal Models: Are 3D Cultures the Ideal Tool to Study Cancer-Microenvironment Interactions? *Int. J. Mol. Sci.* **19**, 181 (2018).

80. Ravi, M., Paramesh, V., Kaviya, S. R., Anuradha, E. & Paul Solomon, F. D. 3D cell culture systems: Advantages and applications. *J. Cell. Physiol.* **230**, 16–26 (2015).

81. Friedrich, J. *et al.* A reliable tool to determine cell viability in complex 3-d culture: the acid phosphatase assay. *J. Biomol. Screen. Off. J. Soc. Biomol. Screen.* **12**, 925–937 (2007).

82. Hirschhaeuser, F. *et al.* Multicellular tumor spheroids: An underestimated tool is catching up again. *J. Biotechnol.* **148**, 3–15 (2010).

83. Stilbo, I. M. Phase I, II, III, and IV Studies: Good Clinical Practice. *Trends in Contrast Media* 57–61 (1999).

84. Derhaschnig, U. & Jilma, B. Phase I studies and first-in-human trials. in *Clinical Pharmacology: Current Topics and Case Studies: Second Edition* 85–95 (Springer International Publishing, 2016).

85. Fang, Y. & Eglen, R. M. Three-Dimensional Cell Cultures in Drug Discovery and Development. *SLAS Discov. Adv. Life Sci. R&D* **22**, 456–472 (2017).

86. Hickman, J. A. *et al.* Three-dimensional models of cancer for pharmacology and cancer cell biology: Capturing tumor complexity in vitro/ex vivo. *Biotechnology Journal* **9**, 1115–1128 (2014).

87. Harrison, R. G. Observations on the living developing nerve fiber. *Exp. Biol. Med.* **4**, 140–143 (1906).

88. Jedrzejczak-Silicka, M. History of Cell Culture. in *New Insights into Cell Culture Technology* 1–41 (InTech, 2017).

89. Scherer, W. F., Syverton, J. T. & Gey, G. O. Studies on the propagation in vitro of

poliomyelitis viruses: IV. Viral multiplication in a stable strain of human malignant epithelial cells (strain hela) derived from an epidermoid carcinoma of the cervix. *J. Exp. Med.* **97**, 695–710 (1953).

90. Gillet, J.-P., Varma, S. & Gottesman, M. M. The Clinical Relevance of Cancer Cell Lines. *JNCI J. Natl. Cancer Inst.* **105**, 452–458 (2013).
91. Longati, P. *et al.* 3D pancreatic carcinoma spheroids induce a matrix-rich, chemoresistant phenotype offering a better model for drug testing. *BMC Cancer* **13**, 95 (2013).
92. Stock, K. *et al.* Capturing tumor complexity in vitro: Comparative analysis of 2D and 3D tumor models for drug discovery. *Sci. Rep.* **6**, 28951 (2016).
93. Hamilton, G. Multicellular spheroids as an in vitro tumor model. *Cancer Lett.* **131**, 29–34 (1998).
94. Friedrich, J., Seidel, C., Ebner, R. & Kunz-Schughart, L. A. Spheroid-based drug screen: considerations and practical approach. *Nat. Protoc.* **4**, 309–324 (2009).
95. Lovitt, C., Shelper, T. & Avery, V. Advanced Cell Culture Techniques for Cancer Drug Discovery. *Biology (Basel).* **3**, 345–367 (2014).
96. Costa, E. C. *et al.* 3D tumor spheroids: an overview on the tools and techniques used for their analysis. *Biotechnol. Adv.* **34**, 1427–1441 (2016).
97. Weiswald, L.-B., Bellet, D. & Dangles-Marie, V. Spherical Cancer Models in Tumor Biology. *Neoplasia* **17**, 1–15 (2015).
98. Mehta, G., Hsiao, A. Y., Ingram, M., Luker, G. D. & Takayama, S. Opportunities and challenges for use of tumor spheroids as models to test drug delivery and efficacy. *J. Control. Release* **164**, 192–204 (2012).
99. Foty, R. A Simple Hanging Drop Cell Culture Protocol for Generation of 3D Spheroids. **20**, 4–7 (2011).
100. Lv, D., Hu, Z., Lu, L., Lu, H. & Xu, X. Three-dimensional cell culture: A powerful tool in tumor research and drug discovery. *Oncology Letters* **14**, 6999–7010 (2017).
101. Knight, E. & Przyborski, S. Advances in 3D cell culture technologies enabling tissue-like structures to be created *in vitro*. *J. Anat.* **227**, 746–756 (2015).

102. Nunes, A. S., Barros, A. S., Costa, E. C., Moreira, A. F. & Correia, I. J. 3D tumor spheroids as in vitro models to mimic in vivo human solid tumors resistance to therapeutic drugs. *Biotechnol. Bioeng.* **116**, 206–226 (2019).

103. Friedrich, J., Seidel, C., Ebner, R. & Kunz-schughart, L. a. Spheroid-based drug screen: considerations and practical approach. *Nat. Protoc.* **4**, 309–324 (2009).

104. Abercrombie, J. *Pathological and Practical Researches on the Diseases of the Stomach, the Intestinal Canal, the Liver, and Other Viscera of the Abdomen*. (1828).

105. Aldis, C. *Observations on the Nature and Cure of Glandular Diseases, especially those denominated Cancer, and on the too frequent use of mercury, etc*. (1820).

106. Hajdu, S. I. A note from history: Landmarks in history of cancer, part 3. *Cancer* **118**, 1155–1168 (2012).

107. Davey, P. & Tudhope, G. R. Anticancer chemotherapy. *Bmj* **287**, 110–113 (1983).

108. da Rocha, A. B., Lopes, R. M. & Schwartsmann, G. Natural products in anticancer therapy. *Curr. Opin. Pharmacol.* **1**, 364–369 (2001).

109. Ta, S., Seino, Y., Nagao, M. & Yahagi, T. Mutagenicity of Several Classes of Antitumor Agents to Mutagenicity of Several Classes of Antitumor Agents to Salmonella. *Cancer Res.* **38**, 2148–2156 (1978).

110. Bull, J. M. An update on the anticancer effects of a combination of chemotherapy and hyperthermia. *Cancer Res.* **44**, 4853s-4856s (1984).

111. Espinosa, E., Zamora, P., Feliu, J. & González Barón, M. Classification of anticancer drugs - A new system based on therapeutic targets. *Cancer Treat. Rev.* **29**, 515–523 (2003).

112. Lee, K.-H. Novel antitumor agents from higher plants. *Med. Res. Rev.* **19**, 569–596 (1999).

113. Malhotra, V. & Perry, M. C. Classical Chemotherapy: Mechanisms, Toxicities and the Therapeutc Window. *Cancer Biol. Ther.* **2**, 1–3 (2003).

114. Gibson, R. J. & Keefe, D. M. K. Cancer chemotherapy-induced diarrhoea and constipation: mechanisms of damage and prevention strategies. *Support. Care Cancer* **14**, 890–900 (2006).

115. Chadha, V. & Shenoi, S. D. Hair loss in cancer chemotherapeutic patients. *Indian J.*

Dermatol. Venereol. Leprol. **69**, 131–132 (2003).

116. Shaikh, A. Y. & Shih, J. A. Chemotherapy-Induced Cardiotoxicity. *Curr. Heart Fail. Rep.* **9**, 117–127 (2012).
117. Dominguez-Brauer, C. *et al.* Targeting Mitosis in Cancer: Emerging Strategies. *Mol. Cell* **60**, 524–536 (2015).
118. Weaver, B. A. How Taxol/paclitaxel kills cancer cells. *Mol. Biol. Cell* **25**, 2677–2681 (2014).
119. Gascoigne, K. E. & Taylor, S. S. How do anti-mitotic drugs kill cancer cells? *J. Cell Sci.* **122**, 2579–2585 (2009).
120. Marzo, I. & Naval, J. Antimitotic drugs in cancer chemotherapy: Promises and pitfalls. *Biochem. Pharmacol.* **86**, 703–710 (2013).
121. Jordan, M. A. & Wilson, L. Microtubules as a target for anticancer drugs. *Nat. Rev. Cancer* **4**, 253–265 (2004).
122. Tinley, T. L. *et al.* Novel 2-Methoxyestradiol Analogues with Antitumor Activity. *Cancer Res.* **63**, 1538–1549 (2003).
123. Tevaarwerk, A. J. *et al.* Phase I trial of 2-methoxyestradiol NanoCrystal dispersion in advanced solid malignancies. *Clin. Cancer Res.* **15**, 1460–1465 (2009).
124. Casey, T. *et al.* Molecular signatures suggest a major role for stromal cells in development of invasive breast cancer. *Breast Cancer Res. Treat.* **114**, 47–62 (2009).
125. Keen, N. & Taylor, S. Mitotic drivers—inhibitors of the Aurora B Kinase. *Cancer Metastasis Rev.* **28**, 185–195 (2009).
126. Mueck, A. O. & Seeger, H. 2-Methoxyestradiol—Biology and mechanism of action. *Steroids* **75**, 625–631 (2010).
127. Parada-Bustamante, A. *et al.* Role of 2-methoxyestradiol, an Endogenous Estrogen Metabolite, in Health and Disease. *Rev. Med. Chem.* **15**, 427–438 (2015).
128. Verenich, S. & Gerk, P. M. Therapeutic promises of 2-methoxyestradiol and its drug disposition challenges. *Mol. Pharm.* **7**, 2030–2039 (2010).
129. Visagie, M. H. & Joubert, A. M. In vitro effects of 2-methoxyestradiol-bis-sulphamate on reactive oxygen species and possible apoptosis induction in a breast adenocarcinoma

cell line. *Cancer Cell Int.* **11**, 43 (2011).

130. Riedl, S. J. & Salvesen, G. S. The apoptosome: signalling platform of cell death. *Nat. Rev. Mol. Cell Biol.* **8**, 405–413 (2007).
131. Kamath, K. *et al.* 2-Methoxyestradiol suppresses microtubule dynamics and arrests mitosis without depolymerizing microtubules. *Mol. Cancer Ther.* **5**, 2225–2233 (2006).
132. D'Amato, R. J., Lin, C. M., Flynn, E., Folkman, J. & Hamel, E. 2-Methoxyestradiol, an endogenous mammalian metabolite, inhibits tubulin polymerization by interacting at the colchicine site. *Proc. Natl. Acad. Sci. U. S. A.* **91**, 3964–3968 (1994).
133. Yue, T. L. *et al.* 2-Methoxyestradiol, an endogenous estrogen metabolite, induces apoptosis in endothelial cells and inhibits angiogenesis: possible role for stress-activated protein kinase signaling pathway and Fas expression. *Mol. Pharmacol.* **51**, 951–62 (1997).
134. Hamel, E., Lin, C. M., Flynn, E. & D'Amato, R. J. Interactions of 2-Methoxyestradiol, an Endogenous Mammalian Metabolite, with Unpolymerized Tubulin and with Tubulin Polymers. *Biochemistry* **35**, 1304–1310 (1996).
135. Ireson, C. R. *et al.* Pharmacokinetics and efficacy of 2-methoxyoestradiol and 2-methoxyoestradiol-bis-sulphamate in vivo in rodents. *Br. J. Cancer* **90**, 932–927 (2004).
136. Stander, A., Joubert, F. & Joubert, A. Docking, Synthesis, and in vitro Evaluation of Antimitotic Estrone Analogs. **77**, 173–181 (2011).
137. Sippel, K. *et al.* Characterization of Carbonic Anhydrase Isozyme Specific Inhibition by Sulfamated 2-Ethylestra Compounds. *Lett. Drug Des. Discov.* **8**, 678–684 (2011).
138. Gieling, R. G. *et al.* Antimetastatic effect of sulfamate carbonic anhydrase IX inhibitors in breast carcinoma xenografts. *J. Med. Chem.* **55**, 5591–600 (2012).
139. Theron, A. *et al.* Novel in silico-designed estradiol analogues are cytotoxic to a multidrug-resistant cell line at nanomolar concentrations. *Cancer Chemother. Pharmacol.* **75**, 431–437 (2014).
140. Mqoco, T. & Joubert, A. 2-methoxyestradiol-bis-sulphamate induces apoptosis and autophagy in an oesophageal carcinoma (SNO) cell line. *Biomed. Res.* **23**, 469–474 (2012).

141. Repsold, L., Pretorius, E. & Joubert, A. An estrogen analogue and promising anticancer agent refrains from inducing morphological damage and reactive oxygen species generation in erythrocytes, fibrin and platelets: a pilot study. *Cancer Cell Int.* **14**, 48 (2014).

142. Visagie, M. H., Birkholtz, L.-M. & Joubert, A. M. 17-Beta-Estradiol Analog Inhibits Cell Proliferation By Induction of Apoptosis in Breast Cell Lines. *Microsc. Res. Tech.* **77**, 236–242 (2014).

143. Visagie, M. H. & Joubert, A. M. 2-Methoxyestradiol-bis-sulphamate refrains from inducting apoptosis and autophagy in a non-tumorigenic breast cell line. *Cancer Cell Int.* **12**, 37 (2012).

144. Wolmarans, E. *et al.* Novel estradiol analogue induces apoptosis and autophagy in esophageal carcinoma cells. *Cell. Mol. Biol. Lett.* **19**, 98–115 (2014).

145. Potter, C. P. S. & Harris, a L. Diagnostic, prognostic and therapeutic implications of carbonic anhydrases in cancer. *Br. J. Cancer* **89**, 2–7 (2003).

146. Theron, A. E., Nolte, E. M., Lafanechère, L. & Joubert, A. M. Molecular crosstalk between apoptosis and autophagy induced by a novel 2-methoxyestradiol analogue in cervical adenocarcinoma cells. *Cancer Cell Int.* **13**, 87 (2013).

147. Lasfargues, E. & Ozzello, L. Cultivation of human breast carcinomas. *J. Natl. Cancer Inst.* **21**, 1131–1147 (1958).

148. Chandrasekaran, S., Geng, Y., DeLouise, L. a. & King, M. R. Effect of homotypic and heterotypic interaction in 3D on the E-selectin mediated adhesive properties of breast cancer cell lines. *Biomaterials* **33**, 9037–9048 (2012).

149. Chandrasekaran, S., Marshall, J. R., Messing, J. a, Hsu, J.-W. & King, M. R. TRAIL-mediated apoptosis in breast cancer cells cultured as 3D spheroids. *PLoS One* **9**, e111487 (2014).

150. Sameni, M., Dosescu, J., Moin, K. & Sloane, B. F. Functional Imaging of Proteolysis: Stromal and Inflammatory Cells Increase Tumor Proteolysis. *Mol. Imaging* **2**, 159–175 (2003).

151. Levenson, A. S. & Jordan, V. C. MCF-7: the first hormone-responsive breast cancer cell

line. *Cancer Res.* **57**, 3071–3078 (1997).

152. Soule, H. D., Vazguez, J., Long, A., Albert, S. & Brennan, M. A human cell line from a pleural effusion derived from a breast carcinoma. *J. Natl. Cancer Inst.* **51**, 1409–1416 (1973).

153. Nicholson, K. M., Bibby, M. C. & Phillips, R. M. Influence of drug exposure parameters on the activity of paclitaxel in multicellular spheroids. *Eur. J. Cancer Part A* **33**, 1291–1298 (1997).

154. Froehlich, K. *et al.* Generation of Multicellular Breast Cancer Tumor Spheroids : Comparison of Different Protocols. *J. Mammary Gland Biol. Neoplasia* **21**, 89–98 (2016).

155. Chandrasekaran, S., Geng, Y., DeLouise, L. A. & King, M. R. Effect of homotypic and heterotypic interaction in 3D on the E-selectin mediated adhesive properties of breast cancer cell lines. *Biomaterials* **33**, 9037–9048 (2012).

156. Kelm, J. M., Timmins, N. E., Brown, C. J., Fussenegger, M. & Nielsen, L. K. Method for generation of homogeneous multicellular tumor spheroids applicable to a wide variety of cell types. *Biotechnol. Bioeng.* **83**, 173–180 (2003).

157. Abràmoff, M. D., Magalhães, P. J. & Ram, S. J. Image processing with imageJ. *Biophotonics Int.* **11**, 36–41 (2004).

158. Julious, S. A. Sample sizes for clinical trials with Normal data. *Stat. Med.* **23**, 1921–1986 (2004).

159. Power calculator for continuous outcome superiority trial. *Sealed Envelope Ltd.* (2012). Available at: https://www.sealedenvelope.com/power/continuous-superiority/. (Accessed: 20th September 2017)

160. Power calculator for continuous outcome equivalence trial. *Sealed Envelope Ltd.* (2012). Available at: www.sealedenvelope.com/power/continuous-equivalence/. (Accessed: 20th September 2017)

161. Kueng, W., Silber, E. & Eppenberger, U. Quantification of cells cultured on 96-well plates. *Anal. Biochem.* **182**, 16–19 (1989).

162. Horning, J. L. *et al.* 3-D tumor model for in vitro evaluation of anticancer drugs. *Mol. Pharm.* **5**, 849–862 (2008).

163. Breslin, S. & O'Driscoll, L. The relevance of using 3D cell cultures, in addition to 2D monolayer cultures, when evaluating breast cancer drug sensitivity and resistance. *Oncotarget* **7**, 45745–45756 (2016).

164. Breslin, S. & O'Driscoll, L. Three-dimensional cell culture: the missing link in drug discovery. *Drug Discov. Today* **18**, 240–249 (2013).

165. Burleson, K. M., Boente, M. P., Pambuccian, S. E. & Skubitz, A. P. N. Disaggregation and invasion of ovarian carcinoma ascites spheroids. *J. Transl. Med.* **4**, 1–16 (2006).

166. Vinci, M. *et al.* Advances in establishment and analysis of three- dimensional tumor spheroid-based functional assays for target validation and drug evaluation. *BMC Biol.* **10**, 29 (2012).

167. Nagelkerke, A., Bussink, J., Sweep, F. C. G. J. & Span, P. N. Generation of multicellular tumor spheroids of breast cancer cells: How to go three-dimensional. *Anal. Biochem.* **437**, 17–19 (2013).

168. Longati, P. *et al.* 3D pancreatic carcinoma spheroids induce a matrix-rich, chemoresistant phenotype offering a better model for drug testing. *BMC Cancer* **13**, 95 (2013).

169. Abràmofff, M. D., Magalhães, P. J. & Ram, S. J. Image processing with ImageJ Part II. *Biophotonics Int.* **11**, 36–43 (2005).

170. Weaver, B. A. How Taxol/paclitaxel kills cancer cells. *Mol. Biol. Cell* **25**, 2677–2681 (2014).

171. Escuin, D., Kline, E. R. & Giannakakou, P. Both microtubule-stabilizing and microtubule-destabilizing drugs inhibit hypoxia-inducible factor-1alpha accumulation and activity by disrupting microtubule function. *Cancer Res.* **65**, 9021–9028 (2005).

172. Ciocca, D. R. *et al.* Response of human breast cancer cells to heat shock and chemotherapeutic drugs. *Cancer Res.* **52**, 3648–3654 (1992).

173. Fan, G., Liu, D. & Lin, Q. Fluorescein diacetate and propidium iodide FDA-PI double staining detect the viability of Microcystis sp. after ultrasonic irradiation. *J. Food, Agric. Environ.* **11**, 2419–2421 (2013).

174. Wartenberg, M. & Acker, H. Quantitative recording of vitality patterns in living

multicellular spheroids by confocal microscopy. *Micron* **26**, 395–404 (1995).

175. Kanade, S., Nataraj, G., Ubale, M. & Mehta, P. Fluorescein diacetate vital staining for detecting viability of acid-fast bacilli in patients on antituberculosis treatment. *Int. J. Mycobacteriology* **5**, 294–298 (2016).
176. Rieger, A. M., Nelson, K. L., Konowalchuk, J. D. & Barreda, D. R. Modified annexin V/propidium iodide apoptosis assay for accurate assessment of cell death. *J. Vis. Exp.* 37–40 (2011).
177. Crowley, L. C. *et al.* Measuring Cell Death by Propidium Iodide Uptake and Flow Cytometry. *Cold Spring Harb. Protoc.* 1 (2016).
178. Jourdan, F. *et al.* Structure–Activity Relationships of C-17-Substituted Estratriene-3- *O* -sulfamates as Anticancer Agents. *J. Med. Chem.* **54**, 4863–4879 (2011).
179. Jourdan, F. *et al.* Synthesis, antitubulin, and antiproliferative SAR of analogues of 2-methoxyestradiol-3,17-O,O-bis-sulfamate. *J. Med. Chem.* **53**, 2942–2951 (2010).
180. Oudin, M. J. *et al.* MENA Confers Resistance to Paclitaxel in Triple-Negative Breast Cancer. *Mol. Cancer Ther.* **16**, 143–155 (2017).
181. O'Reilly, E. A. *et al.* The fate of chemoresistance in triple negative breast cancer (TNBC). *BBA Clin.* **3**, 257–275 (2015).
182. Wahba, H. A. & El-Hadaad, H. A. Current approaches in treatment of triple-negative breast cancer. *Cancer Biol. Med.* **12**, 106–116 (2015).
183. Jeong, Y. J. *et al.* Breast cancer cells evade paclitaxel-induced cell death by developing resistance to dasatinib. *Oncol. Lett.* **12**, 2153–2158 (2016).
184. Balasubramanian, R. *et al.* Functionally compromised CHD7 alleles in patients with isolated GnRH deficiency. *Proc. Natl. Acad. Sci. U. S. A.* **111**, 17953–17958 (2014).
185. Stanton, R. A., Gernert, K. M., Nettles, J. H. & Aneja, R. Drugs that target dynamic microtubules: A new molecular perspective. *Med. Res. Rev.* **31**, 443–481 (2011).
186. Larocque, K. *et al.* Novel analogue of colchicine induces selective pro-death autophagy and necrosis in human cancer cells. *PLoS One* **9**, e87064 (2014).
187. Zinchuk, V., Zinchuk, O. & Okada, T. Quantitative colocalization analysis of multicolor confocal immunofluorescence microscopy images: pushing pixels to explore biological

phenomena. *Acta Histochem. Cytochem.* **40**, 101–111 (2007).

188. Majcher, U. *et al.* Antiproliferative Activity and Molecular Docking of Novel Double-Modified Colchicine Derivatives. *Cells* **7**, 192 (2018).
189. Meehan, J. *et al.* Inhibition of pH regulation as a therapeutic strategy in hypoxic human breast cancer cells. *Oncotarget* **8**, 1–19 (2017).
190. Robertson, N., Potter, C. & Harris, A. L. Role of Carbonic Anhydrase IX in Human Tumor Cell Growth , Survival , and Invasion. *Cancer Res.* **64**, 6160–6165 (2004).
191. Watson, P. H. *et al.* Carbonic anhydrase XII is a marker of good prognosis in invasive breast carcinoma. *Br. J. Cancer* **88**, 1065–1070 (2003).
192. Ivanov, S. *et al.* Expression of Hypoxia-Inducible Cell-Surface Transmembrane Carbonic Anhydrases in Human Cancer. *Am. J. Pathol.* **158**, 905–919 (2001).
193. Karakashev, S. V & Reginato, M. J. Progress toward overcoming hypoxia-induced resistance to solid tumor therapy. *Cancer Manag. Res.* **7**, 253–64 (2015).
194. Huang, L. *et al.* Hypoxia induced paclitaxel resistance in human ovarian cancers via hypoxia-inducible factor 1alpha. *J. Cancer Res. Clin. Oncol.* **136**, 447–456 (2010).
195. Samanta, D., Gilkes, D. M., Chaturvedi, P., Xiang, L. & Semenza, G. L. Hypoxia-inducible factors are required for chemotherapy resistance of breast cancer stem cells. *Proc. Natl. Acad. Sci. U. S. A.* **111**, E5429-38 (2014).
196. Oh, J.-M., Ryu, Y.-K., Lim, J.-S. & Moon, E.-Y. Hypoxia Induces Paclitaxel-Resistance through ROS Production. *Biomol. Ther.* **18**, 145–151 (2010).
197. Labat-Robert, J. Cell-Matrix interactions, the role of fibronectin and integrins. A survey. *Pathol. Biol. (Paris).* **60**, 15–19 (2012).
198. Adams, J. C. & Watt, F. M. Regulation of development and differentiation by the extracellular matrix. *Development* **117**, 1183–1198 (1993).
199. Kleinman, H. K., Luckenbill-Edds, L., Cannon, F. W. & Sephel, G. C. Use of extracellular matrix components for cell culture. *Anal. Biochem.* **166**, 1–13 (1987).
200. Khalili, A. A. & Ahmad, M. R. A Review of cell adhesion studies for biomedical and biological applications. *Int. J. Mol. Sci.* **16**, 18149–18184 (2015).
201. Green, S. K., Francia, G., Isidoro, C. & Kerbel, R. S. Antiadhesive antibodies targeting E-

cadherin sensitize multicellular tumor spheroids to chemotherapy in vitro. *Mol. Cancer Ther.* **3**, 149–159 (2004).

202. Kaur, P. *et al.* Human breast cancer histoid: an in vitro 3-dimensional co-culture model that mimics breast cancer tissue. *J. Histochem. Cytochem.* **59**, 1087–1100 (2011).
203. Luebke-Wheeler, J. L., Nedredal, G., Yee, L., Amiot, B. P. & Nyberg, S. L. E-Cadherin Protects Primary Hepatocyte Spheroids From Cell Death by a Caspase-Independent Mechanism. *Cell Transpl.* **18**, 1281–1287 (2009).
204. Xu, S. *et al.* Construction and characteristics of an E-cadherin-related three-dimensional suspension growth model of ovarian cancer. *Sci. Rep.* **4**, 10–19 (2014).
205. Kim, D.-H. *et al.* Testosterone-induced matrix metalloproteinase activation is a checkpoint for neuronal addition to the adult songbird brain. *J. Neurosci.* **28**, 208–16 (2008).
206. Sorour, M. H., Hani, H. A., Shaalan, H. F. & El-Sayed, M. M. H. Experimental screening of some chelating agents for calcium and magnesium removal from saline solutions. *Desalin. Water Treat.* **57**, 22799–22808 (2016).
207. Filippakopoulos, P. *et al.* Selective inhibition of BET bromodomains. *Nature* **468**, 1067–1073 (2010).
208. Shu, S. *et al.* Response and resistance to BET bromodomain inhibitors in triple-negative breast cancer. *Nature* **529**, 1–24 (2016).
209. Jeffers, V., Yang, C., Huang, S. & Sullivan, W. J. Bromodomains in Protozoan Parasites: Evolution, Function, and Opportunities for Drug Development. *Microbiol. Mol. Biol. Rev.* **81**, 1–16 (2017).
210. Edmondson, R., Broglie, J. J., Adcock, A. F. & Yang, L. Three-Dimensional Cell Culture Systems and Their Applications in Drug Discovery and Cell-Based Biosensors. *Assay Drug Dev. Technol.* **12**, 207–218 (2014).
211. Santini, M. T. & Rainaldi, G. Three-dimensional spheroid model in tumor biology. *Pathobiology* **67**, 148–157 (1999).
212. Sant, S. & Johnston, P. A. The production of 3D tumor spheroids for cancer drug discovery. *Drug Discov. Today Technol.* **23**, 27–36 (2017).

213. Hughes, C. S., Postovit, L. M. & Lajoie, G. A. Matrigel: A complex protein mixture required for optimal growth of cell culture. *Proteomics* **10**, 1886–1890 (2010).

214. Reddel, R. R., Murphy, L. C., Hall, R. E. & Sutherland, R. L. Differential Sensitivity of Human Breast Cancer Cell Lines to the Growth- inhibitory Effects of Tamoxifen. *Cancer Res.* **45**, 1525–1531 (2006).

215. Chandrasekaran, S., Geng, Y., DeLouise, L. A. & King, M. R. Effect of homotypic and heterotypic interaction in 3D on the E-selectin mediated adhesive properties of breast cancer cell lines. *Biomaterials* **33**, 9037–9048 (2012).

216. Benien, P. & Swami, A. 3D tumor models: History, advances and future perspectives. *Future Oncology* **10**, (2014).

217. Yip, D. & Cho, C. H. A multicellular 3D heterospheroid model of liver tumor and stromal cells in collagen gel for anti-cancer drug testing. *Biochem. Biophys. Res. Commun.* **433**, (2013).

218. Stander, B. A. *et al.* In vitro evaluation of ESE-15-ol, an estradiol analogue with nanomolar antimitotic and carbonic anhydrase inhibitory activity. *PLoS One* **7**, e52205 (2012).

219. Stander, B. A., Marais, S., Vorster, C. J. J. & Joubert, A. M. In vitro effects of 2-methoxyestradiol on morphology, cell cycle progression, cell death and gene expression changes in the tumorigenic MCF-7 breast epithelial cell line. *J. Steroid Biochem. Mol. Biol.* **119**, 149–160 (2010).

220. Belotti, D. *et al.* The microtubule-affecting drug paclitaxel has antiangiogenic activity. *Clin. Cancer Res.* **2**, 1843–1849 (1996).

221. Horwitz, S. B. Taxol (paclitaxel): mechanisms of action. *Ann. Oncol.* **5**, 3–6 (1994).

222. Mqoco, T., Marais, S. & Joubert, A. 2-Methoxyestradiol-bis-sulphamate : A promising anticancer agent in an esophageal carcinoma (SNO) cell line . **24**, 115–122 (2013).

223. Theron, A. *et al.* Novel in silico-designed estradiol analogues are cytotoxic to a multidrug-resistant cell line at nanomolar concentrations. *Cancer Chemother. Pharmacol.* **75**, 431–437 (2015).

224. Botes, M. *et al.* A novel non-sulphamoylated 2-methoxyestradiol derivative causes

detachment of breast cancer cells by rapid disassembly of focal adhesions 06 Biological Sciences 0601 Biochemistry and Cell Biology. *Cancer Cell Int.* **18**, 1–12 (2018).

225. Cooke, M. J. *et al.* Enhanced cell attachment using a novel cell culture surface presenting functional domains from extracellular matrix proteins. *Cytotechnology* **56**, 71–79 (2008).
226. Keselowsky, B. G., Collard, D. M. & García, A. J. Integrin binding specificity regulates biomaterial surface chemistry effects on cell differentiation. *Proc. Natl. Acad. Sci. U. S. A.* **102**, 5953–5957 (2005).
227. Grimes, D. R., Kelly, C., Bloch, K. & Partridge, M. A method for estimating the oxygen consumption rate in multicellular tumour spheroids. *J. R. Soc. Interface* **11**, 20131124 (2014).
228. Zhang, W. *et al.* Optimization of the formation of embedded multicellular spheroids of MCF-7 cells: How to reliably produce a biomimetic 3D model. *Anal. Biochem.* **515**, 47–54 (2016).
229. Millard, M. *et al.* Drug delivery to solid tumors: The predictive value of the multicellular tumor spheroid model for nanomedicine screening. *International Journal of Nanomedicine* **12**, 7993–8007 (2017).

6 APPENDICES

I. PhD approval letter

II. Title change approval letter

III. Ethics approval letter

IV. Ethics approval letter – Amendment

V. Ethics approval letter – Amendment for title change

I. PhD approval letter

DOCTORAL STUDIES: PROTOCOL FORM

UNIVERSITY OF PRETORIA
FACULTY OF HEALTH SCIENCES
DOCTORAL DEGREE STUDIES

IMPORTANT:
Mark A or B:

A X	First submission (Without external examiners)	B	Second submission

N.B: FORMS COMPLETED BY HAND WILL NOT BE ACCEPTED – THE FORM IS AVAILABLE, ON REQUEST, IN ELECTRONIC FORMAT (KINDLY INQUIRE AT STUDENT ADMINISTRATION)

1. **DETAILS OF CANDIDATE:** T Perks **STUDENT NO:** 28169982
Title, Initials and Surname: Ms T Perks
Address: 15 Rupee Place, Eldoglen
Postal Code: 0171
Present qualifications and where obtained: MSc Biochemistry (Rhodes University)
Field of Study: PhD Physiology

2. **TOPIC OF THESIS**
Investigation into the effects of a novel estradiol analogue on hypoxic breast cancer tumour cells

2.1 **In the case of an amended topic, does this influence the protocol already approved, in any way?**
Mark the applicable block: N/A

YES	NO

N.B.: If YES, an amended protocol must accompany this form.

3. **PROMOTER:**
Dr Iman van den bout; PhD (Medical Biology, University of Amsterdam)
DEPARTMENT/DIVISION:
Physiology

4. **CO-PROMOTER(S):** (State highest qualification (e.g. PhD), address(es) and attach abridged CV if not from the University of Pretoria
N.B.: If not attached to the University of Pretoria, kindly submit, with this form, an additional motivation by the head of department and/or promoter for the appointment of such a co-promoter. (See Gen. Reg. G.57.2 (b))

Prof Annie Joubert; PhD (Biochemistry; University of Pretoria)
Department of Physiology
Basic Medical Sciences Building
Room 9-31
Prinshof Campus
University of Pretoria
Pretoria
0002

5. **MAIN SUBJECT:** MFG 990, MFG900

6. **SUBSIDIARY SUBJECT(S):** BSCH 5602700
(completed (2012) at Rhodes University Grahamstown)

AM Joubert
RECOMMENDED: ACTING HEAD OF DEPARTMENT **DATE: 14 September 2015**

AMJoubert

APPROVED, CHAIRPERSON: DOCTORAL PROTOCOL COMMITTEE

DEPUTY DEAN/CHAIR
School of Medicine
DATE 2015 -11- -9
Faculty of Health Sciences
UNIVERSITY OF PRETORIA

II. Title amendment approval

UNIVERSITEIT VAN PRETORIA
UNIVERSITY OF PRETORIA
YUNIBESITHI YA PRETORIA

Faculty of Health Sciences

04 December 2019

Dr I van den Bout
Department of Physiology
Faculty of Health Sciences

Dear Dr I van den Bout

STUDENT: JURGENS T (PhD PHYSIOLOGY)

TITLE: Development of a breast cancer spheroid model for use in drug discovery and cancer biology research

The above-mentioned student's protocol title amendment has been approved by the PhD committee.

We wish the student all the best with her studies.

Kind regards

PROF V STEENKAMP
CHAIR: PhD COMMITTEE

Deputy Dean: Teaching and Learning
Room 5-20.1, Level 5, Health Sciences Building
University of Pretoria, Private Bag X323
Gezina 0031, South Africa
Tel +27 (0)12 319 2174
Email vanessa.steenkamp@up.ac.za
www.up.ac.za

Fakulteit Gesondheidswetenskappe
Lefapha la Disaense tša Maphelo

III. Ethics approval letter

The Research Ethics Committee, Faculty Health Sciences, University of Pretoria complies with ICH-GCP guidelines and has US Federal wide Assurance.
- FWA 00002567, Approved dd 22 May 2002 and Expires 20 Oct 2016.
- IRB 0000 2235 IORG0001762 Approved dd 22/04/2014 and Expires 22/04/2017.

UNIVERSITEIT VAN PRETORIA
UNIVERSITY OF PRETORIA
YUNIBESITHI YA PRETORIA

Faculty of Health Sciences Research Ethics Committee

31/03/2016

Approval Certificate
New Application

Ethics Reference No.: 51/2016

Title: Cell Lines - Investigation into the effects of a novel estradiol analogue on hypoxic breast cancer tumour cells

Dear Miss Tamarin Perks

The **New Application** as supported by documents specified in your cover letter dated 12/02/2016 for your research received on the 12/02/2016, was approved by the Faculty of Health Sciences Research Ethics Committee on its quorate meeting of 30/03/2016.

Please note the following about your ethics approval:
- Ethics Approval is valid for 3 years
- Please remember to use your protocol number (**51/2016**) on any documents or correspondence with the Research Ethics Committee regarding your research.
- Please note that the Research Ethics Committee may ask further questions, seek additional information, require further modification, or monitor the conduct of your research.

Ethics approval is subject to the following:
- The ethics approval is conditional on the receipt of 6 monthly written Progress Reports, and
- The ethics approval is conditional on the research being conducted as stipulated by the details of all documents submitted to the Committee. In the event that a further need arises to change who the investigators are, the methods or any other aspect, such changes must be submitted as an Amendment for approval by the Committee.

We wish you the best with your research.

Yours sincerely

Professor Werdie (CW) Van Staden
MBChB MMed(Psych) MD FCPsych FTCL UPLM
Chairperson: Faculty of Health Sciences Research Ethics Committee

The Faculty of Health Sciences Research Ethics Committee complies with the SA National Act 61 of 2003 as it pertains to health research and the United States Code of Federal Regulations Title 45 and 46. This committee abides by the ethical norms and principles for research, established by the Declaration of Helsinki, the South African Medical Research Council Guidelines as well as the Guidelines for Ethical Research: Principles Structures and Processes 2004 (Department of Health).

☎ 012 354 1677 🖷 0866516047 deepeka.behari@up.ac.za http://www.up.ac.za/healthethics
✉ Private Bag X323, Arcadia, 0007 - 31 Bophelo Road, HW Snyman South Building, Level 2, Room 2.33, Gezina, Pretoria

IV. Ethics approval letter – Amendment

The Research Ethics Committee, Faculty Health Sciences, University of Pretoria complies with ICH-GCP guidelines and has US Federal wide Assurance.
- FWA 00002567, Approved dd 22 May 2002 and Expires 20 Oct 2016.
- IRB 0000 2235 IORG0001762 Approved dd 22/04/2014 and Expires 22/04/2017.

UNIVERSITEIT VAN PRETORIA
UNIVERSITY OF PRETORIA
YUNIBESITHI YA PRETORIA

Faculty of Health Sciences Research Ethics Committee

28/07/2016

Approval Certificate
Amendment
(to be read in conjunction with the main approval certificate)

Ethics Reference No.: 51/2016

Title: Investigation into the effects of a novel estradiol analogue on hypoxic breast cancer tumour cells

Dear Miss Tamarin Perks

The **Amendment** as described in your documents specified in your cover letter dated 30/06/2016 received on 30/06/2016 was approved by the Faculty of Health Sciences Research Ethics Committee on its quorate meeting of 27/07/2016.

Please note the following about your ethics amendment:
- Please remember to use your protocol number (**51/2016**) on any documents or correspondence with the Research Ethics Committee regarding your research.
- Please note that the Research Ethics Committe may ask further questions, seek additional information, require further modification, or monitor the conduct of your research.

Ethics amendment is subject to the following:
- The ethics approval is conditional on the receipt of **6 monthly written Progress Reports**, and
- The ethics approval is conditional on the research being conducted as stipulated by the details of all documents submitted to the Committee. In the event that a further need arises to change who the investigators are, the methods or any other aspect, such changes must be submitted as an Amendment for approval by the Committee.

We wish you the best with your research.

Yours sincerely

Dr R Sommers; MBChB; MMed (Int); MPharMed,PhD
Deputy Chairperson of the Faculty of Health Sciences Research Ethics Committee, University of Pretoria

The Faculty of Health Sciences Research Ethics Committee complies with the SA National Act 61 of 2003 as it pertains to health research and the United States Code of Federal Regulations Title 45 and 46. This committee abides by the ethical norms and principles for research, established by the Declaration of Helsinki, the South African Medical Research Council Guidelines as well as the Guidelines for Ethical Research: Principles Structures and Processes 2004 (Department of Health).

☎ 012 356 3084 deepeka.behari@up.ac.za / fhsethics@up.ac.za http://www.up.ac.za/healthethics
✉ Private Bag X323, Arcadia, 0007 - Tswelopele Building, Level 4, Room 60, Gezina, Pretoria

V. Ethics approval letter – Amendment for title change

UNIVERSITEIT VAN PRETORIA
UNIVERSITY OF PRETORIA
YUNIBESITHI YA PRETORIA

Faculty of Health Sciences

Institution: The Research Ethics Committee, Faculty Health Sciences, University of Pretoria complies with ICH-GCP guidelines and has US Federal wide Assurance.

- FWA 00002567, Approved dd 22 May 2002 and Expires 03/20/2022.
- IORG #: IORG0001762 OMB No. 0990-0279 Approved for use through February 28, 2022 and Expires: 03/04/2023.

10 June 2020

Approval Certificate
Amendment

Ethics Reference No.: 51/2016
Title: Development of a breast cancer spheroid model for use in drug discovery and cancer biology research

Dear Mrs T Jurgens

The **Amendment** as supported by documents received between 2020-04-16 and 2020-06-10 for your research, was approved by the Faculty of Health Sciences Research Ethics Committee on its quorate meeting of 2020-06-10.

Please note the following about your ethics approval:

- Please remember to use your protocol number (51/2016) on any documents or correspondence with the Research Ethics Committee regarding your research.
- Please note that the Research Ethics Committee may ask further questions, seek additional information, require further modification, monitor the conduct of your research, or suspend or withdraw ethics approval.

Ethics approval is subject to the following:

- The ethics approval is conditional on the research being conducted as stipulated by the details of all documents submitted to the Committee. In the event that a further need arises to change who the investigators are, the methods or any other aspect, such changes must be submitted as an Amendment for approval by the Committee.

We wish you the best with your research.

Yours sincerely

Dr R Sommers
MBChB MMed (Int) MPharmMed PhD
Deputy Chairperson of the Faculty of Health Sciences Research Ethics Committee, University of Pretoria

The Faculty of Health Sciences Research Ethics Committee complies with the SA National Act 61 of 2003 as it pertains to health research and the United States Code of Federal Regulations Title 45 and 46. This committee abides by the ethical norms and principles for research, established by the Declaration of Helsinki, the South African Medical Research Council Guidelines as well as the Guidelines for Ethical Research: Principles Structures and Processes, Second Edition 2015 (Department of Health).

Research Ethics Committee
Room 4-60, Level 4, Tswelopele Building
University of Pretoria, Private Bag x323
Gezina 0031, South Africa
Tel +27 (0)12 356 3084
Email: deepeka.behari@up.ac.za
www.up.ac.za

Fakulteit Gesondheidswetenskappe
Lefapha la Disaense tša Maphelo